ISSN 1007-9327 (print)
ISSN 2219-2840 (online)

World Journal of *Gastroenterology*

World J Gastroenterol 2022 February 14; 28(6): 608-692

Published by Baishideng Publishing Group Inc

World Journal of Gastroenterology

Contents

Weekly Volume 28 Number 6 February 14, 2022

Contents

ABOUT COVER

Editorial Board Member of *World Journal of Gastroenterology*, Naoki Hashimoto, MD, PhD, Professor, Surgeon, Department of Surgery, Kindai University, Osaka 577-8502, Japan. gojigen000@gmail.com

AIMS AND SCOPE

The primary aim of *World Journal of Gastroenterology* (*WJG*, *World J Gastroenterol*) is to provide scholars and readers from various fields of gastroenterology and hepatology with a platform to publish high-quality basic and clinical research articles and communicate their research findings online. *WJG* mainly publishes articles reporting research results and findings obtained in the field of gastroenterology and hepatology and covering a wide range of topics including gastroenterology, hepatology, gastrointestinal endoscopy, gastrointestinal surgery, gastrointestinal oncology, and pediatric gastroenterology.

INDEXING/ABSTRACTING

The *WJG* is now indexed in Current Contents®/Clinical Medicine, Science Citation Index Expanded (also known as SciSearch®), Journal Citation Reports®, Index Medicus, MEDLINE, PubMed, PubMed Central, and Scopus. The 2021 edition of Journal Citation Report® cites the 2020 impact factor (IF) for *WJG* as 5.742; Journal Citation Indicator: 0.79; IF without journal self cites: 5.590; 5-year IF: 5.044; Ranking: 28 among 92 journals in gastroenterology and hepatology; and Quartile category: Q2. The *WJG*'s CiteScore for 2020 is 6.9 and Scopus CiteScore rank 2020: Gastroenterology is 19/136.

RESPONSIBLE EDITORS FOR THIS ISSUE

Production Editor: *Hua-Ge Yu*; **Production Department Director:** *Xu Guo*; **Editorial Office Director:** *Ze-Mao Gong*.

NAME OF JOURNAL
World Journal of Gastroenterology

ISSN
ISSN 1007-9327 (print) ISSN 2219-2840 (online)

LAUNCH DATE
October 1, 1995

FREQUENCY
Weekly

EDITORS-IN-CHIEF
Andrzej S Tarnawski

EDITORIAL BOARD MEMBERS
http://www.wjgnet.com/1007-9327/editorialboard.htm

PUBLICATION DATE
February 14, 2022

INSTRUCTIONS TO AUTHORS
https://www.wjgnet.com/bpg/gerinfo/204

GUIDELINES FOR ETHICS DOCUMENTS
https://www.wjgnet.com/bpg/GerInfo/287

GUIDELINES FOR NON-NATIVE SPEAKERS OF ENGLISH
https://www.wjgnet.com/bpg/gerinfo/240

PUBLICATION ETHICS
https://www.wjgnet.com/bpg/GerInfo/288

PUBLICATION MISCONDUCT
https://www.wjgnet.com/bpg/gerinfo/208

ARTICLE PROCESSING CHARGE
https://www.wjgnet.com/bpg/gerinfo/242

STEPS FOR SUBMITTING MANUSCRIPTS
https://www.wjgnet.com/bpg/GerInfo/239

ONLINE SUBMISSION
https://www.f6publishing.com

World Journal of Gastroenterology

Submit a Manuscript: https://www.f6publishing.com

World J Gastroenterol 2022 February 14; 28(6): 608-623

DOI: 10.3748/wjg.v28.i6.608

ISSN 1007-9327 (print) ISSN 2219-2840 (online)

OPINION REVIEW

Is precision medicine for colorectal liver metastases still a utopia? New perspectives by modern biomarkers, radiomics, and artificial intelligence

Luca Viganò, Visala S Jayakody Arachchige, Francesco Fiz

ORCID number: Luca Viganò 0000-0001-5798-5021; Visala S Jayakody Arachchige 0000-0003-0754-5516; Francesco Fiz 0000-0003-3932-1330.

Author contributions: Viganò L and Fiz F designed the study; Viganò L, Jayakody Arachchige VS, and Fiz F performed the literature review; Jayakody Arachchige VS, and Fiz F wrote the manuscript draft; Viganò L revised the manuscript; all authors reviewed the final version of the manuscript and approved it.

Conflict-of-interest statement: The authors have no conflicts of interest to disclose.

Supported by the Italian Association for Cancer Research, No. #2019−23822 (Luca Viganò).

Country/Territory of origin: Italy

Specialty type: Gastroenterology and hepatology

Provenance and peer review: Invited article; Externally peer reviewed.

Peer-review model: Single blind

Peer-review report's scientific quality classification

Grade A (Excellent): 0

Grade B (Very good): 0

Luca Viganò, Visala S Jayakody Arachchige, Department of Hepatobiliary and General Surgery, IRCCS Humanitas Research Hospital, Rozzano 20089, MI, Italy

Luca Viganò, Visala S Jayakody Arachchige, Department of Biomedical Sciences, Humanitas University, Pieve Emanuele 20072, MI, Italy

Francesco Fiz, Nuclear Medicine, IRCCS Humanitas Research Hospital, Rozzano 20089, MI, Italy

Corresponding author: Luca Viganò, MD, PhD, Professor, Department of Hepatobiliary and General Surgery, IRCCS Humanitas Research Hospital, Via Manzoni 56, Rozzano 20089, MI, Italy. luca.vigano@hunimed.eu

Abstract

The management of patients with liver metastases from colorectal cancer is still debated. Several therapeutic options and treatment strategies are available for an extremely heterogeneous clinical scenario. Adequate prediction of patients' outcomes and of the effectiveness of chemotherapy and loco-regional treatments are crucial to reach a precision medicine approach. This has been an unmet need for a long time, but recent studies have opened new perspectives. New morphological biomarkers have been identified. The dynamic evaluation of the metastases across a time interval, with or without chemotherapy, provided a reliable assessment of the tumor biology. Genetics have been explored and, thanks to their strong association with prognosis, have the potential to drive treatment planning. The liver-tumor interface has been identified as one of the main determinants of tumor progression, and its components, in particular the immune infiltrate, are the focus of major research. Image mining and analyses provided new insights on tumor biology and are expected to have a relevant impact on clinical practice. Artificial intelligence is a further step forward. The present paper depicts the evolution of clinical decision-making for patients affected by colorectal liver metastases, facing modern biomarkers and innovative opportunities that will characterize the evolution of clinical research and practice in the next few years.

Key Words: Colorectal liver metastases; Biomarkers; Genetics; Immune infiltrate; Radiomics; Artificial Intelligence

Grade C (Good): C
Grade D (Fair): 0
Grade E (Poor): 0

Received: June 22, 2021
Peer-review started: June 22, 2021
First decision: July 14, 2021
Revised: July 29, 2021
Accepted: January 20, 2022
Article in press: January 20, 2021
Published online: February 14, 2022

P-Reviewer: Tanabe S
S-Editor: Chang KL
L-Editor: Filipodia
P-Editor: Chang KL

Core Tip: The management of patients with colorectal liver metastases is challenging because the choice among different therapeutic options and strategies is not supported by strong evidence. A precision medicine approach has been an unmet need for a long time, but recent studies have opened new perspectives. In this paper, we will discuss new morphological approaches to assess tumor biology, the promising data from genetic analyses, the raising clinical relevance of the liver-tumor interface, and the potentialities of advanced imaging analysis and artificial intelligence. These are the keys to reach an effective personalized treatment in the near future.

Citation: Viganò L, Jayakody Arachchige VS, Fiz F. Is precision medicine for colorectal liver metastases still a utopia? New perspectives by modern biomarkers, radiomics, and artificial intelligence. *World J Gastroenterol* 2022; 28(6): 608-623
URL: https://www.wjgnet.com/1007-9327/full/v28/i6/608.htm
DOI: https://dx.doi.org/10.3748/wjg.v28.i6.608

INTRODUCTION

During the last decades, the surgeons and medical oncologists drove the multidisciplinary teams to the ambitious aim of curing patients with colorectal liver metastases [1]. Systemic therapy had a progressively increasing effectiveness[2,3]. To date, the median life expectancy of patients receiving state-of-the-art treatment exceeds 30 mo[1,2]. The new immunotherapies could further raise the bar. Liver surgery has been the game-changer: It rapidly became the standard thanks to its proven safety (mortality risk lower than 2%) and oncological effectiveness (actual 5- and 10-year survival rates of about 50% and 20%, respectively)[1,4-6]. All patients with technically resectable disease, sufficient future liver remnant volume, and disease control by chemotherapy are now considered for surgery[1,7]. The liver surgeons pursued aggressive indications and developed complex techniques to maximize the resectability rate, even considering liver transplantation in the most recent years[7-9]. However, this generated a paradox: We are now searching for criteria to identify patients that are technically resectable but do not benefit from surgery because of their unfavorable tumor biology (10%-15% of patients have an early recurrence and early cancer-related death after surgery)[10]. Finally, thermal ablation gained momentum. After having demonstrated its effectiveness in patients with hepatocellular carcinoma, radiofrequency and microwave ablation have been successfully applied to patients with colorectal liver metastases, achieving adequate disease control[11,12]. Percutaneous treatments are now even tested as alternative to surgery in randomized trials[13,14].

The management of such a complex scenario should rely on an adequate understanding of tumor biology and several decisions need for a precision medicine approach (*e.g.*, the identification of the most appropriate schedule of systemic therapy, the selection of candidates to surgery, the indication to perioperative chemotherapy, the timing of colorectal and hepatic surgery in patients with synchronous metastases, and the choice between surgery and ablation). However, a recent study demonstrated that hepatobiliary surgeons have a huge heterogeneity in the treatment planning and surgical indications, the choice among different options being almost a throw of the dice[15]. Reliable biomarkers are urgently needed to drive a patient-tailored evidence-based approach.

In 2012, we depicted an evolving scenario with some preliminary evidence[16]. Where do we stand almost a decade later? In the present paper, we will provide a critical overview of traditional biomarkers, new proposals, and future perspectives (Figure 1 and Table 1).

MORPHOLOGY: AN OUTDATED BIOMARKER?

The tumor morphology is still the basis of several clinical decisions. The tumor burden defines the resectability of patients, and, in resectable ones, the need for perioperative

Table 1 Characteristics of different biomarkers of colorectal liver metastases.

	Biomarker characteristics					
	Standardized	Reproducibility	Robustness (across series)	Early assessment	Reliability in prediction	(Potential) Clinical impact
Morphology and clinical data	d	e	c	e	b	c
Dynamic evaluation	d	e	e	b	d	e
Genetics	c	d	d	e	e	e
Peritumoral tissue data	c	d	c	a	d	d
Radiomics	b	c	c	e	c	d
Artificial intelligence	a	a	b	d	d	e

The performances of every biomarker are evaluated by a score, ranging from "a" if very low to "e" if very high.

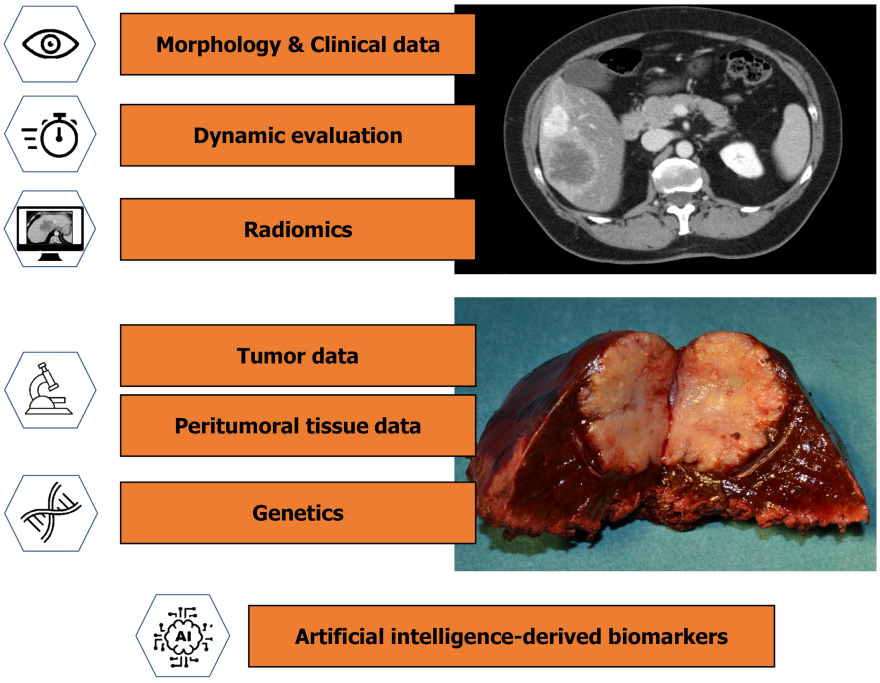

Figure 1 Available biomarkers for patients affected by colorectal liver metastases. A biomarker is defined as any parameter (molecular, cellular, clinical, imaging or identified by an artificial intelligence process) having a clinical role in narrowing or guiding treatment decisions and contributing to the estimation of the overall patient prognosis (prognostic biomarker), the clinical outcome after a treatment (predictive biomarker), or the properties of a clinical condition /disease (diagnostic biomarker).

chemotherapy[1,7]. The size of liver metastases determines the indication to thermal ablation (effective in nodules ≤ 30 mm)[17]. Several morphological parameters, including primary tumor data and tumor markers, have a prognostic value, and they have been combined into multiple scores to optimize their prognostic performance (Table 2)[18-23].

Recent studies reaffirmed the role of tumor morphology as a biomarker and determinant of the treatment strategy. First, Sasaki *et al*[24] proposed to combine the number and size of metastases into a "Tumor Burden Score", mimicking the Metroticket evidence for hepatocellular carcinoma[25]. They classified the patients into three groups and achieved a good stratification of survival, better than the stratification achieved by the size or the number of metastases when separately considered. Nevertheless, the Tumor Burden Score failed to select the candidates to surgery, the patients of the high-risk group (score ≥ 9) having an expected 5-year survival rate over 20%. Second, the primary tumor site has gained momentum. In comparison with patients having a left colonic tumor, those having a right colonic tumor are characterized by a lower response to chemotherapy, survival after surgery, and effectiveness

Table 2 Some of the available scores for outcome prediction of patients with colorectal liver metastases candidates to surgery

	Morphology-based scores				Morphology- and Genetics-based scores		
	Nordlinger *et al*[18], 1996	CRS, Fong *et al*[19], 1999	Iwatsuki *et al*[20], 1999	Rees *et al*[21], 2008	RAS Mutation CRS, Brudvik *et al*[60] 2017	GAME score, Margonis *et al*[61] 2018	Extended CRS, Lang *et al*[65], 2019
Morphological parameters							
Age	Yes (60 yr)						
Primary tumor							
Extension into the serosa	Yes						
N status primary tumor	Yes	Yes		Yes	Yes	Yes	Yes
Grading primary tumor				Yes			
Liver metastases							
Number	Yes (3)	Yes (1)	Yes (2)	Yes (3)		Yes (TBS)	
Size	Yes (50 mm)	Yes (50 mm)	Yes (80 mm)	Yes (50 mm)	Yes (50 mm)		Yes (50 mm)
Bilobar			Y				
DFI	Yes (24 mo)	Yes (12 mo)	Yes (30 mo)				
Surgical margin	Yes (10 mm)						
Extrahepatic disease				Yes		Yes	
CEA value		Yes (200 ng/mL)		Yes (60 ng/mL)		Yes (20 ng/mL)	
Genetic parameters							
RAS					Yes	Yes[1]	
RAS/RAF pathway							Yes
SMAD							Yes

[1]KRAS status.

DFI: Disease-free interval from primary to metastases; CEA: Carcinoembryonic antigen; CRS: Clinical risk score; GAME: Genetic and morphological evaluation; TBS: Tumor Burden Score.

of thermal ablation[26-29]. The embryological origin of the two parts of the colon (midgut for the right colon and hindgut for the left one) and the different genetic profiles of the tumors could explain such results. However, the impact of the primary tumor side on the treatment strategy is still to be defined, and, in this distinction (right *vs* left colonic cancer), the rectal cancers remain a blurred entity to elucidate. Third, a recent study based on the LiverMetSurvey data suggested that patients with synchronous multiple bilobar metastases should undergo a liver-first approach because this strategy achieves better survival than the alternative ones (*i.e.* the simultaneous and primary tumor-first approaches)[30]. This evidence could lead to a major change in current practice and definitively prioritizes the treatment of liver metastases in presence of a severe hepatic tumor burden. Fourth, in patients with liver and lung metastases, the pulmonary disease has shown a limited prognostic relevance [31]. Such data should be paired with those provided by Viganò *et al*[32], who demonstrated that the pathological response of colorectal metastases to systemic therapy changes according to the involved organ, being low in the lung and lymph nodes metastases, intermediate in the hepatic ones, and high in the peritoneal ones. The inhomogeneous prognostic relevance and chemosensitivity of the different tumor sites open new perspectives in treatment strategies and oncological research.

Despite its extensive adoption in current practice, tumor morphology is not a robust biomarker for several reasons. First, in patients undergoing systemic therapy,

morphology gives a limited prediction of the response to treatment. Second, in resectable patients, it does not allow for an adequate selection of candidates. The number of colorectal metastases and the presence of extrahepatic disease are paradigmatic examples. Even if the number of nodules is a strong prognostic factor, there is not a numeric cut-off value beyond which resection is contraindicated, and some patients with numerous metastases may benefit from surgery[33-35]. Similarly, the presence of extrahepatic disease contraindicates surgery in a limited proportion of patients (unresectable lesions, distant lymph node metastases, and diffuse peritoneal disease combined with multiple hepatic metastases)[36-38]. Third, different morphological parameters have been reported by different studies, and none has been confirmed by all authors. Fourth, morphological criteria can be modified by chemotherapy (*e.g.*, the tumor size), and it is unclear which value (before or after treatment) should be considered. Finally, tumor morphology offers a snapshot of the tumor and misses its evolution.

MOVING TOWARD A DYNAMIC VIEW

The tumor behavior is intuitively an effective surrogate biomarker of its biology. In the early 2000s, some authors proposed to adopt a time-test before surgery in patients with resectable colorectal liver metastases (*i.e.* an observation period to evaluate the tumor evolution)[39-41]. One-third to half of the patients developed additional lesions during the time-test and were excluded from resection. This policy has been early abandoned because of the advent of effective chemotherapy regimens, which combine observation and treatment. To date, neoadjuvant systemic therapy is a standard, and the tumor behavior during treatment is one of the most powerful prognostic factors. Since 2004, progression while on chemotherapy is even considered a contraindication to resection in resectable patients with few exceptions[42].

The prognostic role of the response to chemotherapy is indisputable, but three main limitations of this parameter should be highlighted: It excludes from surgery less than 10% of candidates[43]; the pathological evaluation of response has a poor agreement with the radiological one (about one-third of responders at imaging has no tumor regression at the pathology analysis)[44,45]; the no-progression during short chemotherapy (2-3 mo, the present standard) does not necessarily correspond to favorable biology and prognosis (about 15% of patients develop early recurrence after surgery)[10].

There is another time interval during which the tumor behavior can be analyzed. Patients must respect a 4-wk pause between the end of the systemic therapy and surgery (6 wk in case of anti-vascular endothelial growth factor treatment)[46,47]. We observed that about 15% of patients with tumor response or stabilization during chemotherapy have an early tumor progression in the interval between chemotherapy and surgery and an extremely poor outcome (0% survival at 2 years)[48]. Such a progression should contraindicate resection and dictates the need for restaging immediately before surgery.

Finally, percutaneous thermal ablation could contribute to the dynamic evaluation of colorectal liver metastases. It has been proposed as a time-test in patients with a synchronous disease or early recurrence after liver surgery with several benefits: Ablation provided a minimally invasive and effective treatment of the metastases, with high salvageability in case of local failure; avoided futile surgery in some cases; and spared chemotherapy for further disease progression[49,50].

Despite its effectiveness, the dynamic evaluation of colorectal metastases should be applied with caution. First, the time-test must be adequate. Progression during prolonged systemic therapy or after a long chemotherapy-surgery interval represents a loss of chance for resectable patients rather than a selection[48]. Even a disease progression in the interval between the two stages of a staged hepatectomy should not be considered *tout-court* an adequate selection of candidates[51]. Second, selected patients with a dimensional-only progression of the tumor and a limited hepatic tumor burden can be considered for surgery despite progression[52]. Finally, progression is not a definitive contraindication to resection, and surgery can be scheduled if the disease is controlled by a further line of chemotherapy[53,54].

GENETIC DATA: THE PANACEA FOR ALL THE UNCERTAINTIES?

Tumor genetics is the key to design a precision medicine approach. The sequencing of large series of metastases highlighted few high-frequency mutations, which have been extensively investigated for their association with the outcome. Tumor protein p53 (TP53) and APC gene mutations are the commonest ones (65%-75% and 45%-85% of patients, respectively)[55,56], but most studies focused on the RAS genes. KRAS and NRAS mutations are evident in one-third to half of the patients and have an established clinical impact: They preclude anti-epidermal growth factor receptor treatments and are associated with a lower response rate to chemotherapy, poorer survival, and higher risk of pulmonary metastases[57-59]. RAS status has been recently included in two prognostic scores for patients undergoing liver surgery (Table 2): The RAS Mutation Clinical Risk Score that considers the RAS status, metastases size, and N status of the primary tumor[60]; the Genetic And Morphological Evaluation (GAME) score that considers the KRAS status, carcinoembryonic antigen level, N status of the primary tumor, Tumor Burden Score, and presence of extrahepatic disease[61]. Both have been externally validated and outperformed the standard morphology-based scores. The patients with the highest scores had extremely poor outcome (0% recurrence-free survival at 2 years after surgery if RAS Mutation Clinical Risk Score = 3 or GAME score ≥ 6), but they were a marginal part of the cohort (14/564, 2.5%, and 18/1249, 1.4%, respectively).

The analysis of BRAF mutations generated a major interest despite their low frequency (4%-10%)[56,62]. The oncologists reported extremely poor survival of BRAF mutated patients, raising doubts about their candidacy to surgery[57,62]. Nevertheless, surgical series achieved an adequate outcome in selected BRAF mutated patients, suggesting that this genetic profile is a strong prognostic factor but should not be an absolute contraindication when the disease is adequately controlled by chemotherapy [63,64]. Additional mutations have been associated with prognosis, such as those of the TP53, PIK3CA, APC, and SMAD genes[65]. The Mainz group suggested that the performances of the aforementioned RAS score can be improved by replacing the RAS with the RAS-RAF pathway and adding the SMAD family (Table 2)[65]. The patients with all four negative prognostic factors (metastasis size > 50 mm, N+ primary tumors, and double mutation of the RAS-RAF pathway and SMAD family) had an extremely low median survival (1 year after surgery), but they were very few (only 5 out of 123, 4%). The MD Anderson Cancer Center group reported a cumulative negative prognostic impact of the mutations of TP53, RAS, and SMAD4: Survival progressively decreased with the increase in the number of the altered genes[66].

Those are the first steps of genetic-based precision medicine, but we have still to face some major challenges: Evidence is preliminary and needs robust validation to drive clinical practice; some criteria to select the candidates to surgery have been proposed, but they concern a minimal proportion of patients (< 5%)[60,61,65]; the discordance of the genetic profile between the primary tumor and metastases and their corresponding prognostic impact remain to be elucidated; tumor heterogeneity may lead to clonal populations with different mutations into a single metastasis, but their assessment is not yet standardized.

THE SOLUTION COULD BE OUTSIDE THE TUMOR

The liver-tumor interface could be the true battlefield where the interaction between the neoplastic cells and the "host" determines the prognosis. Several data are in favor of this hypothesis.

First, the pathology analysis of the peritumoral parenchyma highlighted the presence of the micrometastases (*i.e.* vascular and lymphatic tumoral emboli, perineural tissue infiltration, and satellite nodules)[44]. They are mainly localized within the first 2 mm of tissue surrounding the tumor, are reduced by chemotherapy, and negatively impact prognosis[44,67,68]. Micrometastases are the true determinants of the local recurrence risk after resection and thermal ablation.

Second, the profile of liver metastases has prognostic relevance. In 2009, Mentha *et al*[69] depicted the so-called "dangerous-halo" (*i.e.* a neoplastic regrowth at the tumor periphery due to an early reactivation of the metastases after the end of chemotherapy). This could represent the pathology counterpart of the radiological tumor progression that we observed in the interval chemotherapy-surgery. To date, the metastases' profile has been named "tumor growth pattern" and has been distinguished into three types: Pushing, desmoplastic, and replacement[70]. The types

correspond to different growing modalities: The metastases with a replacement pattern grow by co-opting the stroma and sinusoids; those with a pushing pattern have signs of active hypoxia-induced angiogenesis[71,72]. The replacement pattern is the most aggressive one and is associated with a lower response rate to chemotherapy, higher recurrence risk, and poorer survival[73-75]. In patients with a replacement pattern, we also observed an increased risk of local recurrence after surgery and the need for a wider surgical margin (unpublished data).

Third, a growing interest concerns the peri-tumoral immune infiltrate, especially after the introduction of modern immunotherapies. As for the primary colorectal cancers, an immunoscore, based on the presence of $CD3^+$ and $CD8^+$ cells in the core of liver metastases and at their invasion margin, achieved a good stratification of prognosis[76]. Additional cell populations have been investigated for their association with the outcome, such as the macrophages[77], but data are still preliminary.

Unfortunately, the biomarkers of the liver-tumor interface can be assessed only by the pathologist on the surgical specimen. The lack of an adequate non-invasive evaluation strongly reduces their clinical relevance. In addition, a comprehensive overview of the liver-tumor interface, merging the different pathology details, is still lacking, precluding a definitive understanding of the tumor-host interaction.

A further aspect deserves consideration; some features of the non-tumoral liver parenchyma could impact prognosis. Chemotherapy-associated sinusoidal injuries have been associated with the tumor response to chemotherapy; the more severe the sinusoidal dilatation the lower the response rate[44,78]. Nevertheless, the response to therapy and not the sinusoidal dilatation impacted survival[44]. In contrast, Viganò *et al*[44] depicted moderate/severe steatosis as a positive prognostic factor after surgery (5-year survival rate 53% *vs* 35%). These results have been confirmed by a subsequent analysis of the LiverMetSurvey database[79] and are in line with some studies reporting a favorable association between body mass index and prognosis[80,81]. We are still far from conclusive evidence and reliable explanation, but further investigations should be performed to potentially outline new therapeutic approaches.

RADIOMICS: IMAGING BEYOND THE VISIBLE DATA

Radiomics, or texture analysis, uses mathematical formulas to extract from medical imaging modalities invisible-to-the-eye patterns, which correlate with the biological properties of the analyzed tissue[82,83]. The complexity of analyses progressively increased, moving from histogram-based values to different types of matrices, filters, and transforms[84,85]. In patients with colorectal liver metastases, several potential applications of radiomics have been proposed[86]. First, it can predict the effectiveness of chemotherapy[87-95]. The decrease in entropy and increase in homogeneity of liver lesions after chemotherapy have been associated with the radiological tumor response. Some authors even reported the possibility to predict response to systemic therapy by analyzing the images at diagnosis before chemotherapy; higher entropy and lower homogeneity of liver metastases were associated with a subsequent higher response rate. When compared with the standard RECIST criteria, texture analysis achieved earlier and more accurate prediction. Second, radiomics have been associated with patients' prognosis, metastases with higher entropy and lower homogeneity having a better survival[88,90,96]. The comparative analysis of the imaging modalities before and after chemotherapy further refined the prediction of the long-term outcome[89,91,92,94], and there is accumulating evidence that both radiomic scores and combined clinical-radiomic models outperform traditional predictors of survival[92]. Third, textural features of the tumor before thermal ablation can predict the risk of local recurrence[97]. Fourth, radiomics are associated with the pathology data (*e.g.*, tumor grading, growth pattern, and regression grade after chemotherapy[88,98,99]). Finally, texture analysis has the potential to provide a non-invasive evaluation of the chemotherapy-associated liver injuries, which at present are poorly evaluated by standard imaging modalities[46,100].

The strength of radiomics relies on its capability to provide early prediction of the outcome and to reach a non-invasive estimation of the pathology details of colorectal metastases, anticipating data that are usually collected only after surgery. Further, the possibility to interpret the biological value of some radiomic features facilitates their implementation into clinical practice. For instance, entropy and heterogeneity, especially after contrast enhancement, clearly suggest the presence of active disease with heterogeneous clones, while homogeneity after chemotherapy reflects tumor necrosis due to a response to treatment. Finally, the development of technological tools

to perform automatic segmentation of liver tumors will enable easier extraction of radiomic features, contributing to the spread of such data. However, the texture analysis suffers from some limitations: Some features, in particular the second-order ones, lack interpretability; radiomics has instability across different devices and acquisition protocols, especially for magnetic resonance images; studies differ in terms of software packages, analyzed phases, and reported features; and reliable cut-off values of radiomic parameters are lacking. Those issues have to be solved to speed up the application of radiomics into clinical practice.

ARTIFICIAL INTELLIGENCE: WHERE DO WE STAND?

In the most recent years, the so-called "artificial intelligence" (AI) is the object of major interest and investments, with a consequent spike of AI-related publications[101]. Introduced in the 1950s, the term AI defines a computer program that, in a very specific setting, can "learn" and self-improve over time[102,103]. A demonstration of its potentialities took place in 1997, when a chess-playing AI, named Deep Blue, was able to beat the world champion Kasparov[104]. In medicine, AI is expected not only to optimize the prediction of an outcome by combining all available variables but also to update and improve continuously prediction according to the experienced results (Figure 2). AI can represent a major support to the decision-making processes, especially in the clinical scenarios with several therapeutic and strategical options and lack of consensus among experts, exactly as occurs for colorectal metastases[15]. In this sense, AI is not *per se* a biomarker but maximizes the profitability of all available data. However, AI may also have an additional role. It can be applied to medical imaging to identify new patterns that can contribute to diagnosis or prediction[105]. Such patterns, extractable from any type of imaging modality in a completely unbiased and unsupervised way, can be considered AI-derived biomarkers, subject to clinical validation[106]. Analogously, AI can identify biomarkers from any source of data, including clinical charts, medical reports, and images scan.

A first attempt in using AI-based therapy guidance dates to 2005, when a decision matrix platform, named OncoSurge, was introduced to help clinicians deciding the best treatment of patients at first diagnosis of colorectal liver metastases (*i.e.* when the treatment planning has the greatest impact)[107]. This method was later validated against the multidisciplinary team meeting achieving an almost perfect agreement [108]. Since then, few studies have been published, but they outlined a progressive increase in AI performances[109-113]. The AI predicted the recurrence risk after surgery by taking into account clinical, pathology, and laboratory data[110,112]. The addition of radiomic features into the machine learning models further optimized and anticipated the prediction[109,111]. Wei *et al*[113] compared a clinical, radiomic, and AI-based model to predict response to first-line chemotherapy; the deep-learning model had the best results, outperforming not only the model based on clinical parameters but also the one including texture analysis.

So far, the AI implementation into everyday practice is a priority to fill the quantum leap toward personalized computer-assisted medicine and will probably become a standard for clinical decision-making in the near future. It will allow merging all biomarkers, from morphological criteria to radiomics and genetic ones, weighing their prognostic role. Nevertheless, some current limitations of AI should be kept in mind. First, it needs training on large datasets, as Deep Blue did analyzing data from millions of chess matches[104]. Big data are crucial, but their availability is still limited by legal constraints and privacy policies. Shared databases and advanced interlinked frameworks could be the starting point. Second, AI supports decisions and does not replace clinical judgment yet, but computer-derived recommendations could lead to some legal and insurance critical issues. Finally, several technical and technological obstacles currently relegate AI-based approaches to highly specialized centers into a research setting.

CONCLUSION

To date, we are still far from a solid precision medicine for patients affected by colorectal liver metastases because of the limited capability of the available biomarkers to predict survival, response to chemotherapy, and the effectiveness of loco-regional therapies. Nevertheless, major (r)evolutions are ongoing, and the clinical approach to patients with metastatic colorectal cancer is going to change in the near future. The

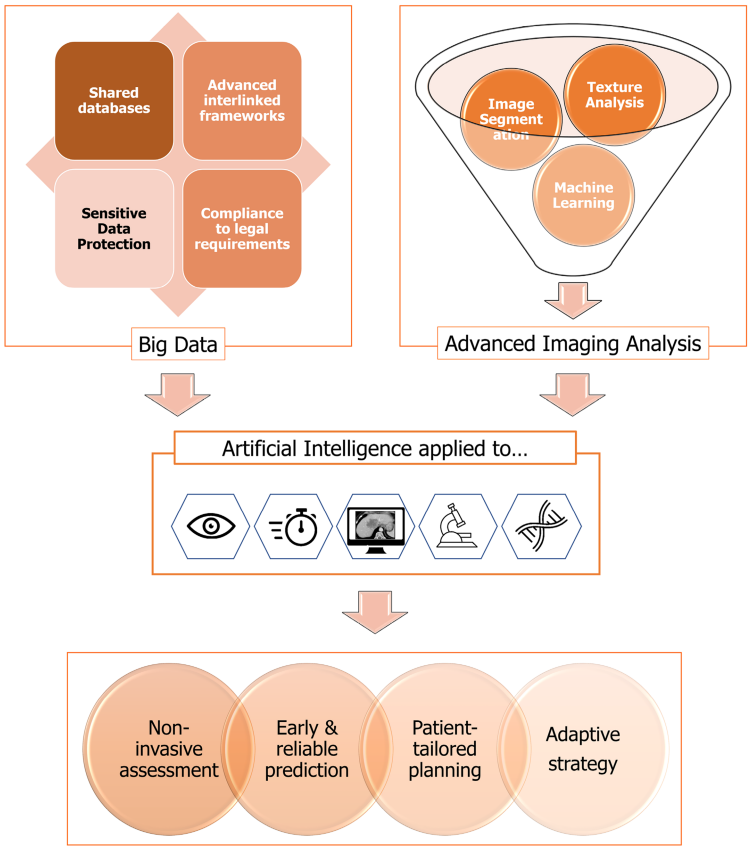

Figure 2 Future developments in the treatment planning for patients with colorectal liver metastases based on radiomics, big data, and artificial intelligence.

genetic analyses will definitively unveil the tumor biology, becoming the consistent basis of treatment planning; new biomarkers, based on radiomics and liver-tumor interface characteristics, will further enrich our comprehension and prediction of the tumor evolution; AI will merge and balance all data to drive decision-making processes.

REFERENCES

1 **Van Cutsem E**, Cervantes A, Adam R, Sobrero A, Van Krieken JH, Aderka D, Aranda Aguilar E, Bardelli A, Benson A, Bodoky G, Ciardiello F, D'Hoore A, Diaz-Rubio E, Douillard JY, Ducreux M, Falcone A, Grothey A, Gruenberger T, Haustermans K, Heinemann V, Hoff P, Köhne CH, Labianca R, Laurent-Puig P, Ma B, Maughan T, Muro K, Normanno N, Österlund P, Oyen WJ, Papamichael D, Pentheroudakis G, Pfeiffer P, Price TJ, Punt C, Ricke J, Roth A, Salazar R, Scheithauer W, Schmoll HJ, Tabernero J, Taïeb J, Tejpar S, Wasan H, Yoshino T, Zaanan A, Arnold D. ESMO consensus guidelines for the management of patients with metastatic colorectal cancer. *Ann Oncol* 2016; **27**: 1386-1422 [PMID: 27380959 DOI: 10.1093/annonc/mdw235]

2 **Tomasello G**, Petrelli F, Ghidini M, Russo A, Passalacqua R, Barni S. FOLFOXIRI Plus Bevacizumab as Conversion Therapy for Patients With Initially Unresectable Metastatic Colorectal Cancer: A Systematic Review and Pooled Analysis. *JAMA Oncol* 2017; **3**: e170278 [PMID: 28542671 DOI: 10.1001/jamaoncol.2017.0278]

3 **Petrelli F**, Barni S; Anti-EGFR agents for liver metastases. Resectability and outcome with anti-EGFR agents in patients with KRAS wild-type colorectal liver-limited metastases: a meta-analysis. *Int J Colorectal Dis* 2012; **27**: 997-1004 [PMID: 22358385 DOI: 10.1007/s00384-012-1438-2]

4 **Viganò L**, Ferrero A, Lo Tesoriere R, Capussotti L. Liver surgery for colorectal metastases: results after 10 years of follow-up. Long-term survivors, late recurrences, and prognostic role of morbidity. *Ann Surg Oncol* 2008; **15**: 2458-2464 [PMID: 18463927 DOI: 10.1245/s10434-008-9935-9]

5 **Creasy JM**, Sadot E, Koerkamp BG, Chou JF, Gonen M, Kemeny NE, Balachandran VP, Kingham TP, DeMatteo RP, Allen PJ, Blumgart LH, Jarnagin WR, D'Angelica MI. Actual 10-year survival after hepatic resection of colorectal liver metastases: what factors preclude cure? *Surgery* 2018; **163**: 1238-1244 [PMID: 29455841 DOI: 10.1016/j.surg.2018.01.004]

6 **Torzilli G**, Viganò L, Gatti A, Costa G, Cimino M, Procopio F, Donadon M, Del Fabbro D. Twelve-

year experience of "radical but conservative" liver surgery for colorectal metastases: impact on surgical practice and oncologic efficacy. *HPB (Oxford)* 2017; **19**: 775-784 [PMID: 28625391 DOI: 10.1016/j.hpb.2017.05.006]

7 **Adam R**, De Gramont A, Figueras J, Guthrie A, Kokudo N, Kunstlinger F, Loyer E, Poston G, Rougier P, Rubbia-Brandt L, Sobrero A, Tabernero J, Teh C, Van Cutsem E; Jean-Nicolas Vauthey of the EGOSLIM (Expert Group on OncoSurgery management of LIver Metastases) group. The oncosurgery approach to managing liver metastases from colorectal cancer: a multidisciplinary international consensus. *Oncologist* 2012; **17**: 1225-1239 [PMID: 22962059 DOI: 10.1634/theoncologist.2012-0121]

8 **Torzilli G**, Adam R, Viganò L, Imai K, Goransky J, Fontana A, Toso C, Majno P, de Santibañes E. Surgery of Colorectal Liver Metastases: Pushing the Limits. *Liver Cancer* 2016; **6**: 80-89 [PMID: 27995092 DOI: 10.1159/000449495]

9 **Line PD**, Ruffolo LI, Toso C, Dueland S, Nadalin S, Hernandez-Alejandro R. Liver transplantation for colorectal liver metastases: What do we need to know? *Int J Surg* 2020; **82S**: 87-92 [PMID: 32305529 DOI: 10.1016/j.ijsu.2020.03.079]

10 **Viganò L**, Gentile D, Galvanin J, Corleone P, Costa G, Cimino M, Procopio F, Torzilli G. Very Early Recurrence After Liver Resection for Colorectal Metastases: Incidence, Risk Factors, and Prognostic Impact. *J Gastrointest Surg* 2021 [PMID: 34508293 DOI: 10.1007/s11605-021-05123-w]

11 **Gillams A**, Goldberg N, Ahmed M, Bale R, Breen D, Callstrom M, Chen MH, Choi BI, de Baere T, Dupuy D, Gangi A, Gervais D, Helmberger T, Jung EM, Lee F, Lencioni R, Liang P, Livraghi T, Lu D, Meloni F, Pereira P, Piscaglia F, Rhim H, Salem R, Sofocleous C, Solomon SB, Soulen M, Tanaka M, Vogl T, Wood B, Solbiati L. Thermal ablation of colorectal liver metastases: a position paper by an international panel of ablation experts, The Interventional Oncology Sans Frontières meeting 2013. *Eur Radiol* 2015; **25**: 3438-3454 [PMID: 25994193 DOI: 10.1007/s00330-015-3779-z]

12 **Solbiati L**, Ahmed M, Cova L, Ierace T, Brioschi M, Goldberg SN. Small liver colorectal metastases treated with percutaneous radiofrequency ablation: local response rate and long-term survival with up to 10-year follow-up. *Radiology* 2012; **265**: 958-968 [PMID: 23091175 DOI: 10.1148/radiol.12111851]

13 **Gurusamy K**, Corrigan N, Croft J, Twiddy M, Morris S, Woodward N, Bandula S, Hochhauser D, Napp V, Pullan A, Jakowiw N, Prasad R, Damink SO, van Laarhoven CJHM, de Wilt JHW, Brown J, Davidson BR. Liver resection surgery versus thermal ablation for colorectal LiVer MetAstases (LAVA): study protocol for a randomised controlled trial. *Trials* 2018; **19**: 105 [PMID: 29439711 DOI: 10.1186/s13063-018-2499-5]

14 **Puijk RS**, Ruarus AH, Vroomen LGPH, van Tilborg AAJM, Scheffer HJ, Nielsen K, de Jong MC, de Vries JJJ, Zonderhuis BM, Eker HH, Kazemier G, Verheul H, van der Meijs BB, van Dam L, Sorgedrager N, Coupé VMH, van den Tol PMP, Meijerink MR; COLLISION Trial Group. Colorectal liver metastases: surgery versus thermal ablation (COLLISION) - a phase III single-blind prospective randomized controlled trial. *BMC Cancer* 2018; **18**: 821 [PMID: 30111304 DOI: 10.1186/s12885-018-4716-8]

15 **Ignatavicius P**, Oberkofler CE, Chapman WC, DeMatteo RP, Clary BM, D'Angelica MI, Tanabe KK, Hong JC, Aloia TA, Pawlik TM, Hernandez-Alejandro R, Shah SA, Vauthey JN, Torzilli G, Lang H, Line PD, Soubrane O, Pinto-Marques H, Robles-Campos R, Boudjema K, Lodge P, Adam R, Toso C, Serrablo A, Aldrighetti L, DeOliveira ML, Dutkowski P, Petrowsky H, Linecker M, Reiner CS, Braun J, Alikhanov R, Barauskas G, Chan ACY, Dong J, Kokudo N, Yamamoto M, Kang KJ, Fong Y, Rela M, De Aretxabala X, De Santibañes E, Mercado MÁ, Andriani OC, Torres OJM, Pinna AD, Clavien PA. Choices of Therapeutic Strategies for Colorectal Liver Metastases Among Expert Liver Surgeons: A Throw of the Dice? *Ann Surg* 2020; **272**: 715-722 [PMID: 32833764 DOI: 10.1097/SLA.0000000000004331]

16 **Viganò L**. Treatment strategy for colorectal cancer with resectable synchronous liver metastases: Is any evidence-based strategy possible? *World J Hepatol* 2012; **4**: 237-241 [PMID: 22993665 DOI: 10.4254/wjh.v4.i8.237]

17 **Crocetti L**, de Baére T, Pereira PL, Tarantino FP. CIRSE Standards of Practice on Thermal Ablation of Liver Tumours. *Cardiovasc Intervent Radiol* 2020; **43**: 951-962 [PMID: 32382856 DOI: 10.1007/s00270-020-02471-z]

18 **Nordlinger B**, Guiguet M, Vaillant JC, Balladur P, Boudjema K, Bachellier P, Jaeck D. Surgical resection of colorectal carcinoma metastases to the liver. A prognostic scoring system to improve case selection, based on 1568 patients. Association Française de Chirurgie. *Cancer* 1996; **77**: 1254-1262 [PMID: 8608500]

19 **Fong Y**, Fortner J, Sun RL, Brennan MF, Blumgart LH. Clinical score for predicting recurrence after hepatic resection for metastatic colorectal cancer: analysis of 1001 consecutive cases. *Ann Surg* 1999; **230**: 309-18; discussion 318 [PMID: 10493478 DOI: 10.1097/00000658-199909000-00004]

20 **Iwatsuki S**, Dvorchik I, Madariaga JR, Marsh JW, Dodson F, Bonham AC, Geller DA, Gayowski TJ, Fung JJ, Starzl TE. Hepatic resection for metastatic colorectal adenocarcinoma: a proposal of a prognostic scoring system. *J Am Coll Surg* 1999; **189**: 291-299 [PMID: 10472930 DOI: 10.1016/s1072-7515(99)00089-7]

21 **Rees M**, Tekkis PP, Welsh FK, O'Rourke T, John TG. Evaluation of long-term survival after hepatic resection for metastatic colorectal cancer: a multifactorial model of 929 patients. *Ann Surg* 2008; **247**: 125-135 [PMID: 18156932 DOI: 10.1097/SLA.0b013e31815aa2c2]

22 **Nagashima I**, Takada T, Matsuda K, Adachi M, Nagawa H, Muto T, Okinaga K. A new scoring system to classify patients with colorectal liver metastases: proposal of criteria to select candidates for hepatic resection. *J Hepatobiliary Pancreat Surg* 2004; **11**: 79-83 [PMID: 15127268 DOI: 10.1007/s00534-002-0778-7]

23 **Konopke R**, Kersting S, Distler M, Dietrich J, Gastmeier J, Heller A, Kulisch E, Saeger HD. Prognostic factors and evaluation of a clinical score for predicting survival after resection of colorectal liver metastases. *Liver Int* 2009; **29**: 89-102 [PMID: 18673436 DOI: 10.1111/j.1478-3231.2008.01845.x]

24 **Sasaki K**, Morioka D, Conci S, Margonis GA, Sawada Y, Ruzzenente A, Kumamoto T, Iacono C, Andreatos N, Guglielmi A, Endo I, Pawlik TM. The Tumor Burden Score: A New "Metro-ticket" Prognostic Tool For Colorectal Liver Metastases Based on Tumor Size and Number of Tumors. *Ann Surg* 2018; **267**: 132-141 [PMID: 27763897 DOI: 10.1097/SLA.0000000000002064]

25 **Mazzaferro V**, Llovet JM, Miceli R, Bhoori S, Schiavo M, Mariani L, Camerini T, Roayaie S, Schwartz ME, Grazi GL, Adam R, Neuhaus P, Salizzoni M, Bruix J, Forner A, De Carlis L, Cillo U, Burroughs AK, Troisi R, Rossi M, Gerunda GE, Lerut J, Belghiti J, Boin I, Gugenheim J, Rochling F, Van Hoek B, Majno P; Metroticket Investigator Study Group. Predicting survival after liver transplantation in patients with hepatocellular carcinoma beyond the Milan criteria: a retrospective, exploratory analysis. *Lancet Oncol* 2009; **10**: 35-43 [PMID: 19058754 DOI: 10.1016/S1470-2045(08)70284-5]

26 **Loupakis F**, Yang D, Yau L, Feng S, Cremolini C, Zhang W, Maus MK, Antoniotti C, Langer C, Scherer SJ, Müller T, Hurwitz HI, Saltz L, Falcone A, Lenz HJ. Primary tumor location as a prognostic factor in metastatic colorectal cancer. *J Natl Cancer Inst* 2015; 107 [PMID: 25713148 DOI: 10.1093/jnci/dju427]

27 **Moretto R**, Cremolini C, Rossini D, Pietrantonio F, Battaglin F, Mennitto A, Bergamo F, Loupakis F, Marmorino F, Berenato R, Marsico VA, Caporale M, Antoniotti C, Masi G, Salvatore L, Borelli B, Fontanini G, Lonardi S, De Braud F, Falcone A. Location of Primary Tumor and Benefit From Anti-Epidermal Growth Factor Receptor Monoclonal Antibodies in Patients With RAS and BRAF Wild-Type Metastatic Colorectal Cancer. *Oncologist* 2016; **21**: 988-994 [PMID: 27382031 DOI: 10.1634/theoncologist.2016-0084]

28 **Sagawa T**, Sato Y, Hirakawa M, Hamaguchi K, Fukuya A, Okamoto K, Miyamoto H, Muguruma N, Fujikawa K, Takahashi Y, Takayama T. Clinical impact of primary tumour location, early tumour shrinkage, and depth of response in the treatment of metastatic colorectal cancer with first-line chemotherapy plus cetuximab or bevacizumab. *Sci Rep* 2020; **10**: 19815 [PMID: 33188279 DOI: 10.1038/s41598-020-76756-1]

29 **Zhou F**, Yu X, Liang P, Han Z, Cheng Z, Yu J, Liu F, Hu Y. Does primary tumor location impact the prognosis of colorectal liver metastases patients after microwave ablation? *Oncotarget* 2017; **8**: 100791-100800 [PMID: 29246023 DOI: 10.18632/oncotarget.18764]

30 **Giuliante F**, Viganò L, De Rose AM, Mirza DF, Lapointe R, Kaiser G, Barroso E, Ferrero A, Isoniemi H, Lopez-Ben S, Popescu I, Ouellet JF, Hubert C, Regimbeau JM, Lin JK, Skipenko OG, Ardito F, Adam R. Liver-First Approach for Synchronous Colorectal Metastases: Analysis of 7360 Patients from the LiverMetSurvey Registry. *Ann Surg Oncol* 2021; **28**: 8198-8208 [PMID: 34212254 DOI: 10.1245/s10434-021-10220-w]

31 **Andres A**, Mentha G, Adam R, Gerstel E, Skipenko OG, Barroso E, Lopez-Ben S, Hubert C, Majno PE, Toso C. Surgical management of patients with colorectal cancer and simultaneous liver and lung metastases. *Br J Surg* 2015; **102**: 691-699 [PMID: 25789941 DOI: 10.1002/bjs.9783]

32 **Vigano L**, Corleone P, Darwish SS, Turri N, Famularo S, Viggiani L, Rimassa L, Del Fabbro D, Di Tommaso L, Torzilli G. Hepatic and Extrahepatic Colorectal Metastases Have Discordant Responses to Systemic Therapy. Pathology Data from Patients Undergoing Simultaneous Resection of Multiple Tumor Sites. *Cancers (Basel)* 2021; **13** [PMID: 33530435 DOI: 10.3390/cancers13030464]

33 **Viganò L**, Capussotti L, Majno P, Toso C, Ferrero A, De Rosa G, Rubbia-Brandt L, Mentha G. Liver resection in patients with eight or more colorectal liver metastases. *Br J Surg* 2015; **102**: 92-101 [PMID: 25451181 DOI: 10.1002/bjs.9680]

34 **Allard MA**, Adam R, Giuliante F, Lapointe R, Hubert C, Ijzermans JNM, Mirza DF, Elias D, Laurent C, Gruenberger T, Poston G, Letoublon C, Isoniemi H, Lucidi V, Popescu I, Figueras J. Long-term outcomes of patients with 10 or more colorectal liver metastases. *Br J Cancer* 2017; **117**: 604-611 [PMID: 28728167 DOI: 10.1038/bjc.2017.218]

35 **Vigano L**, Di Tommaso L, Mimmo A, Sollai M, Cimino M, Donadon M, Roncalli M, Torzilli G. Prospective Evaluation of Intrahepatic Microscopic Occult Tumor Foci in Patients with Numerous Colorectal Liver Metastases. *Dig Surg* 2019; **36**: 340-347 [PMID: 29879717 DOI: 10.1159/000489274]

36 **Elias D**, Viganò L, Orsi F, Scorsetti M, Comito T, Lerut J, Cosola D, Torzilli G. New Perspectives in the Treatment of Colorectal Metastases. *Liver Cancer* 2016; **6**: 90-98 [PMID: 27995093 DOI: 10.1159/000449492]

37 **Hasselgren K**, Isaksson B, Ardnor B, Lindell G, Rizell M, Strömberg C, Loftås P, Björnsson B, Sandström P. Liver resection is beneficial for patients with colorectal liver metastases and extrahepatic disease. *Ann Transl Med* 2020; **8**: 109 [PMID: 32175402 DOI: 10.21037/atm.2019.12.125]

38 **Adam R**, de Haas RJ, Wicherts DA, Aloia TA, Delvart V, Azoulay D, Bismuth H, Castaing D. Is hepatic resection justified after chemotherapy in patients with colorectal liver metastases and lymph

node involvement? *J Clin Oncol* 2008; **26**: 3672-3680 [PMID: 18669451 DOI: 10.1200/JCO.2007.15.7297]

39 **Shimizu Y**, Yasui K, Sano T, Hirai T, Kanemitsu Y, Komori K, Kato T. Validity of observation interval for synchronous hepatic metastases of colorectal cancer: changes in hepatic and extrahepatic metastatic foci. *Langenbecks Arch Surg* 2008; **393**: 181-184 [PMID: 18175143 DOI: 10.1007/s00423-007-0258-2]

40 **Lambert LA**, Colacchio TA, Barth RJ Jr. Interval hepatic resection of colorectal metastases improves patient selection. *Arch Surg* 2000; **135**: 473-9; discussion 479 [PMID: 10768715 DOI: 10.1001/archsurg.135.4.473]

41 **Yoshidome H**, Kimura F, Shimizu H, Ohtsuka M, Kato A, Yoshitomi H, Furukawa K, Mitsuhashi N, Takeuchi D, Iida A, Miyazaki M. Interval period tumor progression: does delayed hepatectomy detect occult metastases in synchronous colorectal liver metastases? *J Gastrointest Surg* 2008; **12**: 1391-1398 [PMID: 18491195 DOI: 10.1007/s11605-008-0540-9]

42 **Adam R**, Pascal G, Castaing D, Azoulay D, Delvart V, Paule B, Levi F, Bismuth H. Tumor progression while on chemotherapy: a contraindication to liver resection for multiple colorectal metastases? *Ann Surg* 2004; **240**: 1052-61; discussion 1061 [PMID: 15570210 DOI: 10.1097/01.sla.0000145964.08365.01]

43 **Nordlinger B**, Sorbye H, Glimelius B, Poston GJ, Schlag PM, Rougier P, Bechstein WO, Primrose JN, Walpole ET, Finch-Jones M, Jaeck D, Mirza D, Parks RW, Collette L, Praet M, Bethe U, Van Cutsem E, Scheithauer W, Gruenberger T; EORTC Gastro-Intestinal Tract Cancer Group; Cancer Research UK; Arbeitsgruppe Lebermetastasen und-tumoren in der Chirurgischen Arbeitsgemeinschaft Onkologie (ALM-CAO); Australasian Gastro-Intestinal Trials Group (AGITG); Fédération Francophone de Cancérologie Digestive (FFCD). Perioperative chemotherapy with FOLFOX4 and surgery versus surgery alone for resectable liver metastases from colorectal cancer (EORTC Intergroup trial 40983): a randomised controlled trial. *Lancet* 2008; **371**: 1007-1016 [PMID: 18358928 DOI: 10.1016/S0140-6736(08)60455-9]

44 **Viganò L**, Capussotti L, De Rosa G, De Saussure WO, Mentha G, Rubbia-Brandt L. Liver resection for colorectal metastases after chemotherapy: impact of chemotherapy-related liver injuries, pathological tumor response, and micrometastases on long-term survival. *Ann Surg* 2013; **258**: 731-40; discussion 741 [PMID: 24045448 DOI: 10.1097/SLA.0b013e3182a6183e]

45 **Brouquet A**, Blot C, Allard MA, Lazure T, Sebbagh M, Gayet M, Lewin M, Adam R, Penna C, Sa Cunha A, Benoist S. What is the Prognostic Value of a Discordant Radiologic and Pathologic Response in Patients Undergoing Resection of Colorectal Liver Metastases After Preoperative Chemotherapy? *Ann Surg Oncol* 2020; **27**: 2877-2885 [PMID: 32144619 DOI: 10.1245/s10434-020-08284-1]

46 **Vigano L**, Sollini M, Ieva F, Fiz F, Torzilli G. Chemotherapy-Associated Liver Injuries: Unmet Needs and New Insights for Surgical Oncologists. *Ann Surg Oncol* 2021; **28**: 4074-4079 [PMID: 33929618 DOI: 10.1245/s10434-021-10069-z]

47 **Vigano L**, De Rosa G, Toso C, Andres A, Ferrero A, Roth A, Sperti E, Majno P, Rubbia-Brandt L. Reversibility of chemotherapy-related liver injury. *J Hepatol* 2017; **67**: 84-91 [PMID: 28284915 DOI: 10.1016/j.jhep.2017.02.031]

48 **Vigano L**, Darwish SS, Rimassa L, Cimino M, Carnaghi C, Donadon M, Procopio F, Personeni N, Del Fabbro D, Santoro A, Torzilli G. Progression of Colorectal Liver Metastases from the End of Chemotherapy to Resection: A New Contraindication to Surgery? *Ann Surg Oncol* 2018; **25**: 1676-1685 [PMID: 29488188 DOI: 10.1245/s10434-018-6387-8]

49 **Livraghi T**, Solbiati L, Meloni F, Ierace T, Goldberg SN, Gazelle GS. Percutaneous radiofrequency ablation of liver metastases in potential candidates for resection: the "test-of-time approach". *Cancer* 2003; **97**: 3027-3035 [PMID: 12784338 DOI: 10.1002/cncr.11426]

50 **Viganò L**, Galvanin J, Poretti D, Del Fabbro D, Gentile D, Pedicini V, Solbiati L, Torzilli G. Percutaneous ablation of post-surgical solitary early recurrence of colorectal liver metastases is an effective "test-of-time" approach. *Updates Surg* 2021; **73**: 1349-1358 [PMID: 33844146 DOI: 10.1007/s13304-021-01047-x]

51 **Viganò L**, Torzilli G, Cimino M, Imai K, Vibert E, Donadon M, Castaing D, Adam R. Drop-out between the two liver resections of two-stage hepatectomy. Patient selection or loss of chance? *Eur J Surg Oncol* 2016; **42**: 1385-1393 [PMID: 27316601 DOI: 10.1016/j.ejso.2016.03.020]

52 **Viganò L**, Capussotti L, Barroso E, Nuzzo G, Laurent C, Ijzermans JN, Gigot JF, Figueras J, Gruenberger T, Mirza DF, Elias D, Poston G, Letoublon C, Isoniemi H, Herrera J, Sousa FC, Pardo F, Lucidi V, Popescu I, Adam R. Progression while receiving preoperative chemotherapy should not be an absolute contraindication to liver resection for colorectal metastases. *Ann Surg Oncol* 2012; **19**: 2786-2796 [PMID: 22622469 DOI: 10.1245/s10434-012-2382-7]

53 **Brouquet A**, Overman MJ, Kopetz S, Maru DM, Loyer EM, Andreou A, Cooper A, Curley SA, Garrett CR, Abdalla EK, Vauthey JN. Is resection of colorectal liver metastases after a second-line chemotherapy regimen justified? *Cancer* 2011; **117**: 4484-4492 [PMID: 21446046 DOI: 10.1002/cncr.26036]

54 **Adam R**, Yi B, Innominato PF, Barroso E, Laurent C, Giuliante F, Capussotti L, Lapointe R, Regimbeau JM, Lopez-Ben S, Isoniemi H, Hubert C, Lin JK, Gruenberger T, Elias D, Skipenko OG, Guglielmi A; LiverMetSurvey International Contributing Centers. Resection of colorectal liver metastases after second-line chemotherapy: is it worthwhile? *Eur J Cancer* 2017; **78**: 7-15 [PMID: 28407529 DOI: 10.1016/j.ejca.2017.03.009]

55 **Ishaque N**, Abba ML, Hauser C, Patil N, Paramasivam N, Huebschmann D, Leupold JH, Balasubramanian GP, Kleinheinz K, Toprak UH, Hutter B, Benner A, Shavinskaya A, Zhou C, Gu Z, Kerssemakers J, Marx A, Moniuszko M, Kozlowski M, Reszec J, Niklinski J, Eils J, Schlesner M, Eils R, Brors B, Allgayer H. Whole genome sequencing puts forward hypotheses on metastasis evolution and therapy in colorectal cancer. *Nat Commun* 2018; **9**: 4782 [PMID: 30429477 DOI: 10.1038/s41467-018-07041-z]

56 **Cancer Genome Atlas Network**. Comprehensive molecular characterization of human colon and rectal cancer. *Nature* 2012; **487**: 330-337 [PMID: 22810696 DOI: 10.1038/nature11252]

57 **Tosi F**, Magni E, Amatu A, Mauri G, Bencardino K, Truini M, Veronese S, De Carlis L, Ferrari G, Nichelatti M, Sartore-Bianchi A, Siena S. Effect of KRAS and BRAF Mutations on Survival of Metastatic Colorectal Cancer After Liver Resection: A Systematic Review and Meta-Analysis. *Clin Colorectal Cancer* 2017; **16**: e153-e163 [PMID: 28216246 DOI: 10.1016/j.clcc.2017.01.004]

58 **Tsilimigras DI**, Ntanasis-Stathopoulos I, Bagante F, Moris D, Cloyd J, Spartalis E, Pawlik TM. Clinical significance and prognostic relevance of KRAS, BRAF, PI3K and TP53 genetic mutation analysis for resectable and unresectable colorectal liver metastases: A systematic review of the current evidence. *Surg Oncol* 2018; **27**: 280-288 [PMID: 29937183 DOI: 10.1016/j.suronc.2018.05.012]

59 **Vauthey JN**, Zimmitti G, Kopetz SE, Shindoh J, Chen SS, Andreou A, Curley SA, Aloia TA, Maru DM. RAS mutation status predicts survival and patterns of recurrence in patients undergoing hepatectomy for colorectal liver metastases. *Ann Surg* 2013; **258**: 619-26; discussion 626 [PMID: 24018645 DOI: 10.1097/SLA.0b013e3182a5025a]

60 **Brudvik KW**, Jones RP, Giuliante F, Shindoh J, Passot G, Chung MH, Song J, Li L, Dagenborg VJ, Fretland ÅA, Røsok B, De Rose AM, Ardito F, Edwin B, Panettieri E, Larocca LM, Yamashita S, Conrad C, Aloia TA, Poston GJ, Bjørnbeth BA, Vauthey JN. RAS Mutation Clinical Risk Score to Predict Survival After Resection of Colorectal Liver Metastases. *Ann Surg* 2019; **269**: 120-126 [PMID: 28549012 DOI: 10.1097/SLA.0000000000002319]

61 **Margonis GA**, Sasaki K, Gholami S, Kim Y, Andreatos N, Rezaee N, Deshwar A, Buettner S, Allen PJ, Kingham TP, Pawlik TM, He J, Cameron JL, Jarnagin WR, Wolfgang CL, D'Angelica MI, Weiss MJ. Genetic And Morphological Evaluation (GAME) score for patients with colorectal liver metastases. *Br J Surg* 2018; **105**: 1210-1220 [PMID: 29691844 DOI: 10.1002/bjs.10838]

62 **Yokota T**, Ura T, Shibata N, Takahari D, Shitara K, Nomura M, Kondo C, Mizota A, Utsunomiya S, Muro K, Yatabe Y. BRAF mutation is a powerful prognostic factor in advanced and recurrent colorectal cancer. *Br J Cancer* 2011; **104**: 856-862 [PMID: 21285991 DOI: 10.1038/bjc.2011.19]

63 **Bachet JB**, Moreno-Lopez N, Vigano L, Marchese U, Gelli M, Raoux L, Truant S, Laurent C, Herrero A, Le Roy B, Deguelte Lardiere S, Passot G, Hautefeuille V, De La Fouchardiere C, Artru P, Ameto T, Mabrut JY, Schwarz L, Rousseau B, Lepère C, Coriat R, Brouquet A, Sa Cunha A, Benoist S. BRAF mutation is not associated with an increased risk of recurrence in patients undergoing resection of colorectal liver metastases. *Br J Surg* 2019; **106**: 1237-1247 [PMID: 31183866 DOI: 10.1002/bjs.11180]

64 **Margonis GA**, Buettner S, Andreatos N, Kim Y, Wagner D, Sasaki K, Beer A, Schwarz C, Løes IM, Smolle M, Kamphues C, He J, Pawlik TM, Kaczirek K, Poultsides G, Lønning PE, Cameron JL, Burkhart RA, Gerger A, Aucejo FN, Kreis ME, Wolfgang CL, Weiss MJ. Association of BRAF Mutations With Survival and Recurrence in Surgically Treated Patients With Metastatic Colorectal Liver Cancer. *JAMA Surg* 2018; **153**: e180996 [PMID: 29799910 DOI: 10.1001/jamasurg.2018.0996]

65 **Lang H**, Baumgart J, Heinrich S, Tripke V, Passalaqua M, Maderer A, Galle PR, Roth W, Kloth M, Moehler M. Extended Molecular Profiling Improves Stratification and Prediction of Survival After Resection of Colorectal Liver Metastases. *Ann Surg* 2019; **270**: 799-805 [PMID: 31634180 DOI: 10.1097/SLA.0000000000003527]

66 **Kawaguchi Y**, Kopetz S, Newhook TE, De Bellis M, Chun YS, Tzeng CD, Aloia TA, Vauthey JN. Mutation Status of *RAS, TP53*, and *SMAD4* is Superior to Mutation Status of *RAS* Alone for Predicting Prognosis after Resection of Colorectal Liver Metastases. *Clin Cancer Res* 2019; **25**: 5843-5851 [PMID: 31221662 DOI: 10.1158/1078-0432.CCR-19-0863]

67 **Wakai T**, Shirai Y, Sakata J, Kameyama H, Nogami H, Iiai T, Ajioka Y, Hatakeyama K. Histologic evaluation of intrahepatic micrometastases in patients treated with or without neoadjuvant chemotherapy for colorectal carcinoma liver metastasis. *Int J Clin Exp Pathol* 2012; **5**: 308-314 [PMID: 22670174]

68 **Kokudo N**, Miki Y, Sugai S, Yanagisawa A, Kato Y, Sakamoto Y, Yamamoto J, Yamaguchi T, Muto T, Makuuchi M. Genetic and histological assessment of surgical margins in resected liver metastases from colorectal carcinoma: minimum surgical margins for successful resection. *Arch Surg* 2002; **137**: 833-840 [PMID: 12093342 DOI: 10.1001/archsurg.137.7.833]

69 **Mentha G**, Terraz S, Morel P, Andres A, Giostra E, Roth A, Rubbia-Brandt L, Majno P. Dangerous halo after neoadjuvant chemotherapy and two-step hepatectomy for colorectal liver metastases. *Br J Surg* 2009; **96**: 95-103 [PMID: 19109800 DOI: 10.1002/bjs.6436]

70 **van Dam PJ**, van der Stok EP, Teuwen LA, Van den Eynden GG, Illemann M, Frentzas S, Majeed AW, Eefsen RL, Coebergh van den Braak RRJ, Lazaris A, Fernandez MC, Galjart B, Laerum OD, Rayes R, Grünhagen DJ, Van de Paer M, Sucaet Y, Mudhar HS, Schvimer M, Nyström H, Kockx M, Bird NC, Vidal-Vanaclocha F, Metrakos P, Simoneau E, Verhoef C, Dirix LY, Van Laere S, Gao ZH, Brodt P, Reynolds AR, Vermeulen PB. International consensus guidelines for scoring the

histopathological growth patterns of liver metastasis. *Br J Cancer* 2017; **117**: 1427-1441 [PMID: 28982110 DOI: 10.1038/bjc.2017.334]

71 **Vermeulen PB**, Colpaert C, Salgado R, Royers R, Hellemans H, Van Den Heuvel E, Goovaerts G, Dirix LY, Van Marck E. Liver metastases from colorectal adenocarcinomas grow in three patterns with different angiogenesis and desmoplasia. *J Pathol* 2001; **195**: 336-342 [PMID: 11673831 DOI: 10.1002/path.966]

72 **Eefsen RL**, Van den Eynden GG, Høyer-Hansen G, Brodt P, Laerum OD, Vermeulen PB, Christensen IJ, Wettergren A, Federspiel B, Willemoe GL, Vainer B, Osterlind K, Illemann M. Histopathological growth pattern, proteolysis and angiogenesis in chemonaive patients resected for multiple colorectal liver metastases. *J Oncol* 2012; **2012**: 907971 [PMID: 22919385 DOI: 10.1155/2012/907971]

73 **Fernández Moro C**, Bozóky B, Gerling M. Growth patterns of colorectal cancer liver metastases and their impact on prognosis: a systematic review. *BMJ Open Gastroenterol* 2018; **5**: e000217 [PMID: 30073092 DOI: 10.1136/bmjgast-2018-000217]

74 **Eefsen RL**, Vermeulen PB, Christensen IJ, Laerum OD, Mogensen MB, Rolff HC, Van den Eynden GG, Høyer-Hansen G, Osterlind K, Vainer B, Illemann M. Growth pattern of colorectal liver metastasis as a marker of recurrence risk. *Clin Exp Metastasis* 2015; **32**: 369-381 [PMID: 25822899 DOI: 10.1007/s10585-015-9715-4]

75 **Frentzas S**, Simoneau E, Bridgeman VL, Vermeulen PB, Foo S, Kostaras E, Nathan M, Wotherspoon A, Gao ZH, Shi Y, Van den Eynden G, Daley F, Peckitt C, Tan X, Salman A, Lazaris A, Gazinska P, Berg TJ, Eltahir Z, Ritsma L, Van Rheenen J, Khashper A, Brown G, Nystrom H, Sund M, Van Laere S, Loyer E, Dirix L, Cunningham D, Metrakos P, Reynolds AR. Vessel co-option mediates resistance to anti-angiogenic therapy in liver metastases. *Nat Med* 2016; **22**: 1294-1302 [PMID: 27748747 DOI: 10.1038/nm.4197]

76 **Mlecnik B**, Van den Eynde M, Bindea G, Church SE, Vasaturo A, Fredriksen T, Lafontaine L, Haicheur N, Marliot F, Debetancourt D, Pairet G, Jouret-Mourin A, Gigot JF, Hubert C, Danse E, Dragean C, Carrasco J, Humblet Y, Valge-Archer V, Berger A, Pagès F, Machiels JP, Galon J. Comprehensive Intrametastatic Immune Quantification and Major Impact of Immunoscore on Survival. *J Natl Cancer Inst* 2018; **110** [PMID: 28922789 DOI: 10.1093/jnci/djx123]

77 **Donadon M**, Torzilli G, Cortese N, Soldani C, Di Tommaso L, Franceschini B, Carriero R, Barbagallo M, Rigamonti A, Anselmo A, Colombo FS, Maggi G, Lleo A, Cibella J, Peano C, Kunderfranco P, Roncalli M, Mantovani A, Marchesi F. Macrophage morphology correlates with single-cell diversity and prognosis in colorectal liver metastasis. *J Exp Med* 2020; **217** [PMID: 32785653 DOI: 10.1084/jem.20191847]

78 **Zhao J**, Sawo P, Rensen SS, Rouflart MMJ, Winstanley A, Vreuls CPH, Verheij J, van Mierlo KMC, Lodewick TM, van Woerden V, van Tiel FH, van Dam RM, Dejong CHC, Olde Damink SWM. Impact of chemotherapy-associated liver injury on tumour regression grade and survival in patients with colorectal liver metastases. *HPB (Oxford)* 2018; **20**: 147-154 [PMID: 28969959 DOI: 10.1016/j.hpb.2017.08.030]

79 **Parkin E**, O'Reilly DA, Adam R, Kaiser GM, Laurent C, Elias D, Capussotti L, Renehan AG; LiverMetSurvey Centres. The effect of hepatic steatosis on survival following resection of colorectal liver metastases in patients without preoperative chemotherapy. *HPB (Oxford)* 2013; **15**: 463-472 [PMID: 23458109 DOI: 10.1111/hpb.12007]

80 **Aparicio T**, Ducreux M, Faroux R, Barbier E, Manfredi S, Lecomte T, Etienne PL, Bedenne L, Bennouna J, Phelip JM, François E, Michel P, Legoux JL, Gasmi M, Breysacher G, Rougier P, De Gramont A, Lepage C, Bouché O, Seitz JF; for FFCD investigators. Overweight is associated to a better prognosis in metastatic colorectal cancer: A pooled analysis of FFCD trials. *Eur J Cancer* 2018; **98**: 1-9 [PMID: 29807237 DOI: 10.1016/j.ejca.2018.03.031]

81 **Renfro LA**, Loupakis F, Adams RA, Seymour MT, Heinemann V, Schmoll HJ, Douillard JY, Hurwitz H, Fuchs CS, Diaz-Rubio E, Porschen R, Tournigand C, Chibaudel B, Falcone A, Tebbutt NC, Punt CJ, Hecht JR, Bokemeyer C, Van Cutsem E, Goldberg RM, Saltz LB, de Gramont A, Sargent DJ, Lenz HJ. Body Mass Index Is Prognostic in Metastatic Colorectal Cancer: Pooled Analysis of Patients From First-Line Clinical Trials in the ARCAD Database. *J Clin Oncol* 2016; **34**: 144-150 [PMID: 26503203 DOI: 10.1200/JCO.2015.61.6441]

82 **Lambin P**, Leijenaar RTH, Deist TM, Peerlings J, de Jong EEC, van Timmeren J, Sanduleanu S, Larue RTHM, Even AJG, Jochems A, van Wijk Y, Woodruff H, van Soest J, Lustberg T, Roelofs E, van Elmpt W, Dekker A, Mottaghy FM, Wildberger JE, Walsh S. Radiomics: the bridge between medical imaging and personalized medicine. *Nat Rev Clin Oncol* 2017; **14**: 749-762 [PMID: 28975929 DOI: 10.1038/nrclinonc.2017.141]

83 **Lambin P**, Rios-Velazquez E, Leijenaar R, Carvalho S, van Stiphout RG, Granton P, Zegers CM, Gillies R, Boellard R, Dekker A, Aerts HJ. Radiomics: extracting more information from medical images using advanced feature analysis. *Eur J Cancer* 2012; **48**: 441-446 [PMID: 22257792 DOI: 10.1016/j.ejca.2011.11.036]

84 **van Timmeren JE**, Cester D, Tanadini-Lang S, Alkadhi H, Baessler B. Radiomics in medical imaging-"how-to" guide and critical reflection. *Insights Imaging* 2020; **11**: 91 [PMID: 32785796 DOI: 10.1186/s13244-020-00887-2]

85 **Yip SS**, Aerts HJ. Applications and limitations of radiomics. *Phys Med Biol* 2016; **61**: R150-R166 [PMID: 27269645 DOI: 10.1088/0031-9155/61/13/R150]

86 **Fiz F**, Viganò L, Gennaro N, Costa G, La Bella L, Boichuk A, Cavinato L, Sollini M, Politi LS,

Chiti A, Torzilli G. Radiomics of Liver Metastases: A Systematic Review. *Cancers (Basel)* 2020; **12** [PMID: 33036490 DOI: 10.3390/cancers12102881]

87 **Nakanishi R**, Oki E, Hasuda H, Sano E, Miyashita Y, Sakai A, Koga N, Kuriyama N, Nonaka K, Fujimoto Y, Jogo T, Hokonohara K, Hu Q, Hisamatsu Y, Ando K, Kimura Y, Yoshizumi T, Mori M. Radiomics Texture Analysis for the Identification of Colorectal Liver Metastases Sensitive to First-Line Oxaliplatin-Based Chemotherapy. *Ann Surg Oncol* 2021; **28**: 2975-2985 [PMID: 33454878 DOI: 10.1245/s10434-020-09581-5]

88 **Lubner MG**, Stabo N, Lubner SJ, del Rio AM, Song C, Halberg RB, Pickhardt PJ. CT textural analysis of hepatic metastatic colorectal cancer: pre-treatment tumor heterogeneity correlates with pathology and clinical outcomes. *Abdom Imaging* 2015; **40**: 2331-2337 [PMID: 25968046 DOI: 10.1007/s00261-015-0438-4]

89 **Andersen IR**, Thorup K, Andersen MB, Olesen R, Mortensen FV, Nielsen DT, Rasmussen F. Texture in the monitoring of regorafenib therapy in patients with colorectal liver metastases. *Acta Radiol* 2019; **60**: 1084-1093 [PMID: 30612433 DOI: 10.1177/0284185118817940]

90 **Beckers RCJ**, Trebeschi S, Maas M, Schnerr RS, Sijmons JML, Beets GL, Houwers JB, Beets-Tan RGH, Lambregts DMJ. CT texture analysis in colorectal liver metastases and the surrounding liver parenchyma and its potential as an imaging biomarker of disease aggressiveness, response and survival. *Eur J Radiol* 2018; **102**: 15-21 [PMID: 29685529 DOI: 10.1016/j.ejrad.2018.02.031]

91 **Dercle L**, Lu L, Schwartz LH, Qian M, Tejpar S, Eggleton P, Zhao B, Piessevaux H. Radiomics Response Signature for Identification of Metastatic Colorectal Cancer Sensitive to Therapies Targeting EGFR Pathway. *J Natl Cancer Inst* 2020; **112**: 902-912 [PMID: 32016387 DOI: 10.1093/jnci/djaa017]

92 **Dohan A**, Gallix B, Guiu B, Le Malicot K, Reinhold C, Soyer P, Bennouna J, Ghiringhelli F, Barbier E, Boige V, Taieb J, Bouché O, François E, Phelip JM, Borel C, Faroux R, Seitz JF, Jacquot S, Ben Abdelghani M, Khemissa-Akouz F, Genet D, Jouve JL, Rinaldi Y, Desseigne F, Texereau P, Suc E, Lepage C, Aparicio T, Hoeffel C; PRODIGE 9 Investigators and PRODIGE 20 Investigators. Early evaluation using a radiomic signature of unresectable hepatic metastases to predict outcome in patients with colorectal cancer treated with FOLFIRI and bevacizumab. *Gut* 2020; **69**: 531-539 [PMID: 31101691 DOI: 10.1136/gutjnl-2018-316407]

93 **Rahmim A**, Bak-Fredslund KP, Ashrafinia S, Lu L, Schmidtlein CR, Subramaniam RM, Morsing A, Keiding S, Horsager J, Munk OL. Prognostic modeling for patients with colorectal liver metastases incorporating FDG PET radiomic features. *Eur J Radiol* 2019; **113**: 101-109 [PMID: 30927933 DOI: 10.1016/j.ejrad.2019.02.006]

94 **Ravanelli M**, Agazzi GM, Tononcelli E, Roca E, Cabassa P, Baiocchi G, Berruti A, Maroldi R, Farina D. Texture features of colorectal liver metastases on pretreatment contrast-enhanced CT may predict response and prognosis in patients treated with bevacizumab-containing chemotherapy: a pilot study including comparison with standard chemotherapy. *Radiol Med* 2019; **124**: 877-886 [PMID: 31172448 DOI: 10.1007/s11547-019-01046-4]

95 **Shur J**, Orton M, Connor A, Fischer S, Moulton CA, Gallinger S, Koh DM, Jhaveri KS. A clinical-radiomic model for improved prognostication of surgical candidates with colorectal liver metastases. *J Surg Oncol* 2019 [PMID: 31797378 DOI: 10.1002/jso.25783]

96 **van Helden EJ**, Vacher YJL, van Wieringen WN, van Velden FHP, Verheul HMW, Hoekstra OS, Boellaard R, Menke-van der Houven van Oordt CW. Radiomics analysis of pre-treatment [^{18}F]FDG PET/CT for patients with metastatic colorectal cancer undergoing palliative systemic treatment. *Eur J Nucl Med Mol Imaging* 2018; **45**: 2307-2317 [PMID: 30094460 DOI: 10.1007/s00259-018-4100-6]

97 **Taghavi M**, Staal F, Gomez Munoz F, Imani F, Meek DB, Simões R, Klompenhouwer LG, van der Heide UA, Beets-Tan RGH, Maas M. CT-Based Radiomics Analysis Before Thermal Ablation to Predict Local Tumor Progression for Colorectal Liver Metastases. *Cardiovasc Intervent Radiol* 2021; **44**: 913-920 [PMID: 33506278 DOI: 10.1007/s00270-020-02735-8]

98 **Cheng J**, Wei J, Tong T, Sheng W, Zhang Y, Han Y, Gu D, Hong N, Ye Y, Tian J, Wang Y. Prediction of Histopathologic Growth Patterns of Colorectal Liver Metastases with a Noninvasive Imaging Method. *Ann Surg Oncol* 2019; **26**: 4587-4598 [PMID: 31605342 DOI: 10.1245/s10434-019-07910-x]

99 **Rao SX**, Lambregts DM, Schnerr RS, Beckers RC, Maas M, Albarello F, Riedl RG, Dejong CH, Martens MH, Heijnen LA, Backes WH, Beets GL, Zeng MS, Beets-Tan RG. CT texture analysis in colorectal liver metastases: A better way than size and volume measurements to assess response to chemotherapy? *United European Gastroenterol J* 2016; **4**: 257-263 [PMID: 27087955 DOI: 10.1177/2050640615601603]

100 **Costa G**, Cavinato L, Masci C, Fiz F, Sollini M, Politi LS, Chiti A, Balzarini L, Aghemo A, di Tommaso L, Ieva F, Torzilli G, Viganò L. Virtual Biopsy for Diagnosis of Chemotherapy-Associated Liver Injuries and Steatohepatitis: A Combined Radiomic and Clinical Model in Patients with Colorectal Liver Metastases. *Cancers (Basel)* 2021; **13** [PMID: 34203103 DOI: 10.3390/cancers13123077]

101 **Kulkarni S**, Seneviratne N, Baig MS, Khan AHA. Artificial Intelligence in Medicine: Where Are We Now? *Acad Radiol* 2020; **27**: 62-70 [PMID: 31636002 DOI: 10.1016/j.acra.2019.10.001]

102 **Wang P**. On Defining Artificial Intelligence. *JAGI* 2019; **10**: 1-37 [DOI: 10.2478/jagi-2019-0002]

103 **Haenlein M**, Kaplan A. A Brief History of Artificial Intelligence: On the Past, Present, and Future of Artificial Intelligence. *Calif Manage Rev* 2019; **61**: 5-14 [DOI: 10.1177/0008125619864925]

104 **Hassabis D**. Artificial Intelligence: Chess match of the century. *Nature* 2017; **544**: 413-414 [DOI: 10.1038/544413a]

105 **Erickson BJ**, Korfiatis P, Akkus Z, Kline TL. Machine Learning for Medical Imaging. *Radiographics* 2017; **37**: 505-515 [PMID: 28212054 DOI: 10.1148/rg.2017160130]

106 **Waldstein SM**, Seeböck P, Donner R, Sadeghipour A, Bogunović H, Osborne A, Schmidt-Erfurth U. Unbiased identification of novel subclinical imaging biomarkers using unsupervised deep learning. *Sci Rep* 2020; **10**: 12954 [PMID: 32737379 DOI: 10.1038/s41598-020-69814-1]

107 **Poston GJ**, Adam R, Alberts S, Curley S, Figueras J, Haller D, Kunstlinger F, Mentha G, Nordlinger B, Patt Y, Primrose J, Roh M, Rougier P, Ruers T, Schmoll HJ, Valls C, Vauthey NJ, Cornelis M, Kahan JP. OncoSurge: a strategy for improving resectability with curative intent in metastatic colorectal cancer. *J Clin Oncol* 2005; **23**: 7125-7134 [PMID: 16192596 DOI: 10.1200/JCO.2005.08.722]

108 **O'Reilly DA**, Chaudhari M, Ballal M, Ghaneh P, Wu A, Poston GJ. The Oncosurge strategy for the management of colorectal liver metastases - an external validation study. *Eur J Surg Oncol* 2008; **34**: 538-540 [PMID: 17560066 DOI: 10.1016/j.ejso.2007.04.013]

109 **Giannini V**, Rosati S, Defeudis A, Balestra G, Vassallo L, Cappello G, Mazzetti S, De Mattia C, Rizzetto F, Torresin A, Sartore-Bianchi A, Siena S, Vanzulli A, Leone F, Zagonel V, Marsoni S, Regge D. Radiomics predicts response of individual HER2-amplified colorectal cancer liver metastases in patients treated with HER2-targeted therapy. *Int J Cancer* 2020; **147**: 3215-3223 [PMID: 32875550 DOI: 10.1002/ijc.33271]

110 **Paredes AZ**, Hyer JM, Tsilimigras DI, Moro A, Bagante F, Guglielmi A, Ruzzenente A, Alexandrescu S, Makris EA, Poultsides GA, Sasaki K, Aucejo FN, Pawlik TM. A Novel Machine-Learning Approach to Predict Recurrence After Resection of Colorectal Liver Metastases. *Ann Surg Oncol* 2020; **27**: 5139-5147 [PMID: 32779049 DOI: 10.1245/s10434-020-08991-9]

111 **Shu Z**, Fang S, Ding Z, Mao D, Cai R, Chen Y, Pang P, Gong X. MRI-based Radiomics nomogram to detect primary rectal cancer with synchronous liver metastases. *Sci Rep* 2019; **9**: 3374 [PMID: 30833648 DOI: 10.1038/s41598-019-39651-y]

112 **Spelt L**, Nilsson J, Andersson R, Andersson B. Artificial neural networks--a method for prediction of survival following liver resection for colorectal cancer metastases. *Eur J Surg Oncol* 2013; **39**: 648-654 [PMID: 23514791 DOI: 10.1016/j.ejso.2013.02.024]

113 **Wei J**, Cheng J, Gu D, Chai F, Hong N, Wang Y, Tian J. Deep learning-based radiomics predicts response to chemotherapy in colorectal liver metastases. *Med Phys* 2021; **48**: 513-522 [PMID: 33119899 DOI: 10.1002/mp.14563]

World Journal of Gastroenterology

Submit a Manuscript: https://www.f6publishing.com

World J Gastroenterol 2022 February 14; 28(6): 624-634

DOI: 10.3748/wjg.v28.i6.624

ISSN 1007-9327 (print) ISSN 2219-2840 (online)

MINIREVIEWS

Recent advances in the diagnostic evaluation of pancreatic cystic lesions

Devarshi R Ardeshna, Troy Cao, Brandon Rodgers, Chidiebere Onongaya, Dan Jones, Wei Chen, Eugene J Koay, Somashekar G Krishna

ORCID number: Devarshi R Ardeshna 0000-0002-1849-0867; Troy Cao 0000-0003-3718-140X; Brandon Rodgers 0000-0002-6840-9676; Chidiebere Onongaya 0000-0003-2033-1440; Dan Jones 0000-0002-4688-3780; Wei Chen 0000-0002-9028-622X; Eugene J Koay 0000-0001-7675-3461; Somashekar G Krishna 0000-0001-5748-7890.

Author contributions: Ardeshna DR, Cao T, Rodgers B, Onongaya C, Krishna SG performed the majority of the literature search, writing, and preparation of tables/figures; Jones D, Chen W, Koay EJ and Krishna SG provided input in the writing process and review of the final manuscript.

Conflict-of-interest statement: Krishna SG is the principal investigator of an investigator-initiated study. The study in part is funded by a grant to The Ohio State University Wexner Medical Center from Mauna Kea Technologies, Paris, France.

Country/Territory of origin: United States

Specialty type: Gastroenterology and hepatology

Provenance and peer review: Invited article; Externally peer reviewed.

Devarshi R Ardeshna, Chidiebere Onongaya, Department of Internal Medicine, Ohio State University Wexner Medical Center, Columbus, OH 43210, United States

Troy Cao, Brandon Rodgers, College of Medicine, Ohio State University, Columbus, OH 43210, United States

Dan Jones, James Molecular Laboratory, Ohio State University Wexner Medical Center, Columbus, OH 43210, United States

Wei Chen, Department of Pathology, Ohio State University Wexner Medical Center, Columbus, OH 43210, United States

Eugene J Koay, Department of GI Radiation Oncology, The University of Texas MD Anderson, Houston, TX77030, United States

Somashekar G Krishna, Division of Gastroenterology, Department of Internal Medicine, Ohio State University Wexner Medical Center, Columbus, OH 43210, United States

Corresponding author: Somashekar G Krishna, AGAF, FACG, FASGE, MD, Professor, Division of Gastroenterology, Department of Internal Medicine, Ohio State University Wexner Medical Center, 395 W. 12th Avenue, Suite 262, Columbus, OH 43210, United States. somashekar.krishna@osumc.edu

Abstract

Pancreatic cystic lesions (PCLs) are becoming more prevalent due to more frequent abdominal imaging and the increasing age of the general population. It has become crucial to identify these PCLs and subsequently risk stratify them to guide management. Given the high morbidity associated with pancreatic surgery, only those PCLs at high risk for malignancy should undergo such treatment. However, current diagnostic testing is suboptimal at accurately diagnosing and risk stratifying PCLs. Therefore, research has focused on developing new techniques for differentiating mucinous from non-mucinous PCLs and identifying high risk lesions for malignancy. Cross sectional imaging radiomics can potentially improve the predictive accuracy of primary risk stratification of PCLs at the time of detection to guide invasive testing. While cyst fluid glucose has reemerged as a potential biomarker, cyst fluid molecular markers have improved accuracy for identifying specific types of PCLs. Endoscopic ultrasound guided approaches such as confocal laser endomicroscopy and through the needle

Peer-review model: Single blind

Peer-review report's scientific quality classification
Grade A (Excellent): 0
Grade B (Very good): B
Grade C (Good): 0
Grade D (Fair): 0
Grade E (Poor): 0

Received: May 29, 2021
Peer-review started: May 29, 2021
First decision: June 22, 2021
Revised: July 30, 2021
Accepted: January 19, 2022
Article in press: January 19, 2022
Published online: February 14, 2022

P-Reviewer: Okasha HH
S-Editor: Wu YXJ
L-Editor: A
P-Editor: Wu YXJ

microforceps biopsy have shown a good correlation with histopathological findings and are evolving techniques for identifying and risk stratifying PCLs. While most of these recent diagnostics are only practiced at selective tertiary care centers, they hold a promise that management of PCLs will only get better in the future.

Key Words: Pancreatic cystic lesion; Intraductal papillary mucinous neoplasms; Mucinous cystic neoplasm; Microforceps biopsy; Radiomics; Confocal laser endomicroscopy

Core Tip: Pancreatic cystic lesions (PCLs) are highly prevalent. It is critical to accurately diagnose PCLs and risk stratify them to guide management. Current diagnostic techniques are suboptimal; hence, recent investigations have focused on developing, refining, and validating novel technologies for accurately diagnosing specific cyst type and ascertaining high-risk lesions for malignancy. Radiomics, cyst-fluid biomarkers, confocal laser endomicroscopy and microforceps biopsy hold the promise of accurately diagnosing PCLs and improving their management.

Citation: Ardeshna DR, Cao T, Rodgers B, Onongaya C, Jones D, Chen W, Koay EJ, Krishna SG. Recent advances in the diagnostic evaluation of pancreatic cystic lesions. *World J Gastroenterol* 2022; 28(6): 624-634
URL: https://www.wjgnet.com/1007-9327/full/v28/i6/624.htm
DOI: https://dx.doi.org/10.3748/wjg.v28.i6.624

INTRODUCTION

Pancreatic cystic lesions (PCLs) are increasingly detected, largely due to advances in imaging techniques and the increasing age of the general population[1]. With prevalence estimated in the range of 4%-14% in the general population and increasing constantly, it has become essential to characterize and risk stratify these cysts to guide management[2]. Current guidelines for evaluating PCLs are limited to less than optimal diagnostic techniques, resulting in either missed detection of early cancer or surgical over-treatment (see Figure 1). Resection of PCLs should be extremely selective since pancreatic surgery generally has a 20%-40% morbidity rate and an approximate 2% mortality rate[3-5]. Therefore, research and utilization of safe and effective diagnostic modalities with high accuracy are needed to evaluate cysts and introduce properly timed interventions.

Addressing this issue is especially relevant for intraductal papillary mucinous neoplasms (IPMNs), a type of PCL with one of the highest risks for malignancy. Of the two IPMN subtypes, main duct IPMNs are reported to have a risk from 38% to 68% and branch duct IPMNs from 12% to 47%[6]. Substantial research has addressed the use of consensus guidelines for evaluating IPMNs, but all mention that significant areas of improvement is imperative[7-9].

Current standards for the evaluation of cyst morphology include computed tomography (CT) scan, magnetic resonance imaging (MRI), and endoscopic ultrasound (EUS). Fine needle aspiration (FNA) of cyst fluid for carcinoembryonic antigen (CEA) and cytology is performed during EUS. Considerable heterogeneity exists among the five widely used guidelines, which indicate a lack of standardization in diagnostic workups[7-12]. In terms of the target population, American College of Gastroenterology and European guidelines include all PCLs, American College of Radiology guidelines focus on incidental PCLs, Fukuoka guidelines only focuses on IPMNs and American Gastroenterological Association (AGA) includes all PCLs except main-duct IPMNs. Guidelines differ in recommending evaluation with EUS and EUS-FNA, and surgical resection. Multiple studies have compared some of these guidelines for identifying high-risk PCLs. Amongst patients who underwent surgery, the current guidelines directed clinical decision with an accuracy, sensitivity and specificity of 49.6%, 23.5%, 84.3% for 2015 AGA guidelines, 41.2%, 39.7%, 43.1% for revised Fukuoka guidelines and 58%, 67.7%, 45.1% for 2018 European guidelines[13].

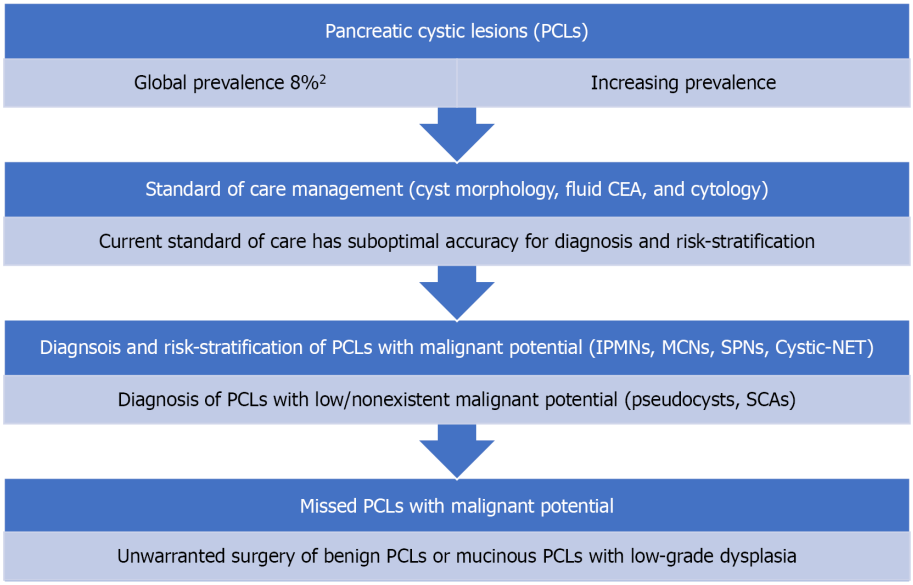

Figure 1 Current standard of care diagnostic methods are suboptimal in the diagnosis of specific types of pancreatic cystic lesions and risk-stratification of mucinous cysts. PCL: Pancreatic cystic lesion, CEA: Carcinoembryonic antigen, IPMN: Intraductal papillary mucinous neoplasms, MCN: Mucinous cystic neoplasm, SPN: Solid pseudopapillary neoplasm, Cystic-NET: Cystic neuroendocrine tumors, SCA: Serous cystadenoma.

A better understanding of investigational characteristics that lead to malignancy is necessary to improve existing criteria and accurately determine associated risks (Figure 1). While cyst fluid glucose has reemerged as a potential biomarker, novel techniques such as cyst fluid molecular analysis, EUS-guided needle-based confocal laser endomicroscopy (EUS-nCLE) and microforceps biopsy (EUS-MFB) have been introduced. The aim of this review is to provide an update of the recent literature in the management of PCLs with an emphasis on novel diagnostic methods.

RADIOMICS

Increasing prevalence of incidental PCLs has placed significant pressure on the necessity of discerning low-risk and high-risk lesions identified in radiological images. Radiomics is the analysis of mathematically derived textural features from cross-sectional imaging studies. The features are generally beyond human visual perception. Using radiometric feature extraction tool, radiomics can quantify individual pixels and their associated gray-scale value from cross-sectional imaging in a temporal and spatial plane to create a cyst impression. While studies have varied in the extraction of radiometric data, these features can potentially risk stratify PCLs. Hence, radiomics can guide downstream invasive diagnostics.

Studies in radiomics can be classified into two broad categories: (1) Differentiating types of PCLs, and (2) Risk stratification of IPMNs. Investigators have applied machine learning algorithms to radiomic features for automatic classification of PCLs. Some recent studies have evaluated nomograms and algorithms combining radiomics, cyst morphology, and clinical features. For differentiating PCLs, several investigations have demonstrated promising results. One of the first studies by Dmitriev *et al*[14], achieved a reasonable accuracy of 83.6% in discriminating PCL types into IPMNs, mucinous cystic neoplasms (MCNs), serous cystadenoma (SCAs) and solid neoplasms [14]. Their model had 93.2%-95.9% accuracy at predicting IPMNs. Subsequently, three investigations utilized CT-Scan radiomics to differentiate serous cystadenomas from other PCLs (area under the curve (AUC) 0.77-0.99, sensitivity 69%-95%, specificity 71%-96%)[15-17]. In one of these studies, radiomics outperformed radiologic characteristics in differentiating MCNs and macrocystic SCAs; comparative diagnostic parameters included sensitivity (93.6% *vs* 74.2%), specificity (96.2% *vs* 80.8%) and accuracy (94.7% *vs* 77.2%), respectively[16]. Combining radiomics with radiological findings or clinical parameters significantly improved the accuracy to distinguish cyst types in comparison to radiomics alone ($P < 0.05$) [16,18].

Only a few studies have evaluated the role of radiomics in differentiating IPMNs with advanced neoplasia, from indolent lesions with low-grade dysplasia (Table 1)[19-

Table 1 Summary of studies evaluating the role of radiomics in differentiating intraductal papillary mucinous neoplasms with advanced neoplasia

Ref.	*n*	Image type	No. of radiomic features	Best model	Performance training set
Hanania *et al*[19], United States, 2016	53	CECT	360	10 radiomic features	AUC: 0.82 SP: 85%, SP: 68%
Permuth *et al*[20], United States, 2016	38	CECT	112	14 radiomic features +blood 5 mi-RNAs	AUC: 0.92 SN: 83%, SP: 89%
Attiyeh *et al*[21], United States, 2019	103	CECT	255	Radiomic + clinical features	AUC: 0.79 SN: 71%, SP: 82%
Williams *et al*[22], United States, 2020	33	CECT	12	Radiomic features + cyst fluid protein markers	AUC: 0.88 SN: 71%, SP: 92%
Hoffman *et al*[23], United States, 2017	18	MRI w/ DWI	N/A	Entropy	AUC: 0.86 SN: 100%; SP: 70%

HGD: High-grade dysplasia; LGD: Low-grade dysplasia; CECT: Contrast-enhanced computed tomography; MRI: Magnetic resonance imaging; mi-RNA: micro-RNA; DWI: Diffusion weighted imaging; AUC: Area under curve; SN: Sensitivity; SP: Specificity; NA: Not application.

23]. Most of the studies evaluating radiomics in IPMNs have used CT scans, and included patients with confirmed surgical histopathology as ground truth. A recent study by Cui *et al*[24], presents the first publication where a radiomic signature incorporating 9 features was combined with clinical variables to predict high-grade dysplasia or adenocarcinoma (advanced neoplasia) in branch duct-IPMNs. Their predictive nomogram diagnosed advanced neoplasia with AUC values of 0.903 (training cohort; sensitivity 95%, specificity 73%), and 0.884 (one of two external validation cohorts; sensitivity 79%, specificity 90%)[24].

Thus, radiomics represents a promising non-invasive approach for the classification and risk stratification of PCLs and will favorably impact patient management. However, radiomics continues to be a novel concept and has been largely used to date in clinical trials at academic centers. While radiomics has demonstrated an immense potential for diagnosis, prognosis, and risk assessment in PCLs; there is a need for standardized protocols for image acquisition, segmentation, feature extraction, and analysis.

TRADITIONAL DIAGNOSTIC APPROACHES USING BIOMARKERS

Cyst fluid analysis

CEA and amylase: Traditionally pancreatic cyst fluid is aspirated using EUS-FNA for biomarker and cytologic analysis. In early studies, cyst fluid CEA levels above 192 ng/mL was shown to correlate with mucinous PCL with 79% (88/111) accuracy ($P < 0.0001$)[25]. However more recent studies, have estimated CEA sensitivity and specificity at 63% and 88%, respectively in differentiating mucinous from non-mucinous cysts[26]. This level of accuracy would result in misdiagnosis of 35%-39% of mucinous cysts. Additionally, CEA levels across sites are difficult to compare and levels have not been shown to correlate with PCL malignant potential[25,27-29]. Regarding amylase levels, a low cyst fluid amylase level has very high specificity for excluding pseudocyst. However, high amylase levels have been shown to have no diagnostic utility[26,30]. As a result, measuring amylase has fallen out of favor for the diagnosis of PCLs.

Cytology: Cyst fluid analysis by cytology has been shown to lack sensitivity for the diagnosis of PCLs. A meta-analysis with 937 patients demonstrated cyst fluid cytology to have 63% sensitivity and 88% specificity for the diagnosis of PCL[31]. Another meta-analysis calculated cytology to have 51% and 94% sensitivity and specificity, respectively[32]. This lack of sensitivity results from cytology evaluations usually detecting only intact exfoliated cells that are typically few in number[25,33].

Glucose: Intracystic glucose has good accuracy at differentiating mucinous and non-mucinous cysts but this economical diagnostic tool has not been used in routine clinical practice. However, recent prospective studies have provided improved and sustained evidence that cyst fluid glucose should be considered for standard of care evaluation of PCLs. Low intra-cystic glucose concentration is predictive of a mucinous cyst while high concentrations are consistent with non-mucinous cysts. In 2020, Ribaldone *et al*[34] reported from 56 patients that intra-cystic glucose concentration < 50 mg/dL had significantly better sensitivity than a CEA level > 192 ng/mL for diagnosing mucinous cysts (93.6% *vs* 54.8%; P = 0.003). Both CEA and intra-cystic glucose had high specificity for diagnosing mucinous cysts (96% *vs* 100%; P = 1). They reported that intra-cystic glucose concentration of more than 50 mg/dL had higher sensitivity than CEA values of less than 5 ng/mL for diagnosing non-mucinous cysts (96% *vs* 72%, P = 0.07).

A meta-analysis of 7 studies encompassing 566 patients reported that lower (cut-off < 50 mg/dL) intra-cystic glucose concentration had a pooled sensitivity of 90.1% (95%CI: 87.2-92.5) and pooled specificity of 85.3% (95%CI: 76.8-91.1) when differentiating mucinous from non-mucinous cysts[35]. In a subset analysis, point-of-care glucometer measurements for intra-cystic glucose (3 studies) also revealed comparable pooled sensitivity of 89.5% (95%CI: 85.5-92.5; I^2 = 0) and pooled specificity of 83.9% (95%CI: 68.5-92.6; I^2 = 43) for the differentiation of PCLs[35]. A more recent (2021) meta-analysis that included 8 studies with 609 PCLs showed pooled sensitivities for glucose *vs* CEA of 91% (95%CI: 88-94) *vs* 56% (95%CI 46-66) (comparative P value < 0.001), pooled specificities were 86% (95%CI: 81-90) *vs* 96% (95%CI: 90-99), P > 0.05, respectively[36].

Estimation of glucose levels is a low-cost diagnostic test that has repeatedly demonstrated better accuracy at differentiating mucinous and non-mucinous cyst. While not being definitive, cyst fluid glucose is a practical and economical diagnostic tool that can help in the differentiation of PCLs.

Molecular markers: With the introduction of next-generation sequencing (NGS), diagnosis of PCLs with either small gene panels and whole exome NGS have been employed. This method allows assessment of intact cell and cell-free nucleic acid that has been shed into the cyst fluid. DNA mutations that are commonly associated with pancreatic adenocarcinoma (*KRAS, CDKN2A, SMAD4, PTEN, PIK3CA,* and *TP53*) may also be present in precursor PCLs, with the latter five associated with advanced neoplasia.

Similar to radiomics, molecular analysis of cyst fluid can contribute to the classification of PCLs, and risk stratification of IPMNs. In a meta-analysis (6 studies, 785 PCLs), McCarty *et al*[37] reported that the dual presence of *KRAS* and *GNAS* mutations detected mucinous PCLs with a sensitivity of 75% (95%CI: 58-87%), specificity of 99% (95%CI: 67-100%), and diagnostic accuracy of 97% (95%CI: 95-98%), respectively. For specifically diagnosing IPMNs, dual *KRAS/GNAS* mutation had 94% (95%CI: 72-99%) sensitivity, 91% (95%CI: 72-98; I^2 = 89.83%) specificity and 97% (95%CI: 95-98%) accuracy, respectively. Recently, our group identified, for the first time, that uncommon *BRAF* mutations (and occasional *MAP2K1* mutations) characterize a significant subset of IPMNs that lack *KRAS* mutations, indicating that RAS-MAPK dysregulation is ubiquitous in these tumors[12]. In the same study, we showed 88.5% sensitivity, 100% specificity, and 90.3% accuracy for NGS differentiation of PCLs[12].

For the risk stratification of IPMNs, Singhi *et al*[38] used next-generation sequencing to evaluate DNA mutations associated with advanced neoplasia. In a subgroup analysis of 102 patients with histopathologic diagnosis, they reported that the presence of TP53, PIK3CA and/or PTEN mutation had 88% (95%CI: 62-98%) sensitivity and 95% (95%CI: 88-98%) specificity, respectively for diagnosing IPMNs with advanced neoplasia.

Cyst fluid molecular analysis by next generation sequencing is superior to measuring cyst CEA levels with superior accuracy and the ability to provide risk stratification for IPMNs. However, it is selectively available and represents a logistical and financial barrier for universal adaptation.

ADVANCED INTERVENTIONAL DIAGNOSTIC APPROACHES

EUS-guided needle confocal laser endomicroscopy

EUS-guided needle confocal laser endomicroscopy (nCLE) permits real-time microscopic imaging of intra-cystic epithelium within a single plane. It allows for *in*

vivo pathological analysis of PCLs. Early studies have established the characteristic features for IPMNs. Investigations by Napoleon *et al*[40] in the CONTACT study established defining criteria for MCNs, SCAs, and cystic neuroendocrine tumors[39, 40]. In 2020, the INDEX study provided further support for nCLE as a viable diagnostic tool by demonstrating high performance in differentiating PCLs amongst the highest number (n = 65) of patients with surgical histopathology[41]. For the differentiation of PCLs into mucinous and non-mucinous lesions, a recent meta-analysis with 7 studies and 324 patients reported a pooled sensitivity, specificity and accuracy of 85% (95%CI: 71-93%), 99% (95%CI: 90-100%) and 99% (95%CI: 98-100%), respectively. The pooled risk of post-procedure acute pancreatitis was 1% (95%CI: 0-3%)[42]. Another recent meta-analysis (10 studies, 536 patients) reported a pooled sensitivity, specificity, and accuracy of 82.4% (95%CI: 74.7-90.1%), 96.6% (95%CI: 94.3-99%), and 88.6% (95%CI: 83.7-93.4%), respectively, for the differentiation of mucinous from non-mucinous PCLs[43].

In addition to the high accuracy of diagnosing IPMNs and other cysts, nCLE can potentially determine the risk for advanced neoplasia in PCLs. To detect advanced neoplasia in IPMNs, multiple nCLE imaging variables were identified in a post-hoc analysis of the INDEX study[44], Figure 2. This study identified that the variables with the highest interobserver agreement were papillary epithelial thickness and darkness. Specifically, nCLE visualized papillary epithelial thickness (width ≥ 50 μm) had a sensitivity, specificity, and AUC of 87.5% (95%CI: 62%-99%), 100% (95%CI: 69%-100%), and 0.95, respectively for the detection of advanced neoplasia. Also, estimation of the papillary epithelial darkness (cut-off ≤ 90 pixel intensity) revealed a sensitivity, specificity, and AUC of 87.5% (95%CI: 62%-99%), 100% (95%CI: 69%-100%), and 0.90, respectively[44]. Analogously for mucinous cysts, Feng *et al*[45] reported that nCLE pattern of "dark aggregates of neoplastic cells" correlated with the morphologic features of "irregular branching and budding" and was diagnostic of malignancy, with 75% sensitivity, 100% specificity and 94% accuracy, respectively.

However, potential limitations of nCLE include differences in interobserver interpretation of images and the tedious nature of manually determining papillary epithelial thickness and darkness. Both of these issues were addressed with the development of a machine learning artificial intelligence model that identified advanced neoplasia in IPMNs with a sensitivity (83%) and specificity (88%) well above the Fukuoka or AGA guidelines[46].

Despite the growing evidence of nCLE as a viable diagnostic technique, its incorporation into standard clinical evaluation is lacking. The primary challenges include equipment costs, optimal training in image acquisition and interpretation, and prevention of adverse events higher than the standard EUS-FNA process.

EUS guided MFB or EUS-through-the-needle biopsy

This technique utilizes an EUS guided approach to pass a specialized device, the Moray micro forceps (Moray micro forceps, US Endoscopy, Mentor, Ohio, United States) through the 19-gauge EUS needle to collect tissue sample from PCLs. Multiple recent studies have demonstrated an improved diagnostic yield and accuracy in the diagnosis of specific types of PCLs[47,48].

Multiple meta-analyses have been published and the most recent studies include the following. Tacelli *et al*[49] (2020) included 9 studies with 454 patients and pooled technical success, histological accuracy and diagnostic yield for specific types of PCLs were 98.5% (95%CI: 97.3%-99.6%), 86.7% (95%CI: 80.1-93.4) and 69.5% (95%CI: 59.2-79.7%), respectively. Additionally sensitivity and specificity for diagnosis of mucinous PCLs were 88.6% and 94.7%, respectively. However, the overall complication rate was 8.6% (95%CI: 4.0-13.1%) with studies reporting rates ranging from 1%-23%. Of the reported complications, 57.1% had self-limiting bleedings (most commonly intra-cystic bleeding), 24.5% had mild pancreatitis, 6.1% had infections and 14.3% had abdominal pain. Westerveld *et al*[50] analyzed 8 studies with 426 patients reporting similar results. The MFB approach had significantly higher diagnostic yield for specific cyst type compared to cytology (72.5%, 95%CI: 60.6-83.0% *vs* 38.1%, 95%CI: 18.0-60.5%). Additionally, MFB had significantly higher diagnostic yield for mucinous cyst compared to cytology (OR: 3.86; 95%CI: 2.0-7.44, I^2 = 72%). Overall MFB procedures had a 7% complication rate with 5% incidence of intra-cystic hemorrhage and 2.3% risk of acute pancreatitis. More importantly, in a subgroup analysis of 92 patients who had surgical resection of their PCLs, MFB findings had concordance of 82.3% (95%CI: 71.9-90.7%) for specific cyst diagnosis. MFB findings for mucinous cysts had a sensitivity of 90.1% (95%CI: 78.4-97.6%) and specificity of 94% (95%CI: 81.5-99.7%). Additionally, the concordance rate for histological grade of dysplasia was 75.6% (95%CI: 62.3-86.8).

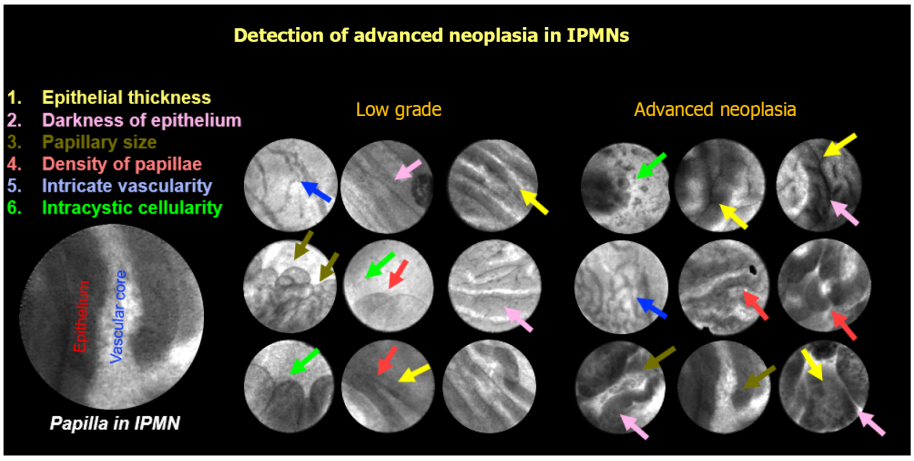

Figure 2 Features identified on endoscopic ultrasound guided needle confocal laser endomicroscopy. IPMN: Intraductal papillary mucinous neoplasms.

In another meta-analysis that included patients with surgical histopathology as reference diagnosis, the pooled sensitivity and specificity for diagnosing mucinous PCL was 86% (95 %CI: 62-96%) and specificity 95% (95%CI: 79-99%) respectively[51]. For diagnosis of specific cyst type, the pooled sensitivity and specificity were 69% (95%CI: 50-83%) and specificity 47% (95%CI: 28-68%), respectively. The authors also grouped IPMNs and MCNs with advanced neoplasia, SPNs, and cystic neuroendocrine tumors as high-risk cysts. MFB demonstrated a pooled sensitivity and specificity of 78% (95%CI: 61-89%) and 99% (95%CI: 90-99%) respectively for diagnosis of a high-risk cyst.

While MFB represents an excellent technique for acquisition of tissue and accurately diagnosing PCLs, the high rates of adverse events including acute pancreatitis and intra-cystic bleeding may deter clinicians from using this technique.

Contrast-enhanced EUS

EUS when combined with contrast enhancers allows detection of vascularity within PCLs. This allowed contrast-enhanced EUS (CE-EUS) to differentiate pseudocysts from true PCLs and identify mural nodules within PCLs. Despite early studies reporting no improvement over traditional EUS at differentiating PCLs[52], recent studies have reported higher diagnostic yield for PCLs using CE-EUS (96% compared to 71% for traditional EUS)[53]. CE-EUS detected small lesions initially missed on contrast-enhanced CT or EUS-FNA[54]. Recent literature on CE-EUS has reported higher accuracy at diagnosing PCLs compared to CT, MRI and traditional EUS[55]. Despite these encouraging results, CE-EUS has not gained traction in clinical management of PCLs.

CONCLUSION

Future directions in the diagnosis of pancreatic cysts

Reliable and accurate diagnosis of PCLs is a bottleneck for appropriate management of these lesions. Although, novel diagnostics have improved the diagnostic accuracy, there is still a dearth of prospective multicenter studies and a need to understand the complementary role of these tests. Radiomics, as a non-invasive tool has the potential for preliminary risk stratification of PCLs into low-and-high risk lesions (Figure 3). The technique holds a potential to allow clinicians to skip expensive and invasive diagnostic techniques on certain low risk PCLs.

For low-risk PCLs, and when EUS-FNA is indicated, low-cost cyst fluid analysis with glucose, CEA, and cytology can guide management (Figure 3). If radiomics and EUS cyst morphology are indicative of a high-risk PCL, advanced diagnostics with cyst fluid molecular analysis, nCLE, or microforceps biopsy can be considered based on the center and endoscopists' expertise. The rate of adverse events with microforceps biopsy needs to be considered when considering this test.

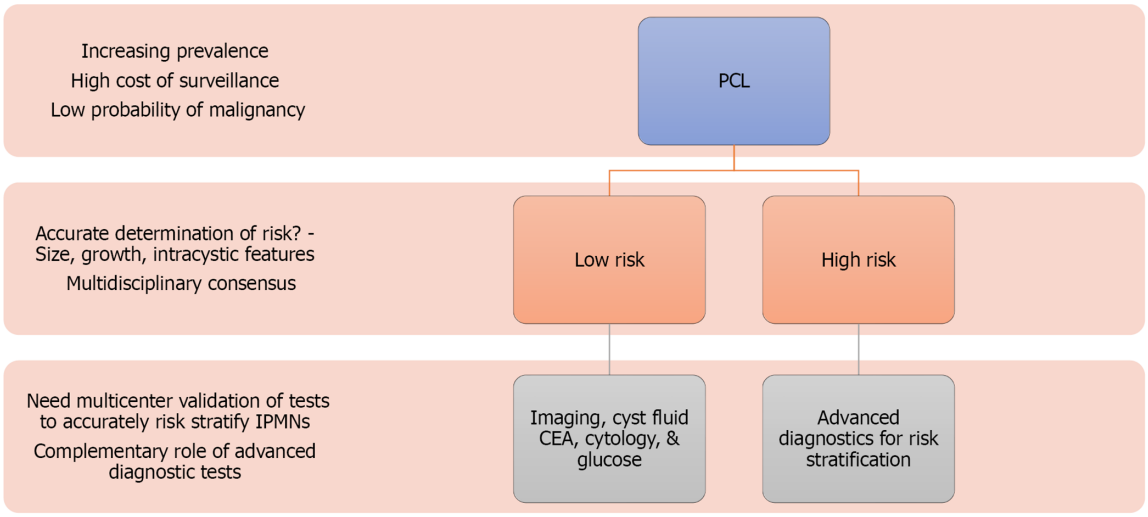

Figure 3 Future directions of detection and risk stratification of pancreatic cystic lesion to guide clinical management. PCL: Pancreatic cystic lesion, CEA: Carcinoembryonic antigen, IPMN: Intraductal papillary mucinous neoplasms.

Despite the availability of multiple diagnostic methods, the diagnosis and management of PCLs continues to be challenging. The more recent diagnostic modalities lack supportive larger multicenter data and there is need to demonstrate cost-effectiveness when compared to using suboptimal techniques and resultant unwarranted resection of otherwise benign or indolent PCLs. Apart from diagnosis, surveillance methods for low-risk lesions needs innovation as current tools are resource-consumptive.

REFERENCES

1 **Kromrey ML**, Bülow R, Hübner J, Paperlein C, Lerch MM, Ittermann T, Völzke H, Mayerle J, Kühn JP. Prospective study on the incidence, prevalence and 5-year pancreatic-related mortality of pancreatic cysts in a population-based study. *Gut* 2018; **67**: 138-145 [PMID: 28877981 DOI: 10.1136/gutjnl-2016-313127]

2 **Zerboni G**, Signoretti M, Crippa S, Falconi M, Arcidiacono PG, Capurso G. Systematic review and meta-analysis: Prevalence of incidentally detected pancreatic cystic lesions in asymptomatic individuals. *Pancreatology* 2019; **19**: 2-9 [PMID: 30503370 DOI: 10.1016/j.pan.2018.11.014]

3 **Oh HC**, Seo DW, Song TJ. Resolution of a septated pancreatic cyst by booster endoscopic ultrasonography-guided ablation. *J Dig Dis* 2011; **12**: 497-499 [PMID: 22118701 DOI: 10.1111/j.1751-2980.2011.00538.x]

4 **Allen PJ**, D'Angelica M, Gonen M, Jaques DP, Coit DG, Jarnagin WR, DeMatteo R, Fong Y, Blumgart LH, Brennan MF. A selective approach to the resection of cystic lesions of the pancreas: results from 539 consecutive patients. *Ann Surg* 2006; **244**: 572-582 [PMID: 16998366 DOI: 10.1097/01.sla.0000237652.84466.54]

5 **Scheiman JM**, Hwang JH, Moayyedi P. American gastroenterological association technical review on the diagnosis and management of asymptomatic neoplastic pancreatic cysts. *Gastroenterology* 2015; **148**: 824-48.e22 [PMID: 25805376 DOI: 10.1053/j.gastro.2015.01.014]

6 **Stark A**, Donahue TR, Reber HA, Hines OJ. Pancreatic Cyst Disease: A Review. *JAMA* 2016; **315**: 1882-1893 [PMID: 27139061 DOI: 10.1001/jama.2016.4690]

7 **Vege SS**, Ziring B, Jain R, Moayyedi P; Clinical Guidelines Committee; American Gastroenterology Association. American gastroenterological association institute guideline on the diagnosis and management of asymptomatic neoplastic pancreatic cysts. *Gastroenterology* 2015; **148**: 819-22; quize12 [PMID: 25805375 DOI: 10.1053/j.gastro.2015.01.015]

8 **Tanaka M**, Fernández-Del Castillo C, Kamisawa T, Jang JY, Levy P, Ohtsuka T, Salvia R, Shimizu Y, Tada M, Wolfgang CL. Revisions of international consensus Fukuoka guidelines for the management of IPMN of the pancreas. *Pancreatology* 2017; **17**: 738-753 [PMID: 28735806 DOI: 10.1016/j.pan.2017.07.007]

9 **Elta GH**, Enestvedt BK, Sauer BG, Lennon AM. ACG Clinical Guideline: Diagnosis and Management of Pancreatic Cysts. *Am J Gastroenterol* 2018; **113**: 464-479 [PMID: 29485131 DOI: 10.1038/ajg.2018.14]

10 **European Study Group on Cystic Tumours of the Pancreas**. European evidence-based guidelines on pancreatic cystic neoplasms. *Gut* 2018; **67**: 789-804 [PMID: 29574408 DOI: 10.1136/gutjnl-2018-316027]

11 **Megibow AJ**, Baker ME, Morgan DE, Kamel IR, Sahani DV, Newman E, Brugge WR, Berland LL, Pandharipande PV. Management of Incidental Pancreatic Cysts: A White Paper of the ACR Incidental Findings Committee. *J Am Coll Radiol* 2017; **14**: 911-923 [PMID: 28533111 DOI: 10.1016/j.jacr.2017.03.010]

12 **Ren R**, Krishna SG, Chen W, Frankel WL, Shen R, Zhao W, Avenarius MR, Garee J, Caruthers S, Jones D. Activation of the RAS pathway through uncommon BRAF mutations in mucinous pancreatic cysts without KRAS mutation. *Mod Pathol* 2021; **34**: 438-444 [PMID: 32792597 DOI: 10.1038/s41379-020-00647-z]

13 **Nijhuis J**, Bosscher F, Liem M. Accuracy of treatment decision-making in pancreatic cystic neoplasms based on available guidelines. European Journal of Surgical Oncology 2020; 46(2): e26-e27 [DOI: 10.1016/j.ejso.2019.11.488]

14 **Dmitriev K**, Kaufman AE, Javed AA, Hruban RH, Fishman EK, Lennon AM, Saltz JH. Classification of Pancreatic Cysts in Computed Tomography Images Using a Random Forest and Convolutional Neural Network Ensemble. *Med Image Comput Comput Assist Interv* 2017; **10435**: 150-158 [PMID: 29881827 DOI: 10.1007/978-3-319-66179-7_18]

15 **Yang J**, Guo X, Zhang H, Zhang W, Song J, Xu H, Ma X. Differential diagnosis of pancreatic serous cystadenoma and mucinous cystadenoma: utility of textural features in combination with morphological characteristics. *BMC Cancer* 2019; **19**: 1223 [PMID: 31842793 DOI: 10.1186/s12885-019-6421-7]

16 **Xie H**, Ma S, Guo X, Zhang X, Wang X. Preoperative differentiation of pancreatic mucinous cystic neoplasm from macrocystic serous cystic adenoma using radiomics: Preliminary findings and comparison with radiological model. *Eur J Radiol* 2020; **122**: 108747 [PMID: 31760275 DOI: 10.1016/j.ejrad.2019.108747]

17 **Wei R**, Lin K, Yan W, Guo Y, Wang Y, Li J, Zhu J. Computer-Aided Diagnosis of Pancreas Serous Cystic Neoplasms: A Radiomics Method on Preoperative MDCT Images. *Technol Cancer Res Treat* 2019; **18**: 1533033818824339 [PMID: 30803366 DOI: 10.1177/1533033818824339]

18 **Shen X**, Yang F, Yang P, Yang M, Xu L, Zhuo J, Wang J, Lu D, Liu Z, Zheng SS, Niu T, Xu X. A Contrast-Enhanced Computed Tomography Based Radiomics Approach for Preoperative Differentiation of Pancreatic Cystic Neoplasm Subtypes: A Feasibility Study. *Front Oncol* 2020; **10**: 248 [PMID: 32185129 DOI: 10.3389/fonc.2020.00248]

19 **Hanania AN**, Bantis LE, Feng Z, Wang H, Tamm EP, Katz MH, Maitra A, Koay EJ. Quantitative imaging to evaluate malignant potential of IPMNs. *Oncotarget* 2016; **7**: 85776-85784 [PMID: 27588410 DOI: 10.18632/oncotarget.11769]

20 **Permuth JB**, Choi J, Balarunathan Y, Kim J, Chen DT, Chen L, Orcutt S, Doepker MP, Gage K, Zhang G, Latifi K, Hoffe S, Jiang K, Coppola D, Centeno BA, Magliocco A, Li Q, Trevino J, Merchant N, Gillies R, Malafa M; Florida Pancreas Collaborative. Combining radiomic features with a miRNA classifier may improve prediction of malignant pathology for pancreatic intraductal papillary mucinous neoplasms. *Oncotarget* 2016; **7**: 85785-85797 [PMID: 27589689 DOI: 10.18632/oncotarget.11768]

21 **Attiyeh MA**, Chakraborty J, Gazit L, Langdon-Embry L, Gonen M, Balachandran VP, D'Angelica MI, DeMatteo RP, Jarnagin WR, Kingham TP, Allen PJ, Do RK, Simpson AL. Preoperative risk prediction for intraductal papillary mucinous neoplasms by quantitative CT image analysis. *HPB (Oxford)* 2019; **21**: 212-218 [PMID: 30097414 DOI: 10.1016/j.hpb.2018.07.016]

22 **Williams TL**, Harrington KA, Lawrence SA, Chakraborty J, Al Efishat MA, Attiyeh MA, Askan G, Chou Y, Pulvirenti A, McIntyre CA. A combined radiomics and cyst fluid inflammatory markers model to predict preoperative risk in pancreatic cystic lesions. Proceedings of the Medical Imaging 2020: Image-Guided Procedures, Robotic Interventions, and Modeling; 2020. International Society for Optics and Photonics: 113151Q [DOI: 10.1117/12.2566425]

23 **Hoffman DH**, Ream JM, Hajdu CH, Rosenkrantz AB. Utility of whole-lesion ADC histogram metrics for assessing the malignant potential of pancreatic intraductal papillary mucinous neoplasms (IPMNs). *Abdom Radiol (NY)* 2017; **42**: 1222-1228 [PMID: 27900458 DOI: 10.1007/s00261-016-1001-7]

24 **Cui S**, Tang T, Su Q, Wang Y, Shu Z, Yang W, Gong X. Radiomic nomogram based on MRI to predict grade of branching type intraductal papillary mucinous neoplasms of the pancreas: a multicenter study. *Cancer Imaging* 2021; **21**: 26 [PMID: 33750453 DOI: 10.1186/s40644-021-00395-6]

25 **Brugge WR**, Lewandrowski K, Lee-Lewandrowski E, Centeno BA, Szydlo T, Regan S, del Castillo CF, Warshaw AL. Diagnosis of pancreatic cystic neoplasms: a report of the cooperative pancreatic cyst study. *Gastroenterology* 2004; **126**: 1330-1336 [PMID: 15131794 DOI: 10.1053/j.gastro.2004.02.013]

26 **Thornton GD**, McPhail MJ, Nayagam S, Hewitt MJ, Vlavianos P, Monahan KJ. Endoscopic ultrasound guided fine needle aspiration for the diagnosis of pancreatic cystic neoplasms: a meta-analysis. *Pancreatology* 2013; **13**: 48-57 [PMID: 23395570 DOI: 10.1016/j.pan.2012.11.313]

27 **Cizginer S**, Turner BG, Bilge AR, Karaca C, Pitman MB, Brugge WR. Cyst fluid carcinoembryonic antigen is an accurate diagnostic marker of pancreatic mucinous cysts. *Pancreas* 2011; **40**: 1024-1028 [PMID: 21775920 DOI: 10.1097/MPA.0b013e31821bd62f]

28 **Park WG**, Mascarenhas R, Palaez-Luna M, Smyrk TC, O'Kane D, Clain JE, Levy MJ, Pearson RK, Petersen BT, Topazian MD, Vege SS, Chari ST. Diagnostic performance of cyst fluid carcinoembryonic antigen and amylase in histologically confirmed pancreatic cysts. *Pancreas* 2011;

40: 42-45 [PMID: 20966811 DOI: 10.1097/MPA.0b013e3181f69f36]
29 **Ngamruengphong S**, Bartel MJ, Raimondo M. Cyst carcinoembryonic antigen in differentiating pancreatic cysts: a meta-analysis. *Dig Liver Dis* 2013; **45**: 920-926 [PMID: 23790480 DOI: 10.1016/j.dld.2013.05.002]
30 **Ngamruengphong S**, Lennon AM. Analysis of Pancreatic Cyst Fluid. *Surg Pathol Clin* 2016; **9**: 677-684 [PMID: 27926366 DOI: 10.1016/j.path.2016.05.010]
31 **Thosani N**, Thosani S, Qiao W, Fleming JB, Bhutani MS, Guha S. Role of EUS-FNA-based cytology in the diagnosis of mucinous pancreatic cystic lesions: a systematic review and meta-analysis. *Dig Dis Sci* 2010; **55**: 2756-2766 [PMID: 20694512 DOI: 10.1007/s10620-010-1361-8]
32 **Wang QX**, Xiao J, Orange M, Zhang H, Zhu YQ. EUS-Guided FNA for Diagnosis of Pancreatic Cystic Lesions: a Meta-Analysis. *Cell Physiol Biochem* 2015; **36**: 1197-1209 [PMID: 26138881 DOI: 10.1159/000430290]
33 **Stelow EB**, Stanley MW, Bardales RH, Mallery S, Lai R, Linzie BM, Pambuccian SE. Intraductal papillary-mucinous neoplasm of the pancreas. The findings and limitations of cytologic samples obtained by endoscopic ultrasound-guided fine-needle aspiration. *Am J Clin Pathol* 2003; **120**: 398-404 [PMID: 14502804 DOI: 10.1309/CEPK-542W-3885-2LP8]
34 **Ribaldone DG**, Bruno M, Gaia S, Cantamessa A, Bragoni A, Caropreso P, Sacco M, Fagoonee S, Saracco GM, De Angelis C. Differential diagnosis of pancreatic cysts: A prospective study on the role of intra-cystic glucose concentration. *Dig Liver Dis* 2020; **52**: 1026-1032 [PMID: 32675041 DOI: 10.1016/j.dld.2020.06.038]
35 **Mohan BP**, Madhu D, Khan SR, Kassab LL, Ponnada S, Chandan S, Facciorusso A, Crino SF, Barresi L, McDonough S, Adler DG. Intracystic Glucose Levels in Differentiating Mucinous From Nonmucinous Pancreatic Cysts: A Systematic Review and Meta-analysis. *J Clin Gastroenterol* 2021 [PMID: 33731599 DOI: 10.1097/MCG.0000000000001507]
36 **McCarty TR**, Garg R, Rustagi R. Pancreatic cyst fluid glucose in differentiating mucinous from non-mucinous pancreatic cysts: a systemic review and meta-analysis. *Gastrointest Endosc* 2021; 94: 698-712.e6 [PMID: 33964311 DOI: 10.1016/j.gie.2021.04.025]
37 **McCarty TR**, Paleti S, Rustagi T. Molecular analysis of EUS-acquired pancreatic cyst fluid for KRAS and GNAS mutations for diagnosis of intraductal papillary mucinous neoplasia and mucinous cystic lesions: a systematic review and meta-analysis. *Gastrointest Endosc* 2021; **93**: 1019-1033.e5 [PMID: 33359054 DOI: 10.1016/j.gie.2020.12.014]
38 **Singhi AD**, McGrath K, Brand RE, Khalid A, Zeh HJ, Chennat JS, Fasanella KE, Papachristou GI, Slivka A, Bartlett DL, Dasyam AK, Hogg M, Lee KK, Marsh JW, Monaco SE, Ohori NP, Pingpank JF, Tsung A, Zureikat AH, Wald AI, Nikiforova MN. Preoperative next-generation sequencing of pancreatic cyst fluid is highly accurate in cyst classification and detection of advanced neoplasia. *Gut* 2018; **67**: 2131-2141 [PMID: 28970292 DOI: 10.1136/gutjnl-2016-313586]
39 **Napoléon B**, Lemaistre AI, Pujol B, Caillol F, Lucidarme D, Bourdariat R, Morellon-Mialhe B, Fumex F, Lefort C, Lepilliez V, Palazzo L, Monges G, Filoche B, Giovannini M. A novel approach to the diagnosis of pancreatic serous cystadenoma: needle-based confocal laser endomicroscopy. *Endoscopy* 2015; **47**: 26-32 [PMID: 25325684 DOI: 10.1055/s-0034-1390693]
40 **Napoleon B**, Lemaistre AI, Pujol B, Caillol F, Lucidarme D, Bourdariat R, Morellon-Mialhe B, Fumex F, Lefort C, Lepilliez V, Palazzo L, Monges G, Poizat F, Giovannini M. In vivo characterization of pancreatic cystic lesions by needle-based confocal laser endomicroscopy (nCLE): proposition of a comprehensive nCLE classification confirmed by an external retrospective evaluation. *Surg Endosc* 2016; **30**: 2603-2612 [PMID: 26428198 DOI: 10.1007/s00464-015-4510-5]
41 **Krishna SG**, Hart PA, Malli A, Kruger AJ, McCarthy ST, El-Dika S, Walker JP, Dillhoff ME, Manilchuk A, Schmidt CR, Pawlik TM, Porter K, Arnold CA, Cruz-Monserrate Z, Conwell DL. Endoscopic Ultrasound-Guided Confocal Laser Endomicroscopy Increases Accuracy of Differentiation of Pancreatic Cystic Lesions. *Clin Gastroenterol Hepatol* 2020; **18**: 432-440.e6 [PMID: 31220640 DOI: 10.1016/j.cgh.2019.06.010]
42 **Konjeti VR**, McCarty TR, Rustagi T. Needle-based Confocal Laser Endomicroscopy (nCLE) for Evaluation of Pancreatic Cystic Lesions: A Systematic Review and Meta-analysis. J Clin Gastroenterol 2020 [DOI: 10.1016/s0016-5085(20)33777-x]
43 **Facciorusso A**, Buccino VR, Sacco R. Needle-based confocal laser endomicroscopy in pancreatic cysts: a meta-analysis. *Eur J Gastroenterol Hepatol* 2020; **32**: 1084-1090 [PMID: 32282543 DOI: 10.1097/MEG.0000000000001728]
44 **Krishna SG**, Hart PA, DeWitt JM, DiMaio CJ, Kongkam P, Napoleon B, Othman MO, Yew Tan DM, Strobel SG, Stanich PP, Patel A, Luthra AK, Chan MQ, Blaszczak AM, Lee D, El-Dika S, McCarthy ST, Walker JP, Arnold CA, Porter K, Conwell DL. EUS-guided confocal laser endomicroscopy: prediction of dysplasia in intraductal papillary mucinous neoplasms (with video). *Gastrointest Endosc* 2020; **91**: 551-563.e5 [PMID: 31542380 DOI: 10.1016/j.gie.2019.09.014]
45 **Feng Y**, Chang X, Zhao Y, Wu D, Meng Z, Wu X, Guo T, Jiang Q, Zhang S, Wang Q, Yang A. A new needle-based confocal laser endomicroscopy pattern of malignant pancreatic mucinous cystic lesions (with video). Endosc Ultrasound 2020 [DOI: 10.4103/eus.eus_35_20]
46 **Machicado JD**, Chao W-L, Carlyn DE, Pan T-Y, Poland S, Alexander VL, Maloof TG, Dubay K, Ueltschi O, Middendorf DM, Jajeh MO, Vishwanath AB, Porter K, Hart PA, Papachristou GI, Cruz-Monserrate Z, Conwell DL, Krishna SG. High performance in risk stratification of intraductal papillary mucinous neoplasms by confocal laser endomicroscopy image analysis with convolutional neural networks (with video). Gastrointestinal Endoscopy 2021 [DOI: 10.1016/j.gie.2020.12.054]

47 **Barresi L**, Tacelli M, Ligresti D, Traina M, Tarantino I. Tissue acquisition in pancreatic cystic lesions. *Dig Liver Dis* 2019; **51**: 286-292 [PMID: 30166219 DOI: 10.1016/j.dld.2018.08.003]

48 **Huelsen A**, Cooper C, Saad N, Gupta S. Endoscopic ultrasound-guided, through-the-needle forceps biopsy in the assessment of an incidental large pancreatic cystic lesion with prior inconclusive fine-needle aspiration. *Endoscopy* 2017; **49**: E109-E110 [PMID: 28192812 DOI: 10.1055/s-0043-100217]

49 **Tacelli M**, Celsa C, Magro B, Barchiesi M, Barresi L, Capurso G, Arcidiacono PG, Cammà C, Crinò SF. Diagnostic performance of endoscopic ultrasound through-the-needle microforceps biopsy of pancreatic cystic lesions: Systematic review with meta-analysis. *Dig Endosc* 2020; **32**: 1018-1030 [PMID: 31912580 DOI: 10.1111/den.13626]

50 **Westerveld DR**, Ponniah SA, Draganov PV, Yang D. Diagnostic yield of EUS-guided through-the-needle microforceps biopsy *vs* EUS-FNA of pancreatic cystic lesions: a systematic review and meta-analysis. *Endosc Int Open* 2020; **8**: E656-E667 [PMID: 32355885 DOI: 10.1055/a-1119-6543]

51 **Rift CV**, Scheie D, Toxværd A, Kovacevic B, Klausen P, Vilmann P, Hansen CP, Lund EL, Hasselby JP. Diagnostic accuracy of EUS-guided through-the-needle-biopsies and simultaneously obtained fine needle aspiration for cytology from pancreatic cysts: A systematic review and meta-analysis. *Pathol Res Pract* 2021; **220**: 153368 [PMID: 33652239 DOI: 10.1016/j.prp.2021.153368]

52 **Kamata K**, Kitano M, Omoto S, Kadosaka K, Miyata T, Yamao K, Imai H, Sakamoto H, Harwani Y, Chikugo T, Chiba Y, Matsumoto I, Takeyama Y, Kudo M. Contrast-enhanced harmonic endoscopic ultrasonography for differential diagnosis of pancreatic cysts. *Endoscopy* 2016; **48**: 35-41 [PMID: 26605974 DOI: 10.1055/s-0034-1393564]

53 **Buxbaum J**, Ko C, Varghese N, Lee A, Sahakian A, King K, Serna J, Lee H, Tchelepi H, Van Dam J, Duddalwar V. Qualitative and Quantitative Contrast-enhanced Endoscopic Ultrasound Improves Evaluation of Focal Pancreatic Lesions. *Clin Gastroenterol Hepatol* 2020; **18**: 917-925.e4 [PMID: 31499247 DOI: 10.1016/j.cgh.2019.08.054]

54 **Kamata K**, Takenaka M, Minaga K, Omoto S, Miyata T, Yamao K, Imai H, Nakai A, Tanaka H, Chiba Y, Watanabe T, Sakurai T, Nishida N, Chikugo T, Matsumoto I, Takeyama Y, Kitano M, Kudo M. Value of additional endoscopic ultrasonography for surveillance after surgical removal of intraductal papillary mucinous neoplasms. *Dig Endosc* 2018; **30**: 659-666 [PMID: 29675938 DOI: 10.1111/den.13176]

55 **Zhong L**, Chai N, Linghu E, Li H, Yang J, Tang P. A Prospective Study on Contrast-Enhanced Endoscopic Ultrasound for Differential Diagnosis of Pancreatic Cystic Neoplasms. *Dig Dis Sci* 2019; **64**: 3616-3622 [PMID: 31290040 DOI: 10.1007/s10620-019-05718-z]

World Journal of Gastroenterology

Submit a Manuscript: https://www.f6publishing.com

World J Gastroenterol 2022 February 14; 28(6): 635-652

DOI: 10.3748/wjg.v28.i6.635

ISSN 1007-9327 (print) ISSN 2219-2840 (online)

ORIGINAL ARTICLE

Basic Study

Effects of viremia and CD4 recovery on gut "microbiome-immunity" axis in treatment-naïve HIV-1-infected patients undergoing antiretroviral therapy

Edda Russo, Giulia Nannini, Gaetana Sterrantino, Seble Tekle Kiros, Vincenzo Di Pilato, Marco Coppi, Simone Baldi, Elena Niccolai, Federica Ricci, Matteo Ramazzotti, Marco Pallecchi, Filippo Lagi, Gian Maria Rossolini, Alessandro Bartoloni, Gianluca Bartolucci, Amedeo Amedei

ORCID number: Edda Russo 0000-0003-3141-1091; Giulia Nannini 0000-0002-6481-6864; Gaetana Sterrantino 0000-0002-0385-0903; Seble Tekle Kiros 0000-0002-9687-0734; Vincenzo Di Pilato 0000-0002-5863-5805; Marco Coppi 0000-0002-4387-4037; Simone Baldi 0000-0002-5151-2618; Elena Niccolai 0000-0002-9205-8079; Federica Ricci 0000-0002-9986-7039; Matteo Ramazzotti 0000-0002-6862-9409; Marco Pallecchi 0000-0002-0057-6531; Filippo Lagi 0000-0003-0999-6070; Gian Maria Rossolini 0000-0002-9386-0434; Alessandro Bartoloni 0000-0001-9758-1523; Gianluca Bartolucci 0000-0002-5631-8769; Amedeo Amedei 0000-0002-6797-9343.

Author contributions: Russo E and Nannini G contributed equally to the work; Sterrantino G, Russo E, and Amedei A designed the study; Russo E and Sterrantino G revised the literature on this topic; Tekle Kiros S, Niccolai E, Ricci F, Russo E, Baldi S, and Nannini G collected the data; Russo E, Coppi M, Di Pilato V, Nannini G, Baldi S, Ricci F, and Lagi F analysed the data; Ramazzotti M and Di Pilato V performed microbiota analysis; Russo E wrote the manuscript; Russo E edited the manuscript;

Edda Russo, Giulia Nannini, Gaetana Sterrantino, Seble Tekle Kiros, Marco Coppi, Simone Baldi, Elena Niccolai, Federica Ricci, Filippo Lagi, Alessandro Bartoloni, Amedeo Amedei, Department of Clinical and Experimental Medicine, University of Florence, Florence 50134, Italy

Vincenzo Di Pilato, Department of Surgical Sciences and Integrated Diagnostics, University of Genoa, Genoa 16126, Italy

Matteo Ramazzotti, Marco Pallecchi, Department of Biomedical, Experimental and Clinical "Mario Serio", University of Florence, Florence 50134, Italy

Gian Maria Rossolini, Microbiology and Virology Unit, Florence Careggi University Hospital, University of Florence, Florence 50134, Italy

Gianluca Bartolucci, Department of Neurosciences, Psychology, Drug Research and Child Health, University of Florence, Florence 50019, Italy

Corresponding author: Amedeo Amedei, BSc, PhD, Professor, Reader (Associate Professor), Department of Clinical and Experimental Medicine, University of Florence, Viale Pieraccini, 6, Florence 50139, Italy. aamedei@unifi.it

Abstract

BACKGROUND

Human immunodeficiency virus type 1 (HIV-1) infection is characterized by persistent systemic inflammation and immune activation, even in patients receiving effective antiretroviral therapy (ART). Converging data from many cross-sectional studies suggest that gut microbiota (GM) changes can occur throughout including human immunodeficiency virus (HIV) infection, treated by ART; however, the results are contrasting. For the first time, we compared the fecal microbial composition, serum and fecal microbial metabolites, and serum cytokine profile of treatment-naïve patients before starting ART and after reaching virological suppression, after 24 wk of ART therapy. In addition, we compared the microbiota composition, microbial metabolites, and cytokine profile of patients with CD4/CD8 ratio < 1 (immunological non-responders [INRs]) and

Amedei A supervised the manuscript; Amedei A, Sterrantino G, Rossolini GM, Bartoucci G, and Bartoloni A revised the manuscript; Russo E, Amedei A, Sterratino G, Bartoloni A, and Rossolini GM provided funding acquisition.

Institutional review board statement: The study was reviewed and approved by the Comitato Etico Area Vasta Centro [(Approval No. 15035)].

Conflict-of-interest statement: The authors declare that they have no competing interests to disclose.

Data sharing statement: No additional data are available.

Supported by University of Florence, No. XXXV PhD Program.

Country/Territory of origin: Italy

Specialty type: Immunology

Provenance and peer review: Invited article; Externally peer reviewed.

Peer-review model: Single blind

Peer-review report's scientific quality classification

Grade A (Excellent): 0
Grade B (Very good): 0
Grade C (Good): C
Grade D (Fair): 0
Grade E (Poor): 0

Received: May 28, 2021
Peer-review started: May 28, 2021

CD4/CD8 > 1 (immunological responders [IRs]), after 24 wk of ART therapy.

AIM

To compare for the first time the fecal microbial composition, serum and fecal microbial metabolites, and serum cytokine profile of treatment-naïve patients before starting ART and after reaching virological suppression (HIV RNA < 50 copies/mL) after 24 wk of ART.

METHODS

We enrolled 12 treatment-naïve HIV-infected patients receiving ART (mainly based on integrase inhibitors). Fecal microbiota composition was assessed through next generation sequencing. In addition, a comprehensive analysis of a blood broad-spectrum cytokine panel was performed through a multiplex approach. At the same time, serum free fatty acid (FFA) and fecal short chain fatty acid levels were obtained through gas chromatography-mass spectrometry.

RESULTS

We first compared microbiota signatures, FFA levels, and cytokine profile before starting ART and after reaching virological suppression. Modest alterations were observed in microbiota composition, in particular in the viral suppression condition, we detected an increase of *Ruminococcus* and *Succinivibrio* and a decrease of *Intestinibacter*. Moreover, in the same condition, we also observed augmented levels of serum propionic and butyric acids. Contemporarily, a reduction of serum IP-10 and an increase of IL-8 levels were detected in the viral suppression condition. In addition, the same components were compared between IRs and INRs. Concerning the microflora population, we detected a reduction of *Faecalibacterium* and an increase of *Alistipes* in INRs. Simultaneously, fecal isobutyric, isovaleric, and 2-methylbutyric acids were also increased in INRs.

CONCLUSION

Our results provided an additional perspective about the impact of HIV infection, ART, and immune recovery on the "microbiome-immunity axis" at the metabolism level. These factors can act as indicators of the active processes occurring in the gastrointestinal tract. Individuals with HIV-1 infection, before ART and after reaching virological suppression with 24 wk of ART, displayed a microbiota with unchanged overall bacterial diversity; moreover, their systemic inflammatory status seems not to be completely restored. In addition, we confirmed the role of the GM metabolites in immune reconstitution.

Key Words: HIV; Antiretroviral therapy; Microbiome-immunity axis; Microbiota; Cytokines; Short chain fatty acid; Inflammation; Immunological responders; Viremia

Core Tip: Even in patients receiving effective antiretroviral therapy (ART), human immunodeficiency virus type 1 infection is characterized by persistent systemic inflammation and immune activation. Changes in the gut microbiota can occur with including human immunodeficiency virus infection and treatment with ART; however, the data are still conflicting. For these reasons, we compared the fecal microbial composition and serum cytokine profile of treatment-naïve patients before starting ART and after virological suppression. Finally, we evaluated the microbiota composition, microbial metabolites, and cytokine profile of patients with CD4/CD8 ratio < 1 and CD4/CD8 > 1 (immunological responders).

Citation: Russo E, Nannini G, Sterrantino G, Kiros ST, Pilato VD, Coppi M, Baldi S, Niccolai E, Ricci F, Ramazzotti M, Pallecchi M, Lagi F, Rossolini GM, Bartoloni A, Bartolucci G, Amedei A. Effects of viremia and CD4 recovery on gut "microbiome-immunity" axis in treatment-naïve HIV-1-infected patients undergoing antiretroviral therapy. *World J Gastroenterol* 2022; 28(6): 635-652
URL: https://www.wjgnet.com/1007-9327/full/v28/i6/635.htm

First decision: June 30, 2021
Revised: July 30, 2021
Accepted: January 13, 2022
Article in press: January 13, 2022
Published online: February 14, 2022

P-Reviewer: Hazafa A
S-Editor: Ma YJ
L-Editor: Wang TQ
P-Editor: Yu HG

DOI: https://dx.doi.org/10.3748/wjg.v28.i6.635

INTRODUCTION

The mutual interaction between the human microbiota and the immune system defines the so-called "microbiome-immune axis". This axis has also been associated with several diseases, including human immunodeficiency virus (HIV) infection[1]. Indeed, a key place for HIV replication is the gastrointestinal tract. HIV replication in the gastrointestinal tract results in a severe depletion of $CD4^+$ T cells that leads to decreased function of the epithelial barrier, allowing microbes and microbial products to be translocated, which contributes to the chronic inflammatory response[2]. HIV replication can also result in a microbial dysbiosis condition[3-5], which has been correlated with increases in markers of disease progression, immune activation, and microbial translocation[3,5-7]. Notably, HIV-infected people harbour a distinct gut microbiota (GM)[8,9] with a *Prevotella*-rich community composition, typically observed in individuals from agrarian cultures or with carbohydrate-rich, protein- and fat-poor diets[10]. In addition, the significant subversion of the *Bacteroidetes* and *Proteobacteria* phyla, with an imbalanced *Prevotella/Bacteroides* species ratio and an abundance in *Enterobacteriaceae,* is one of the most persistent changes documented in untreated HIV infection[11-13]. Moreover, the increased number of gut-resident bacteria capable of directly producing inflammation can be a probable mechanistic link between HIV-associated dysbiosis and high systemic immune activation[14]. However, converging data from cross-sectional studies suggest that the GM composition and its related immune response can change over the progression of HIV infection. In particular, correlating the composition of the gastrointestinal tract microbiome to immune activation, circulating bacterial products and clinical parameters, a decrease of commensal species, and a gain of pathogenic taxa was observed in HIV+ subjects compared to controls[15]. Additionally, analysing the functional gene content of the GM in HIV+ patients and the metabolic pathways of the bacterial community associated with immune dysfunction, the metagenome sequencing revealed an altered functional profile with significant interactions between the bacterial community, their altered metabolic pathways, and systemic markers of immune dysfunction[16]. Furthermore, analysing the associations between the innate lymphoid cell (ILC) cytokines and measures of virologic, immunologic, and microbiome indices, it was observed that inflammatory ILCs contribute to gut mucosal inflammation and epithelial barrier breakdown, important features of HIV-1 mucosal pathogenesis[17]. Despite growing evidence that the GM has a role in HIV pathogenesis[11,18-20], the results were contrasting, with some studies suggesting an influence and others no HIV influence on microbial diversity[1,21] and composition[22,23]. However, many studies on the GM in HIV-infected patients are often carried out with a lack of adjustment for confounding factors, such as diet and use of drugs[24,25].

Currently, antiretroviral therapy (ART) has increased the life expectancy of HIV-infected patients, approximating it to that of the general population[26]. Interestingly, chronic inflammation and GM alterations persist in patients virologically suppressed by ART[27]. These data implicate that re-shaping the microbiota may be an adjuvant therapy in patients commencing successful ART[28]. On the other hand, suppressive ART appears to have a limited effect on the restoration of the GM[13,25,29,30]. Although the gut microbial composition of ART-treated people differs from that of untreated people, the former also have a different microbial community structure compared to the HIV-uninfected population[31,32]. These findings raise the possibility that persistent gut dysbiosis may play a role in the development of residual clinical illness after ART.

Currently, the CD4/CD8 ratio is considered one of the best-used markers of immune reconstitution. Notably, a low CD4/CD8 ratio is associated with an increased risk of non-AIDS-related diseases[33]. Furthermore, the differences between the elements of the microbiome-immune axis between patients with normalized or non-normalized CD4/CD8 ratio during ART have not been elucidated so far[34,35]; however, this question is recognized as a current research gap.

Moreover, with a better understanding of the microbiota-immune axis, it is now known that in addition to the intestinal flora itself, its metabolites are also involved in regulating vital host activities, such as energy metabolism, cell-to-cell communication, and host immunity. Short-chain fatty acids (SCFAs) are important metabolites able to modulate the production of immune mediators, such as key cytokines for the repair

and maintenance of epithelium integrity[36]. In addition, the SCFAs modulate the activity of T cells and decrease the overexpression of histone deacetylase, particularly butyric and valeric acids[37]. SCFAs are an important link between microflora and the immune system; they involve different molecular mechanisms and cellular targets, are essential for the maintenance of intestinal homeostasis, and finally play a role in HIV infection[38].

The purpose of this prospective observational study was to compare for the first time the fecal microbial composition, serum and fecal microbial metabolites, and serum cytokine profile of treatment-naïve patients before starting ART and after reaching virological suppression (HIV RNA < 50 copies/mL) after 24 wk of ART. An additional aim was to correlate the GM composition, microbial metabolites, and cytokine profile of patients with CD4/CD8 ratio < 1 and CD4/CD8 > 1 after antiretroviral therapy.

MATERIALS AND METHODS

Patients

The study population, composed of 12 treatment-naïve HIV-infected patients receiving ART mainly based on integrase inhibitors, was enrolled between April 2018 and May 2019 at the Department of Infective and Tropical Disease at University Hospital of Careggi, Florence, Italy (Table 1). The study was approved by local institutional review boards and written informed consent was obtained from patients before participation (Rif CEAVC 15035).

We conducted a prospective observational cohort study comparing the changes occurring in the fecal microbiota, serum and fecal SCFA, serum free fatty acids (FFAs), and serum cytokines of patients with HIV-1 infection before ART (T0) and after 24 wk (T1). In addition, patients were divided into two groups according to whether they were immunological responders (IRs, n = 6) or not (INRs, n = 6) (INRs and IRs, based on the normalization of CD4/CD8 ratio: < 1 or ≥ 1 after 24 wk of ART, respectively). Patients who had used antibiotics, probiotics, or prebiotics or had experienced diarrhoea or digestive symptoms within the previous 1 mo were excluded.

Personal data, ART regimen, HIV-RNA values, and number of $CD4^+$ and $CD8^+$ T cells prior to ART starting and at the time of virologic suppression were included in the analysis (Table 1). In this pilot exploratory study, no formal sample size calculation was performed. All patients followed a Mediterranean diet.

Plasma HIV-RNA was measured using Test v1.5 Roche COBAS AmpliPrep, Roche TaqMan HIV-1 Test v2.0 (Roche Diagnostics, Branchburg, NJ, United States) and Siemens Versant K PCR (Siemens Healthcare GmbH, Erlangen, Germany), with lower limits of detection of 50, 20, and 37 copies/mL, respectively.

The T cell counts of patients were determined using a FACScanto flow cytometer (BD Immunocytometry Systems)[10]. Immunophenotyping of peripheral blood lymphocytes was analysed by three-color flow cytometry (Epics XL Flow Cytometry System; Beckman Coulter, United States) as previously described[39]. Freshly collected EDTA anticoagulated whole blood was incubated and tested with a panel of monoclonal antibodies directed against fluorescein isothiocyanate/phycoerythrin/peridinin chlorophyll protein combinations of CD3/CD4/CD8, CD3/CD16CD56/CD19, HLA-DR/CD8/CD38, and CD4/CD8/CD28 and isotype controls (Immunotech, France).

At each time point (0 and 24 wk after study enrolment), we collected blood and fecal samples. After collection, stool samples were immediately frozen and stored at −80 °C until DNA extraction. Fecal samples were used to assess the microbiota composition and SCFAs, and while blood samples were used to measure SCFAs and FFAs and a panel of 27 selected cytokines.

Study follow-up

Patients underwent medical visits at 0 and 24 wk after study enrolment. They also underwent a comprehensive physical examination and medical history inquiry, urine toxicology panel testing, clinical laboratory tests including plasma HIV RNA, specimen collection, and detailed behavioural questionnaire survey. Demographic and clinical data were collected in a specific questionnaire and reported in an appropriate database, including the time point of follow-up in months; the participant's gender, age, weight, and height; $CD4^+$ and $CD8^+$ T cell counts; the CD4/CD8 ratio; HIV-1 RNA levels, ART, and antibiotic use. If subjects had to start antibiotics, they provided a last fecal sample and the study follow-up was immediately terminated.

Table 1 Features of the enrolled patients

	Age	Sex	ART regimen	Comorbidities	Timepoints (wk)	Viral load (copies/mL)	CD4+ cells/mm^3	CD8+ cells/mm^3	CD4/CD8 ratio
1	37	Male	3TC/ABC/DTG	No	T0	597463	110	420	0.3
					T24	< 20	520	832	0.6
2	38	Male	FTC/TDF/EVG/C	No	T0	4489	630	670	0.9
					T24	TND	831	740	1.1
3	34	Male	FTC/TDF/EVG/C	No	T0	165516	253	725	0.3
					T24	TND	504	363	1.4
4	39	Male	FTC/TDF/EVG/c	No	T0	859883	360	974	0.4
					T24	33	781	986	0.8
5	38	Male	3TC/ABC/DTG	No	T0	4860	1341	928	1.4
					T24	TND	1881	988	1.9
6	41	Male	FTC/TDF/RPV	Atrial fibrillation	T0	213	814	690	1.2
					T24	TND	845	519	1.6
7	25	Male	3TC/ABC/DTG	No	T0	23098	516	1149	0.4
					T24	< 20	942	1019	0.9
8	22	Male	FTC/TAF/EVG/c	No	T0	12188	654	1055	0.6
					T24	TND	668	733	0.9
9	48	Male	3TC/ABC/DTG	No	T0	175	833	1520	0.5
					T24	TND	941	1258	0.7
10	53	Male	3TC/ABC/DTG	Hypertension, HCV	T0	40545	863	1196	0.7
					T24	TND	612	515	1.2
11	40	Male	3TC/ABC/DTG	No	T0	859000	399	980	0.4
					T24	39	648	652	1
12	51	Male	FTC/TDF DTG	Diabetes	T0	4410	884	1066	0.8
					T24	< 20	1130	1261	0.9

ART: Antiretroviral therapy; 3TC: Lamivudine; ABC: Abacavir; DTG: Dolutegravir; FTC: Emtricitabine; TDF: Tenovir; EVG/c: Elvitegravir/cobi; RPV: Rilpivirine.

Fecal microbiota characterization

Total genomic DNA was extracted from frozen (-80 °C) stool samples, collected at different time points (weeks 0 and 24; T0 and T24), using the DNeasy PowerLyzer PowerSoil Kit (Qiagen, Hilden, Germany) according to the manufacturer's instructions. The quality and quantity of purified DNA were assessed using the NanoDrop ND-1000 (Thermo Fisher Scientific, WalthAP, US) and the Qubit Fluorometer (Thermo Fisher Scientific), respectively.

Extracted DNA samples were sent to IGA Technology Services (Udine, Italy) where amplicons of the variable V3–V4 region of the bacterial 16S rRNA gene were sequenced (2 × 300 bp paired-end) on the Illumina MiSeq platform, according to the Illumina 16S Metagenomic Sequencing Library Preparation protocol[40].

Sequencing results were analysed using the QIIME 2 suite (Quantitative Insights Into Microbial Ecology)[41]. Briefly, following raw reads denoising (*i.e.*, estimation of error rates, removal of chimeric and singleton sequences, and join of denoised paired-end reads) using DADA2 (Divisive Amplicon Denoising Algorithm 2)[42], denoised reads were dereplicated and amplicon sequence variants (ASVs) were inferred. Taxonomic classification of inferred ASVs was performed using a Naive Bayes classifier trained on the SILVA 16S reference database (release 132) (https://www.arb-silva.de/documentation/release-132/).

Evaluation of fecal short chain fatty acids and serum free fatty acids by gas chromatography-mass spectrometry

The fecal SCFAs, in particular acetic, propionic, butyric, isobutyric, isovaleric, 2-methylbutyric, valeric, and hexanoic acids, were analyzed using an Agilent GC-MS system composed with a 5971 single quadrupole mass spectrometer, a 5890 gas-chromatograph, and a 7673 auto sampler. The chemicals, GC-MS conditions, and calibrations parameters are reported in supporting information (Tables S1-S4)[43]. Fecal samples were collected in 15-mL Falcon tubes and stored at -80 °C. Just before the analysis, each sample was thawed, weighted (between 0.5-1.0 g), and added to sodium bicarbonate 10 mmol/L solution (1:1 w/v) in a 1.5 mL centrifuge tube. The obtained suspension was briefly stirred in a vortex apparatus, extracted in an ultrasonic bath (for 5 min), and then centrifuged at 5000 rpm (for 10 min). The supernatant was collected and transferred into a 1.5 mL centrifuge tube (sample solution). The SCFAs were finally extracted as follows: An aliquot of 100 μL of sample solution was added to 50 μL of internal standard mixture, 1 mL of tert-butyl methyl ether, and 50 μL of 1.0 mol/L HCl solution in a 1.5 mL centrifuge tube. Afterwards, each tube was shaken in a vortex apparatus for 2 min and centrifuged at 10000 rpm for 5 min, and finally the solvent layer was transferred into an autosampler vial and analyzed by the GC-MS method. Each sample was prepared and processed, by the method described above, three times. In addition, serum FFAs, classified as SCFAs (acetic, propionic, butyric, isobutyric isovaleric, 2-methylbutyri, and valeric acids), medium chain fatty acids (MCFAs; hexanoic, heptanoic, octanoic, nonanoic, decanoic, and dodecanoic acids), and long chain fatty acids (LCFAs; tetradecanoic, hexadecanoic, and octadecanoic acids) were analyzed with our previous described GC-MS protocol[44]. The chemicals, GC-MS conditions, GC-MS method, and calibrations parameters are reported in supporting information (Tables S5-S7).

Just before the analysis, each sample was thawed. The FFAs were extracted as follows: An aliquot of 300 μL of plasma sample was added to 10 μL of internal standard mixture, 100 μL of tert-butyl methyl ether, and 20 μL of 6 M HCl plus 0.5 mol/L NaCl solution in a 0.5 mL centrifuge tube. Afterwards, each tube was stirred in vortex for 2 min and centrifuged at 10000 rpm for 5 min, and finally the solvent layer was transferred into a vial with a microvolume insert and analyzed.

Molecular inflammatory response in serum

The inflammatory response in serum samples of patients and healthy controls was evaluated using a specifically assembled kit ProCartaPlex MixMatch Human 27 Panel for Luminex MAGPIX detection system (Affymetrix, eBioscience) following the manufacturers' instructions.

In detail, the panel included macrophage inflammatory protein-1α (MIP-1α), interleukin (IL)-27, IL-1β, IL-2, IL-4, IL-5, interferon gamma-induced protein 10 (IP-10), IL-6, IL-8, IL-10, IL-12p70, IL-13, IL-17A, interferon (IFN)-γ, IFN-α, tumor necrosis factor-α (TNF-α), granulocyte-macrophage colony stimulating factor (GM-CSF), monocyte chemotactic protein 1(MCP-1), IL-9, P-selectin, IL-1α, IL-23, IL-18, IL-21, soluble intercellular adhesion molecule-1 (sICAM-1), IL-22, and E-selectin.

All measurements were performed in a blinded manner by a laboratory technician who was experienced in executing the technique. The levels of cytokines were estimated using a 5-parameter polynomial curve (ProcartaPlex Analyst 1.0). A value under the low limit of quantification (LLOQ) was considered as 0 pg/mL.

Statistical analysis

Statistical analyses on ASVs representing the bacterial community were performed in R (R Core Team, 2014) with the help of the packages phyloseq 1.26.1[45] and DESeq2 1.22.2[46], and other packages satisfying their dependencies, in particular vegan 2.5-5 [47]. Rarefaction analysis on ASVs was performed using the function rarecurve (step 50 reads), and further processed to highlight saturated samples (arbitrarily defined as saturated samples with a final slope in the rarefaction curve with an increment in ASV number per reads < 1e-5). For the cluster analysis (complete clustering on euclidean distance) of the entire community, the OTU table was first normalized using the total ASV counts of each sample and then adjusted using square root transformation. The coverage was calculated by Good's estimator using the formula $(1 - n/N) \times 100$, where n is the number of sequences found once in a sample (singletons), and N is the total number of sequences in that sample.

Richness, Shannon, Chao 1, and evenness indices were used to estimate bacterial diversity in each sample using the function estimate_richness from phyloseq[45]. The evenness index was calculated using the formula E = S/Log(R), where S is the

Shannon diversity index and R is the number of ASVs in the sample. Differences in all indices were tested using a paired Wilcoxon signed-rank test. The differential analysis of abundance at the ASVs as well as at the different taxonomic ranks (created using the tax_glom function in phyloseq) was performed with DESeq2[46] using a two group blocked by patient design in order to perform a paired test[48].

In addition, the software GraphPad Prism (v. 5) and Statgraphics Centurion XVI software were used for immunological data analysis. Numerical data are presented as the mean ± SD. The concentrations of several cytokines in some of the samples lay below the curve fit of the standards. To avoid the bias that would have been introduced by excluding these data, the concentrations of the implicated cytokine were set at half of the lower cut off of the test system, which was usually about 1 pg/mL. Outliers at the other end of the spectrum (higher than the mean ± SD) were identified *via* boxplots and were excluded from the statistical analysis. The comparisons between dependent groups were evaluated by the Wilcoxon matched pairs test, while the comparisons between the independent groups were assessed by the Mann-Whitney test. A P value less than 0.05 were considered statistically significant.

Data availability statement

The 16S rRNA sequence dataset has been deposited in the NCBI Sequence Read Archive (SRA) database and is available under the BioProject accession number PRJNA731648.

RESULTS

Comparison of fecal microbiota and metabolic and inflammatory profiles after ART

Modest differences in specific fecal microbiota taxa associated with HIV viremia: In the first part of our study, we compared the fecal microbiota and metabolic and inflammatory profile before and after ART starting, in order to examine potential changes resulting from HIV infection and ART therapy. We first analysed the longitudinal variation of fecal microbiota population in the same patients at T0 (HIV+ viremia - RNA > 50 copies/mL), defined as "high viremia" condition, and T24 (HIV+ suppression - RNA ≤ 50 copies/mL), defined as "viral suppression" condition. The alpha diversity of samples did not display significant differences for Chao, Shannon, and evenness indices (Figure 1). The analysis of the taxonomic composition revealed that more than 99% of the sequences collected were classified into four phyla: *Firmicutes* (65.46%), *Bacteroidetes* (21.54%), *Actinobacteria* (9.40%), and *Proteobacteria* (2.72%). In order to investigate similarity of patients' microbiota abundance profiles and to study the paired nature of sampling (*i.e.*, high viremia condition *vs* viral suppression condition), a cluster analysis and PCoA on normalized ASV counts were performed.

The hierarchical clustering evidenced that microbiota was not sufficiently altered after treatment (24 wk) to break individual compositions apart, resulting in a perfect matching of the two time points from the same patient (Figure 2A). This result was also confirmed by the PCoA (Figure 2B), which showed a substantial proximity of each patient at T0 and T24, indicating that, overall, the abundance profile of the single patient was not affected by the 24-wk therapy.

On the other hand, the paired comparison of the abundance of single microbial ranks revealed some significant (adj. $P < 0.05$, abs (logFC) ≥ 1) differences between the two samples groups. In particular, the genera *Ruminococcus 2* and *Succinivibrio* were found to be significantly increased in higher viral suppression condition. On the contrary, viral suppression was related with a decrease in the *Intestinibacter* genus (median abundance, ~1%) (Figure 3).

Analysis of fecal SCFAs displays no different layout between "high viremia" and "viral suppression" conditions: As we noticed minor changes in fecal microbiome profile (just at the order and genus levels), we wondered if the GM metabolic activity had been altered as well, and whether this activity might be masked by simply examining the microbiota composition. In order to evaluate the presence of alterations in GM metabolic activity, the levels of microbial linear and branched SCFAs were measured in fecal samples for each patient. However, the analysis of linear SCFA (acetic, propionic, butyric, and valeric acids), and branched SCFA (isobutyric, isovaleric, and 2-metilbutyric acids) abundance did not reveal any significant change after 24 wk of therapy for each patient.

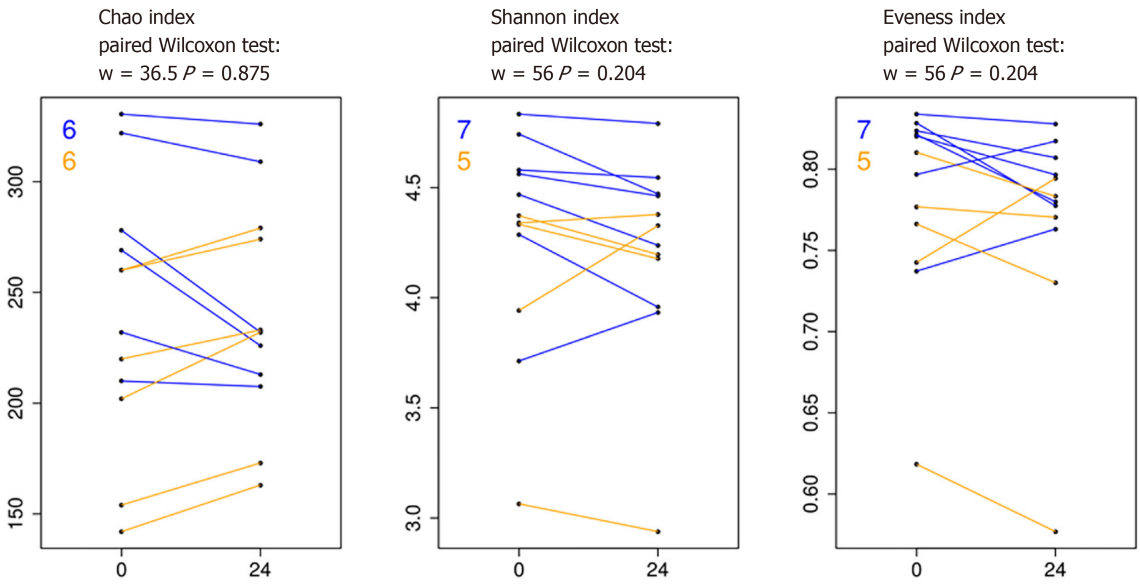

Figure 1 Box-plots showing alpha diversity indices (Chao1, Shannon, and evenness indices) in samples. Statistical differences were evaluated using paired Wilcoxon signed-rank test for Chao, Shannon, and evenness indices. *P* value less than 0.05 were considered statistically significant.

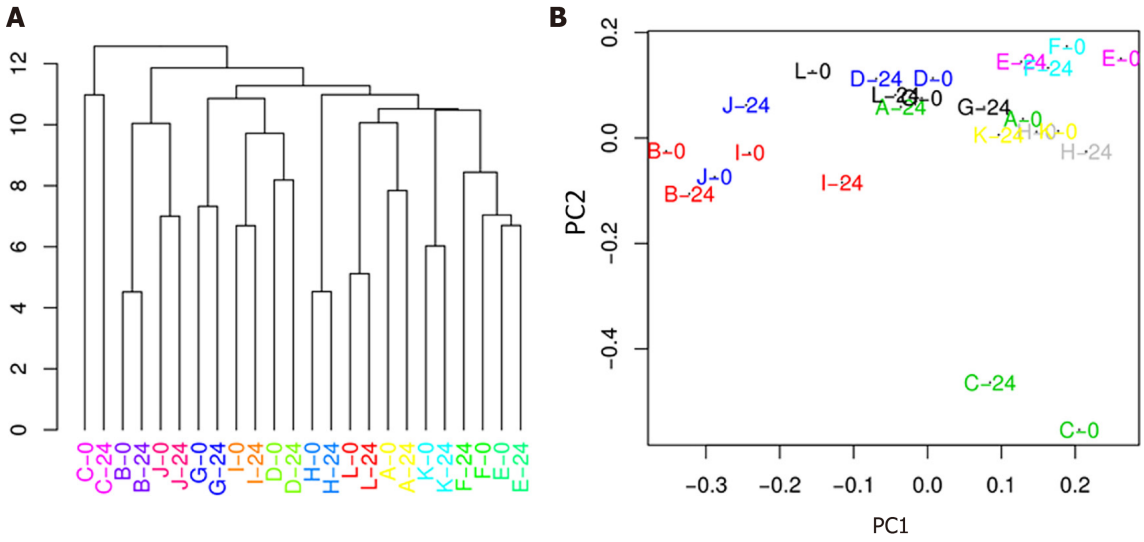

Figure 2 Cluster analysis (A) and principal coordinate analysis showing that samples do not separate into two groups depending on their condition (0-24 wk) (B).

Analysis of serum FFAs reveals a significantly different subgroup of SCFAs between "high viremia" and "viral suppression" conditions: As we did not report alterations in the composition of fecal SCFAs, we wanted to observe if there were any other alterations in metabolic output, by analyzing both microbial and host derived FFAs in serum. As known, the impairment of gut integrity due to dysbiosis condition, leads to translocation of microbial elements from the intestinal mucosa to the bloodstream, which is considered a major driving force of chronic immune activation [49] even in patients successfully treated with ART and achieving stable virological suppression[2].

The analysis of serum FFA levels showed a significant change of two SCFAs at T24 compared to the baseline. In particular, propionic and butyric acids were increased in viral suppression condition (Figure 4).

Inflammatory profile between high viremia and viral suppression conditions: As known, gut microbial dysbiosis is linked to aberrant immune responses, as alterations in the GM may induce the interruption of gut epithelial barrier integrity with subsequent microbial translocation, increased inflammation, and immune activation,

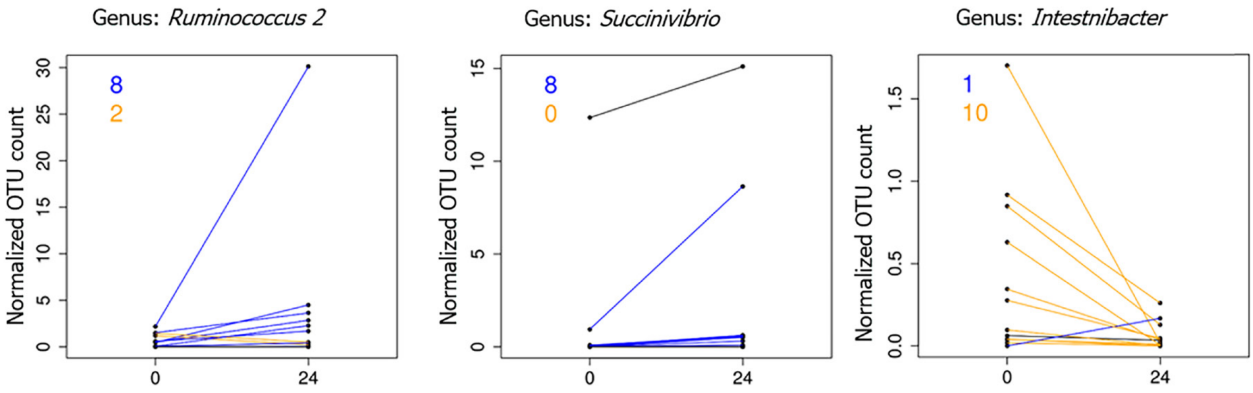

Figure 3 Segment plots depicting taxa with significantly differences between high viremia (time point 0) and viral suppression (time point 24) conditions. Lines connect paired samples and highlight the differences in normalized abundance for the indicated rank. Orange or blue colors highlight decrease or increase, respectively. Numbers in the top-left corner represent counts of increased (orange) and decreased (blue) measurement for paired samples.

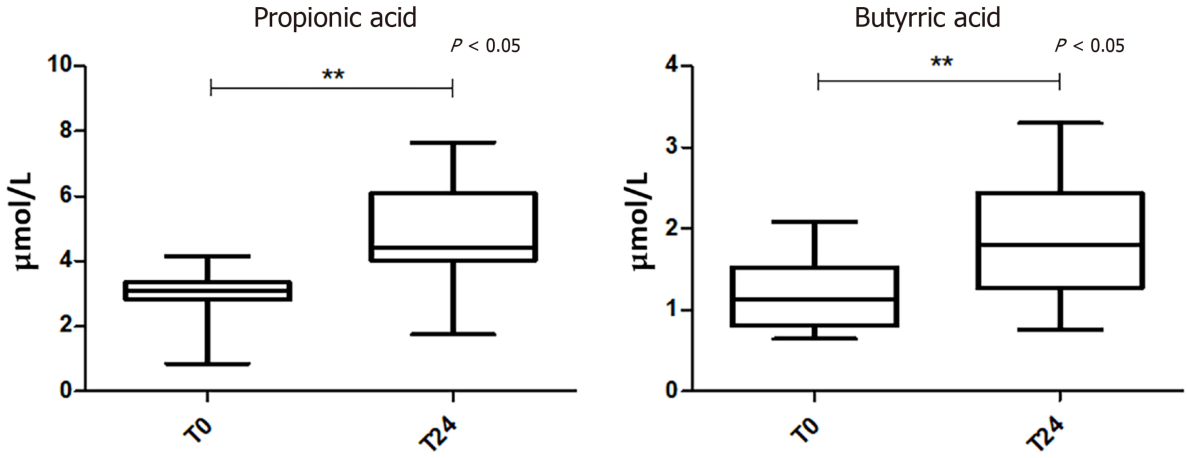

Figure 4 Boxplots showing statistically different levels of serum short-chain fatty acids between high viremia and viral suppressor patients, assessed by the Wilcoxon test. *P* value < 0.05 was considered statistically significant.

which are often accompanied by abnormal differentiation of immunological cells[6, 50]. Since we detected significant variations of microbial communities between high viremia and viral suppression conditions, we decided to characterize also the serum immunological profile by evaluating a panel of 27 cytokines between the two mentioned conditions. Among the 27 cytokines examined, we detected a significant reduction of IP-10 ($P = 0.0244$) and a significant increment of IL-8 levels ($P = 0.0547$) in the high viremia setting (Figure 5).

Association of GM composition and metabolic and inflammatory profiles with CD4⁺ T-cell counts

Correlation between fecal microbiota and CD4/CD8 ratio: In the second part of our study, we divided our cohort of patients into two groups: Immunological responders (IRs) and immunological non-responders (INRs), based on the CD4/CD8 ratio > 1 or < 1. In this condition, the analysis of microbiota revealed that, considering only taxa with an overall abundance higher than 1%, members of the *Faecalibacteria* genus were significantly reduced (adj. $P < 0.05$, logFC = 1.32) while members of the *Alistipes* genus were significantly increased in responders (adj. $P < 0.05$, logFC = 2.5) (Figure 6).

Different branched SCFA profiles in serum and fecal samples between IRs and INRs: As we observed significant variations in the composition of the fecal microbiota between IRs and INRs, we assessed if there were any other alterations in the fecal and serum microbial metabolites as linear and branched SCFAs derived from bacterial metabolism. We documented significant changes in isobutyric ($P = 0.01$), isovaleric ($P = 0.04$), and 2-methylbutyric ($P = 0.04$) acids, which were increased in IR fecal samples

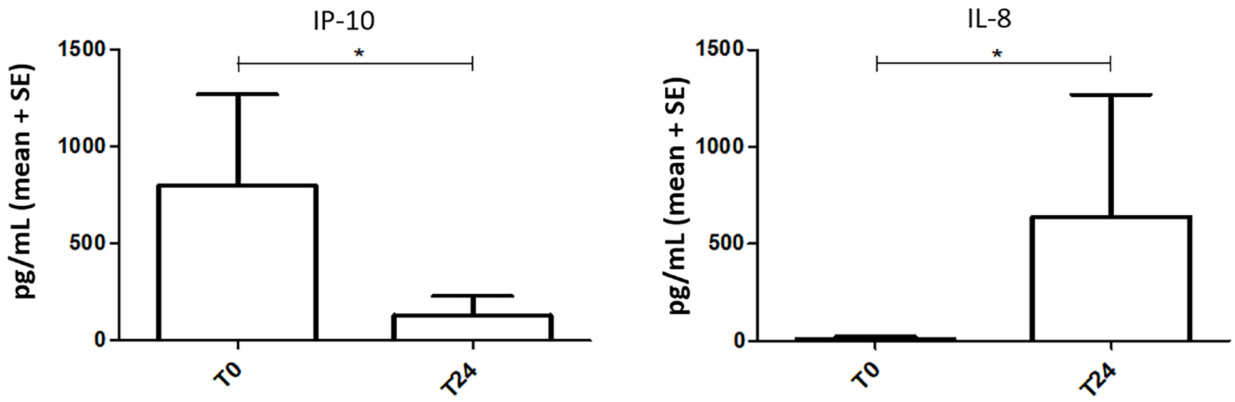

Figure 5 Boxplots showing statistically different levels of serum cytokines between high viremia and viral suppressor patients, assessed by the Wilcoxon test. A *P* value < 0.05 was considered statistically significant.

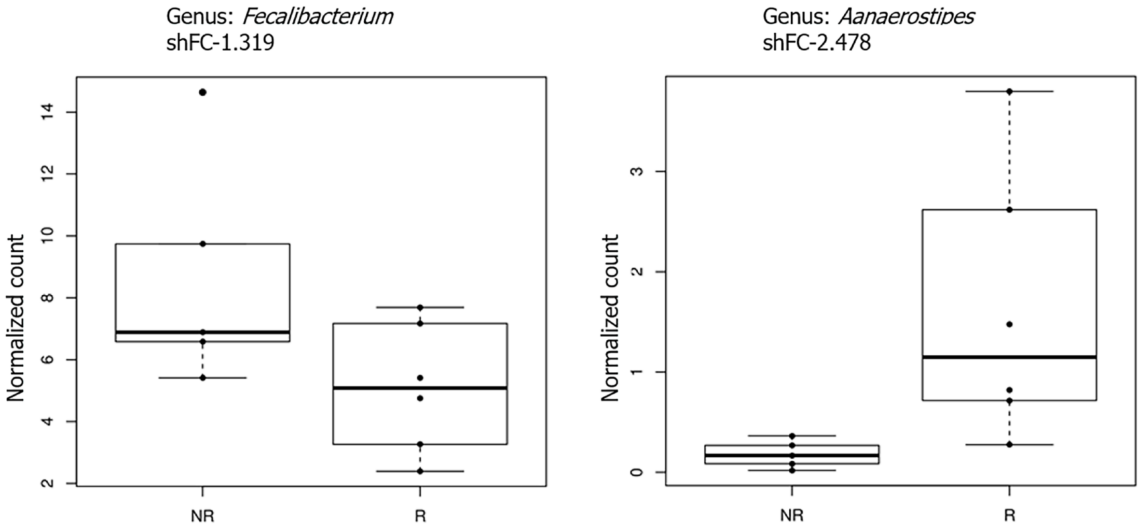

Figure 6 Boxplots showing the results of taxa-level differential abundance analysis between immunological responders and immunological non-responders at 24 wk. Plot titles report the shrunk Log2 fold change (according to the DESeq2 function lfcShrink). All results have a *P* value < 0.05. NR = INRs, R = IRs. IRs: Immunological responders; INRs: Immunological non-responders.

while we did not detect significant differences in serum samples (Figure 7).

Inflammatory profile shows no significant differences between IRs and INRs: Since we detected significant variations of microbial communities between IRs and INRs, we also evaluated the serum immunological profile. However, cytokine levels did not show significant variations between the IRs and INRs.

DISCUSSION

Currently, the mechanisms regulating the interplay between the host immune system and HIV-1, as well as the exact changes occurring in the GM composition and functionality, remain to be defined. To clarify the intricate relationships between the actors of the "microbiota-immunity" axis, we examined microbiota composition and functionality (SCFAs), serum inflammatory response, and FFA composition in individuals undergoing ART in different HIV infection settings.

Today, many studies on microbiota have been performed chiefly comparing HIV-infected and uninfected individuals, revealing a reduced GM diversity (the so-called HIV-associated dysbiosis) and an independent association between alpha-diversity of microbiota and peripheral levels of $CD4^+$ T cell count in treatment-naïve HIV-infected patients[28]. However, cross-sectional studies may not be suitable to provide information about cause-and-effect relationships, whereas longitudinal ones could be

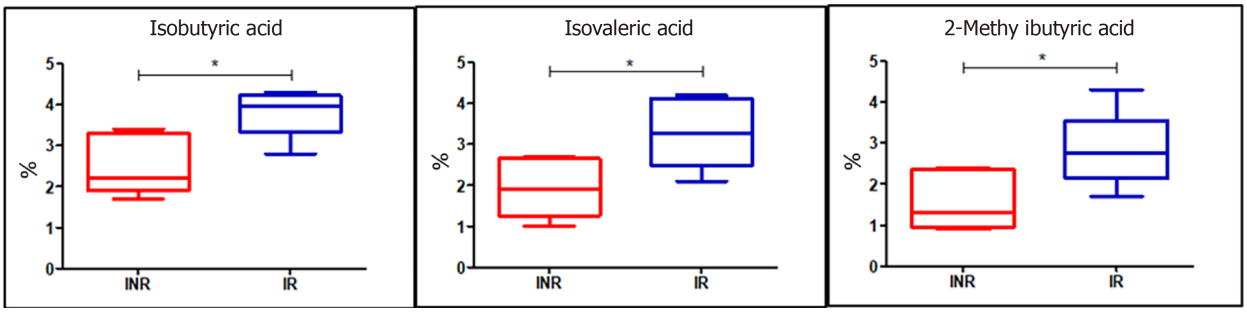

Figure 7 Boxplots showing statistically different fecal short-chain fatty acid abundances between immunological responders and immunological non-responders, assessed by the Mann-Whitney test. [a]*P* value < 0.05 was considered statistically significant.

more valid for examining such relationships. Besides, there is a lack of human longitudinal observations of the "microbiota-immunity" axis before and after first ART administration. Only in few longitudinal studies, where HIV-1-infected participants were followed after ART starting, data obtained on bacterial flora showed that shifts in the fecal microbiota persisted in a number of patients[10,28]. On the other hand, a recent study by Dillon *et al*[14] failed to find a significant change in a single time point study of the stool of HIV-1-infected patients.

In this study, we first performed a longitudinal investigation evaluating the GM before the treatment and after "viral suppression" (T24). According to the longitudinal study conducted by Dillon *et al*[14], our results showed modest changes in the GM composition after ART; indeed, we did not assess significant differences in phylum composition. However, the paired comparison of the abundance of single bacterial taxa revealed a significant alteration at the genus level between the two sample groups (Figure 3). In particular, the genera of *Ruminococcus*, and *Succinivibrio* were significantly increased after ART and the viral suppression. Conversely, the genus of *Intestinibacter* was significantly decreased in the same condition. We hypothesize that the slight change between the two groups may be due to persistent inflammation (related to microbial translocation and reduced immunoregulatory function), HIV latency throughout the gut, and direct effects of antiretroviral drugs on the bacterial population. Moreover, our results are in accordance with other longitudinal previous studies in non-human primates, which allowed to control for confounders affecting human studies[51,52]. We also reported an increase of the genus *Succinivibrio* (*Proteobacteria* phylum) between the two samples groups. In addition, in agreement with our data, the proportion of the rare genus *Succinivibrio*, was also found considerably high in the stool of Japanese patients treated with ART[53]. One of the possible reasons for the contradictory results reported in the examined different studies may include the cross-sectional nature of the study, the used sampling method (stool swab *vs* stool), and the microbial taxon level applied.

Based on our findings, the 24 wk of ART inhibited HIV-1 viral replication effectively (indeed, all enrolled patients reached viral suppression), but did not heavily affect the overall bacterial composition of the gut microenvironment. The modest GM diversity that we observed between the two sample groups might be associated with the lowering of viremia. However, there was evidence that ART also induces changes in the gut microbiome, unrelated to HIV infection. Some authors have implied that ART may enhance dysbiosis, which is consistent with the high frequency of gastrointestinal side effects of this treatment[28,54].

As the GM influences the immune system through their bacterial metabolites, like SCFAs[55,56], we measured SCFA levels in blood and stool samples, in order to have a more accurate assessment of microbial metabolism after the ART. As known, the main SCFAs include, in order of proportion, acetic, propionic, and butyric acids that are produced by fibres fermentation by gut bacteria, particularly by members of the *Firmicutes* phylum[57]. Interestingly, for the first time, we observed a significant change of two serum SCFAs after the ART. In particular, propionic and butyric acids were increased in "viral suppression" condition. This altered SCFA profile may indicate a potential role for the SCFA synthesis pathway in the regulation of the HIV "microbiota-immunity" axis during effective ART. Notably, we did not observe any significant SCFA changes in stool samples, probably because in the colon, about 95% of the produced SCFAs are rapidly absorbed by large intestinal mucosal cells while the remaining 5% are secreted in the feces[58]. Propionate is only present at a low concentration in the periphery because it is metabolized in the liver[59]. It has been shown

that butyrate may reduce gut inflammation by inducing the regulatory T cells (Tregs) and modulating activation of antigen-presenting cells[17]. We may speculate that bacterial flora responds reciprocally to inflammation by increasing the biosynthesis of anti-inflammatory and pro-solving lipid mediators that circulate in the bloodstream. Altogether, it is plausible that immune system-bacteria synergism mediates solutions to inflammation. On the contrary, as previously reported, some studies have found that butyrate-producing bacteria are selectively reduced in stool samples from HIV-infected compared to non-infected subjects[17,54]. In particular, Serrano-Villar *et al*[60] found that HIV-infected individuals had a distinct SCFA profile in stool compared to HIV-negative controls, with increased propionate and lower levels of acetate. No data from the literature are available regarding SCFA levels in HIV$^+$ serum samples, except a study of Segal *et al*[61] reporting that higher values of serum SCFAs, in consequence of an increased abundance of pulmonary anaerobic bacteria in HIV+ patients on ART, inhibited the immune response to *M. tuberculosis*, likely enhancing tuberculosis susceptibility. They observed that baseline serum butyrate and propionate were associated with the subsequent increasing hazard of tuberculosis. Moreover, we also evaluated serum FFA composition before and after ART treatment. Indeed, increased levels of FFA and proinflammatory cytokines have been reported in some HIV-infected patients under ART (reviewed in reference[62]). However, we did not appreciate any difference at the examined two time points.

Regarding the inflammation tone, there is consensus that a pro-inflammatory status remains active even after ART initiation in most patients[63,64]. Since the HIV life cycle is suppressed through ART in treated patients, the chronic inflammatory status observed in patients is maintained by factors secondary to HIV replication, including microbial translocation and reduced immunoregulatory function. In order to evaluate the inflammatory status after ART, we measured a panel of selected multifunctional effector molecules of the immune response in serum. Among the measured cytokines, we observed a decrease of IP-10 (P = 0.0244) after the treatment, confirming the downregulation of this chemokine production in patients with HIV infection during ART[65-69]. IP-10 is involved in trafficking immune cells to inflammatory sites, and it is considered an important pro-inflammatory factor in the HIV disease process. It has been observed that its levels can be reduced, but not to normal levels, by ART administration. Interestingly, IP-10 was consistently associated with HIV disease progression (based on CD4$^+$ counts) during the period[70], suggesting its potential for use as an indicator of HIV infection and/or a therapeutic target for HIV treatment[71]. On the other hand, in agreement with recent data, we observed a significant increased trend of IL-8 levels (P = 0.0547) with suppressed viral load after 24 wk of ART. Indeed, increased IL-8 levels were observed in HIV-infected individuals on ART[72]. It has been shown that during HIV-1 infection, IL-8 plays an important role in the recruitment of CD4$^+$ T cells to the lymph nodes, thus generating more targets for viral replication. Our results may suggest that increased IL-8 Levels may represent a hallmark of chronic inflammation in HIV$^+$ patients on ART. In accordance with our findings, Wada *et al*[73] observed significantly higher circulating IL-8 levels in HIV$^+$ men on ART with suppressed viral load in comparison to HIV-uninfected men.

It is now established that the gut microbiome may play a crucial role in the immune activation in HIV-infected patients treated with ART[5,64,73-75]. Recently, several studies have reported that GM is associated with CD4$^+$ T cell recovery in HIV-infected patients, playing an essential role in the reconstitution of immune function[76-78]. The potential mechanism includes the formation of a virus shelter, resistance to ART, promotion of intestinal mucosal barrier damage, and further entry of intestinal bacteria and their metabolites into the circulatory system, resulting in long-term immune activation, inflammation, and metabolic disorders such as cardiovascular diseases, diabetes mellitus, liver steatosis, and lastly, cancer[8]. Although it remains unclear whether an altered immunity after HIV infection drives dysbiosis or *vice versa*, the gut dysbiosis, immune dysfunction, epithelial damage, and microbial translocation are still evident even in the setting of ART-mediated viral suppression, which might be the treatment dilemma for HIV infection at present. Despite numerous studies of the microbiota in HIV-infected patients, there are relatively few reports discussing the compositional GM changes in patients with different immune responses to ART[79, 80].

To investigate the role of GM in immunomodulation and immune reconstitution and which bacterial metabolites are implicated, in the second part of the study, we divided the patients into two groups: Patients with CD4/CD4 ratio < 1 with insufficient reconstitution of CD4$^+$ T cells despite achieving virological suppression after 24 wk of ART and those with CD4/CD8 ≥ 1 who reached a robust reconstitution of CD4$^+$ T cells. We found that the *Anaerostipes* genus was significantly augmented in IRs; on

the contrary, the *Faecalibacterium* genus was significantly increased in INRs. Notably, *Faecalibacterium* has been reported as the anti-inflammatory commensal genus[81]. It has been positively correlated with the CD4/CD8 ratio and anti-correlated with inflammation markers and LPS in a recent study in HIV-infected patients[82].

Regarding microbial metabolites, we detected a significant increase in fecal isobutyric, isovaleric, and 2-methylbutyric acids in the IRs. However, we found that the changes associated with the IR group were not evident in the blood. Based on our results, we hypothesized that changes at the genus level in the gut ecosystem in HIV-infected patients undergoing ART might thus be both a consequence and a potential cause of the recovery of systemic immunity.

Our study had some limitations. First, a low number of patients were enrolled to investigate the elements of the microbiota-immunity axis and it cannot determine whether the altered GM contributed to or was caused by immune dysfunction. Second, only the effects of 24-wk ART were observed in our study, and to establish a more meaningful connection between GM and microbial/immune parameters, future studies should investigate the GM alterations and the restoration of immune function after long-term effective ART. Finally, the microbiota of feces was a proxy for GM in this study, which was the only realistic sample for a non-invasive study. However, fecal microbiota may only represent the GM composition in the lumen rather than on the mucosal surfaces, which is an important distinction because the mucosa-associated microbiota potentially interacts with the gut-associated lymphoid tissue in HIV-1-infected patients directly.

CONCLUSION

Our results provided an additional vision about the impact of HIV infection, ART, and immune recovery in the microbiota-immunity axis at the metabolism level, which are an indicator of the active processes occurring in the gastrointestinal tract. In summary, we demonstrated that patients infected by HIV-1, after reaching virological suppression with ART, displayed a fecal microbiota with unchanged overall bacterial diversity except for few genera. Although 24 wk of treatment with ART was effective, the systemic inflammatory tone was not completely restored despite the anti-inflammatory serum butyrate increment. In addition, we confirmed the role of the GM in immune reconstitution, with the possible implication of bacterial metabolites; however, changes in the gut ecosystem in HIV$^+$ patients undergoing 24 wk of ART may thus be both a consequence and a potential cause of the recovery of systemic immunity.

Future larger-scale, long-term ART and longitudinal studies that include functional metagenomic and metabolomic approaches to identify the roles of the specific differential phylotypes are required to better define the relationship between microbiota-immunity axis and HIV-1 infection and to provide new insights into the targeted treatment, improving the immune recovery and dampening inflammation.

ARTICLE HIGHLIGHTS

Research background

Human immunodeficiency virus type 1 (HIV-1) infection is characterized by persistent systemic inflammation and immune activation, even in patients receiving effective antiretroviral therapy (ART). Converging data suggest that gut microbiota (GM) changes can occur throughout including human immunodeficiency virus (HIV) infection treated by ART.

Research motivation

ART has increased the life expectancy of HIV-infected patients; however, chronic inflammation and gut microbiota alterations persist in patients virologically suppressed by ART. These data suggest that re-shaping the microbiota may be an adjuvant therapy in patients commencing successful ART.

Research objectives

The purpose of this prospective observational study was to compare for the first time the fecal microbial composition, serum and fecal microbial metabolites, and serum cytokine profile of treatment-naïve patients before starting ART and after reaching

virological suppression (HIV RNA < 50 copies/mL) after 24 wk of ART.

Research methods

The authors enrolled 12 treatment-naïve HIV-infected patients receiving ART. Fecal microbiota composition was assessed through next generation sequencing, and a comprehensive analysis of a broad spectrum of cytokines in blood was performed through a multiplex approach. In addition, serum free fatty acid (FFA) and fecal short chain fatty acid (SCFA) levels were measured through GC-MS.

Research results

The authors compared microbiota signatures, FFA levels, and cytokine profile before starting ART and after reaching virological suppression. Modest alterations were observed on microbiota composition; moreover, in the same condition, we also observed augmented levels of serum propionic and butyric acids. A reduction of serum IP-10 and an increase of IL-8 level were detected in the viral suppression condition. Thereafter, the same components were compared between immunological responders and non-responders. Concerning the microflora population, we detected a reduction of *Faecalibacterium* and an increase of *Alistipes* in immunological non-responders. Simultaneously, fecal isobutyric, isovaleric, and 2-methylbutyric acids were also increased in immunological non-responders.

Research conclusions

The results provid an additional perspective about the impact of HIV infection, ART, and immune recovery on the "microbiome-immunity axis" at the metabolism level. These factors can act as indicators of the active processes occurring in the gastrointestinal tract.

Research perspectives

Future larger-scale, long-term ART and longitudinal studies that include functional metagenomic and metabolomic approaches to identify the roles of the specific differential phylotypes are required to better define the relationship between microbiota-immunity axis and HIV-1 infection and to provide new insights into the targeted treatment, improving the immune recovery and dampening inflammation.

REFERENCES

1 **Vujkovic-Cvijin I**, Dunham RM, Iwai S, Maher MC, Albright RG, Broadhurst MJ, Hernandez RD, Lederman MM, Huang Y, Somsouk M, Deeks SG, Hunt PW, Lynch SV, McCune JM. Dysbiosis of the gut microbiota is associated with HIV disease progression and tryptophan catabolism. *Sci Transl Med* 2013; **5**: 193ra91 [PMID: 23843452 DOI: 10.1126/scitranslmed.3006438]

2 **Brenchley JM**, Price DA, Schacker TW, Asher TE, Silvestri G, Rao S, Kazzaz Z, Bornstein E, Lambotte O, Altmann D, Blazar BR, Rodriguez B, Teixeira-Johnson L, Landay A, Martin JN, Hecht FM, Picker LJ, Lederman MM, Deeks SG, Douek DC. Microbial translocation is a cause of systemic immune activation in chronic HIV infection. *Nat Med* 2006; **12**: 1365-1371 [PMID: 17115046 DOI: 10.1038/nm1511]

3 **Dinh DM**, Volpe GE, Duffalo C, Bhalchandra S, Tai AK, Kane AV, Wanke CA, Ward HD. Intestinal microbiota, microbial translocation, and systemic inflammation in chronic HIV infection. *J Infect Dis* 2015; **211**: 19-27 [PMID: 25057045 DOI: 10.1093/infdis/jiu409]

4 **Guadalupe M**, Reay E, Sankaran S, Prindiville T, Flamm J, McNeil A, Dandekar S. Severe CD4+ T-cell depletion in gut lymphoid tissue during primary human immunodeficiency virus type 1 infection and substantial delay in restoration following highly active antiretroviral therapy. *J Virol* 2003; **77**: 11708-11717 [PMID: 14557656 DOI: 10.1128/jvi.77.21.11708-11717.2003]

5 **Klatt NR**, Funderburg NT, Brenchley JM. Microbial translocation, immune activation, and HIV disease. *Trends Microbiol* 2013; **21**: 6-13 [PMID: 23062765 DOI: 10.1016/j.tim.2012.09.001]

6 **Marchetti G**, Tincati C, Silvestri G. Microbial translocation in the pathogenesis of HIV infection and AIDS. *Clin Microbiol Rev* 2013; **26**: 2-18 [PMID: 23297256 DOI: 10.1128/CMR.00050-12]

7 **Mehandru S**, Poles MA, Tenner-Racz K, Horowitz A, Hurley A, Hogan C, Boden D, Racz P, Markowitz M. Primary HIV-1 infection is associated with preferential depletion of CD4+ T lymphocytes from effector sites in the gastrointestinal tract. *J Exp Med* 2004; **200**: 761-770 [PMID: 15365095 DOI: 10.1084/jem.20041196]

8 **Zilberman-Schapira G**, Zmora N, Itav S, Bashiardes S, Elinav H, Elinav E. The gut microbiome in human immunodeficiency virus infection. *BMC Med* 2016; **14**: 83 [PMID: 27256449 DOI: 10.1186/s12916-016-0625-3]

9 **Rocafort M**, Noguera-Julian M, Rivera J, Pastor L, Guillén Y, Langhorst J, Parera M, Mandomando I, Carrillo J, Urrea V, Rodríguez C, Casadellà M, Calle ML, Clotet B, Blanco J, Naniche D, Paredes

R. Evolution of the gut microbiome following acute HIV-1 infection. *Microbiome* 2019; **7**: 73 [PMID: 31078141 DOI: 10.1186/s40168-019-0687-5]

10 **Lozupone CA**, Li M, Campbell TB, Flores SC, Linderman D, Gebert MJ, Knight R, Fontenot AP, Palmer BE. Alterations in the gut microbiota associated with HIV-1 infection. *Cell Host Microbe* 2013; **14**: 329-339 [PMID: 24034618 DOI: 10.1016/j.chom.2013.08.006]

11 **Mudd JC**, Brenchley JM. Gut Mucosal Barrier Dysfunction, Microbial Dysbiosis, and Their Role in HIV-1 Disease Progression. *J Infect Dis* 2016; **214** Suppl 2: S58-S66 [PMID: 27625432 DOI: 10.1093/infdis/jiw258]

12 **Klase Z**, Ortiz A, Deleage C, Mudd JC, Quiñones M, Schwartzman E, Klatt NR, Canary L, Estes JD, Brenchley JM. Dysbiotic bacteria translocate in progressive SIV infection. *Mucosal Immunol* 2015; **8**: 1009-1020 [PMID: 25586559 DOI: 10.1038/mi.2014.128]

13 **Pinto-Cardoso S**, Lozupone C, Briceño O, Alva-Hernández S, Téllez N, Adriana A, Murakami-Ogasawara A, Reyes-Terán G. Fecal Bacterial Communities in treated HIV infected individuals on two antiretroviral regimens. *Sci Rep* 2017; **7**: 43741 [PMID: 28262770 DOI: 10.1038/srep43741]

14 **Dillon SM**, Lee EJ, Kotter CV, Austin GL, Dong Z, Hecht DK, Gianella S, Siewe B, Smith DM, Landay AL, Robertson CE, Frank DN, Wilson CC. An altered intestinal mucosal microbiome in HIV-1 infection is associated with mucosal and systemic immune activation and endotoxemia. *Mucosal Immunol* 2014; **7**: 983-994 [PMID: 24399150 DOI: 10.1038/mi.2013.116]

15 **Mutlu EA**, Keshavarzian A, Losurdo J, Swanson G, Siewe B, Forsyth C, French A, Demarais P, Sun Y, Koenig L, Cox S, Engen P, Chakradeo P, Abbasi R, Gorenz A, Burns C, Landay A. A compositional look at the human gastrointestinal microbiome and immune activation parameters in HIV infected subjects. *PLoS Pathog* 2014; **10**: e1003829 [PMID: 24586144 DOI: 10.1371/journal.ppat.1003829]

16 **Vázquez-Castellanos JF**, Serrano-Villar S, Latorre A, Artacho A, Ferrús ML, Madrid N, Vallejo A, Sainz T, Martínez-Botas J, Ferrando-Martínez S, Vera M, Dronda F, Leal M, Del Romero J, Moreno S, Estrada V, Gosalbes MJ, Moya A. Altered metabolism of gut microbiota contributes to chronic immune activation in HIV-infected individuals. *Mucosal Immunol* 2015; **8**: 760-772 [PMID: 25407519 DOI: 10.1038/mi.2014.107]

17 **Dillon SM**, Kibbie J, Lee EJ, Guo K, Santiago ML, Austin GL, Gianella S, Landay AL, Donovan AM, Frank DN, McCARTER MD, Wilson CC. Low abundance of colonic butyrate-producing bacteria in HIV infection is associated with microbial translocation and immune activation. *AIDS* 2017; **31**: 511-521 [PMID: 28002063 DOI: 10.1097/QAD.0000000000001366]

18 **Tincati C**, Douek DC, Marchetti G. Gut barrier structure, mucosal immunity and intestinal microbiota in the pathogenesis and treatment of HIV infection. *AIDS Res Ther* 2016; **13**: 19 [PMID: 27073405 DOI: 10.1186/s12981-016-0103-1]

19 **Parbie PK**, Mizutani T, Ishizaka A, Kawana-Tachikawa A, Runtuwene LR, Seki S, Abana CZ, Kushitor D, Bonney EY, Ofori SB, Uematsu S, Imoto S, Kimura Y, Kiyono H, Ishikawa K, Ampofo WK, Matano T. Dysbiotic Fecal Microbiome in HIV-1 Infected Individuals in Ghana. *Front Cell Infect Microbiol* 2021; **11**: 646467 [PMID: 34084754 DOI: 10.3389/fcimb.2021.646467]

20 **Luján JA**, Rugeles MT, Taborda NA. Contribution of the Microbiota to Intestinal Homeostasis and its Role in the Pathogenesis of HIV-1 Infection. *Curr HIV Res* 2019; **17**: 13-25 [PMID: 30854974 DOI: 10.2174/1570162X17666190311114808]

21 **Dillon SM**, Manuzak JA, Leone AK, Lee EJ, Rogers LM, McCarter MD, Wilson CC. HIV-1 infection of human intestinal lamina propria CD4+ T cells in vitro is enhanced by exposure to commensal Escherichia coli. *J Immunol* 2012; **189**: 885-896 [PMID: 22689879 DOI: 10.4049/jimmunol.1200681]

22 **Wu GD**, Chen J, Hoffmann C, Bittinger K, Chen YY, Keilbaugh SA, Bewtra M, Knights D, Walters WA, Knight R, Sinha R, Gilroy E, Gupta K, Baldassano R, Nessel L, Li H, Bushman FD, Lewis JD. Linking long-term dietary patterns with gut microbial enterotypes. *Science* 2011; **334**: 105-108 [PMID: 21885731 DOI: 10.1126/science.1208344]

23 **David LA**, Materna AC, Friedman J, Campos-Baptista MI, Blackburn MC, Perrotta A, Erdman SE, Alm EJ. Host lifestyle affects human microbiota on daily timescales. *Genome Biol* 2014; **15**: R89 [PMID: 25146375 DOI: 10.1186/gb-2014-15-7-r89]

24 **Li SX**, Armstrong A, Neff CP, Shaffer M, Lozupone CA, Palmer BE. Complexities of Gut Microbiome Dysbiosis in the Context of HIV Infection and Antiretroviral Therapy. *Clin Pharmacol Ther* 2016; **99**: 600-611 [PMID: 26940481 DOI: 10.1002/cpt.363]

25 **Pinto-Cardoso S**, Klatt NR, Reyes-Terán G. Impact of antiretroviral drugs on the microbiome: unknown answers to important questions. *Curr Opin HIV AIDS* 2018; **13**: 53-60 [PMID: 29028667 DOI: 10.1097/COH.0000000000000428]

26 **Marcus JL**, Leyden WA, Alexeeff SE, Anderson AN, Hechter RC, Hu H, Lam JO, Towner WJ, Yuan Q, Horberg MA, Silverberg MJ. Comparison of Overall and Comorbidity-Free Life Expectancy Between Insured Adults With and Without HIV Infection, 2000-2016. *JAMA Netw Open* 2020; **3**: e207954 [PMID: 32539152 DOI: 10.1001/jamanetworkopen.2020.7954]

27 **Ancona G**, Merlini E, Tincati C, Barassi A, Calcagno A, Augello M, Bono V, Bai F, Cannizzo ES, d'Arminio Monforte A, Marchetti G. Long-Term Suppressive cART Is Not Sufficient to Restore Intestinal Permeability and Gut Microbiota Compositional Changes. *Front Immunol* 2021; **12**: 639291 [PMID: 33717191 DOI: 10.3389/fimmu.2021.639291]

28 **Nowak P**, Troseid M, Avershina E, Barqasho B, Neogi U, Holm K, Hov JR, Noyan K, Vesterbacka J, Svärd J, Rudi K, Sönnerborg A. Gut microbiota diversity predicts immune status in HIV-1 infection.

AIDS 2015; **29**: 2409-2418 [PMID: 26355675 DOI: 10.1097/QAD.0000000000000869]

29 **Villanueva-Millán MJ**, Pérez-Matute P, Recio-Fernández E, Lezana Rosales JM, Oteo JA. Differential effects of antiretrovirals on microbial translocation and gut microbiota composition of HIV-infected patients. *J Int AIDS Soc* 2017; **20**: 21526 [PMID: 28362071 DOI: 10.7448/IAS.20.1.21526]

30 **Deusch S**, Serrano-Villar S, Rojo D, Martínez-Martínez M, Bargiela R, Vázquez-Castellanos JF, Sainz T, Barbas C, Moya A, Moreno S, Gosalbes MJ, Estrada V, Seifert J, Ferrer M. Effects of HIV, antiretroviral therapy and prebiotics on the active fraction of the gut microbiota. *AIDS* 2018; **32**: 1229-1237 [PMID: 29683848 DOI: 10.1097/QAD.0000000000001831]

31 **McHardy IH**, Li X, Tong M, Ruegger P, Jacobs J, Borneman J, Anton P, Braun J. HIV Infection is associated with compositional and functional shifts in the rectal mucosal microbiota. *Microbiome* 2013; **1**: 26 [PMID: 24451087 DOI: 10.1186/2049-2618-1-26]

32 **Flygel TT**, Sovershaeva E, Claassen-Weitz S, Hjerde E, Mwaikono KS, Odland JØ, Ferrand RA, Mchugh G, Gutteberg TJ, Nicol MP, Cavanagh JP, Flægstad T; BREATHE Study Team. Composition of Gut Microbiota of Children and Adolescents With Perinatal Human Immunodeficiency Virus Infection Taking Antiretroviral Therapy in Zimbabwe. *J Infect Dis* 2020; **221**: 483-492 [PMID: 31549151 DOI: 10.1093/infdis/jiz473]

33 **Serrano-Villar S**, Sainz T, Lee SA, Hunt PW, Sinclair E, Shacklett BL, Ferre AL, Hayes TL, Somsouk M, Hsue PY, Van Natta ML, Meinert CL, Lederman MM, Hatano H, Jain V, Huang Y, Hecht FM, Martin JN, McCune JM, Moreno S, Deeks SG. HIV-infected individuals with low CD4/CD8 ratio despite effective antiretroviral therapy exhibit altered T cell subsets, heightened CD8+ T cell activation, and increased risk of non-AIDS morbidity and mortality. *PLoS Pathog* 2014; **10**: e1004078 [PMID: 24831517 DOI: 10.1371/journal.ppat.1004078]

34 **McBride JA**, Striker R. Imbalance in the game of T cells: What can the CD4/CD8 T-cell ratio tell us about HIV and health? *PLoS Pathog* 2017; **13**: e1006624 [PMID: 29095912 DOI: 10.1371/journal.ppat.1006624]

35 **Serrano-Villar S**, Pérez-Elías MJ, Dronda F, Casado JL, Moreno A, Royuela A, Pérez-Molina JA, Sainz T, Navas E, Hermida JM, Quereda C, Moreno S. Increased risk of serious non-AIDS-related events in HIV-infected subjects on antiretroviral therapy associated with a low CD4/CD8 ratio. *PLoS One* 2014; **9**: e85798 [PMID: 24497929 DOI: 10.1371/journal.pone.0085798]

36 **Kelly CJ**, Zheng L, Campbell EL, Saeedi B, Scholz CC, Bayless AJ, Wilson KE, Glover LE, Kominsky DJ, Magnuson A, Weir TL, Ehrentraut SF, Pickel C, Kuhn KA, Lanis JM, Nguyen V, Taylor CT, Colgan SP. Crosstalk between Microbiota-Derived Short-Chain Fatty Acids and Intestinal Epithelial HIF Augments Tissue Barrier Function. *Cell Host Microbe* 2015; **17**: 662-671 [PMID: 25865369 DOI: 10.1016/j.chom.2015.03.005]

37 **Kim CH**, Park J, Kim M. Gut microbiota-derived short-chain Fatty acids, T cells, and inflammation. *Immune Netw* 2014; **14**: 277-288 [PMID: 25550694 DOI: 10.4110/in.2014.14.6.277]

38 **Corrêa-Oliveira R**, Fachi JL, Vieira A, Sato FT, Vinolo MA. Regulation of immune cell function by short-chain fatty acids. *Clin Transl Immunology* 2016; **5**: e73 [PMID: 27195116 DOI: 10.1038/cti.2016.17]

39 **Effros RB**, Cai Z, Linton PJ. CD8 T cells and aging. *Crit Rev Immunol* 2003; **23**: 45-64 [PMID: 12906259 DOI: 10.1615/critrevimmunol.v23.i12.30]

40 **Pagliai G**, Russo E, Niccolai E, Dinu M, Di Pilato V, Magrini A, Bartolucci G, Baldi S, Menicatti M, Giusti B, Marcucci R, Rossolini GM, Casini A, Sofi F, Amedei A. Influence of a 3-month low-calorie Mediterranean diet compared to the vegetarian diet on human gut microbiota and SCFA: the CARDIVEG Study. *Eur J Nutr* 2020; **59**: 2011-2024 [PMID: 31292752 DOI: 10.1007/s00394-019-02050-0]

41 **Bolyen E**, Rideout JR, Dillon MR, Bokulich NA, Abnet CC, Al-Ghalith GA, Alexander H, Alm EJ, Arumugam M, Asnicar F, Bai Y, Bisanz JE, Bittinger K, Brejnrod A, Brislawn CJ, Brown CT, Callahan BJ, Caraballo-Rodríguez AM, Chase J, Cope EK, Da Silva R, Diener C, Dorrestein PC, Douglas GM, Durall DM, Duvallet C, Edwardson CF, Ernst M, Estaki M, Fouquier J, Gauglitz JM, Gibbons SM, Gibson DL, Gonzalez A, Gorlick K, Guo J, Hillmann B, Holmes S, Holste H, Huttenhower C, Huttley GA, Janssen S, Jarmusch AK, Jiang L, Kaehler BD, Kang KB, Keefe CR, Keim P, Kelley ST, Knights D, Koester I, Kosciolek T, Kreps J, Langille MGI, Lee J, Ley R, Liu YX, Loftfield E, Lozupone C, Maher M, Marotz C, Martin BD, McDonald D, McIver LJ, Melnik AV, Metcalf JL, Morgan SC, Morton JT, Naimey AT, Navas-Molina JA, Nothias LF, Orchanian SB, Pearson T, Peoples SL, Petras D, Preuss ML, Pruesse E, Rasmussen LB, Rivers A, Robeson MS 2nd, Rosenthal P, Segata N, Shaffer M, Shiffer A, Sinha R, Song SJ, Spear JR, Swafford AD, Thompson LR, Torres PJ, Trinh P, Tripathi A, Turnbaugh PJ, Ul-Hasan S, van der Hooft JJJ, Vargas F, Vázquez-Baeza Y, Vogtmann E, von Hippel M, Walters W, Wan Y, Wang M, Warren J, Weber KC, Williamson CHD, Willis AD, Xu ZZ, Zaneveld JR, Zhang Y, Zhu Q, Knight R, Caporaso JG. Reproducible, interactive, scalable and extensible microbiome data science using QIIME 2. *Nat Biotechnol* 2019; **37**: 852-857 [PMID: 31341288 DOI: 10.1038/s41587-019-0209-9]

42 **Callahan BJ**, McMurdie PJ, Rosen MJ, Han AW, Johnson AJ, Holmes SP. DADA2: High-resolution sample inference from Illumina amplicon data. *Nat Methods* 2016; **13**: 581-583 [PMID: 27214047 DOI: 10.1038/nmeth.3869]

43 **Niccolai E**, Baldi S, Ricci F, Russo E, Nannini G, Menicatti M, Poli G, Taddei A, Bartolucci G, Calabrò AS, Stingo FC, Amedei A. Evaluation and comparison of short chain fatty acids composition in gut diseases. *World J Gastroenterol* 2019; **25**: 5543-5558 [PMID: 31576099 DOI:

10.3748/wjg.v25.i36.5543]
44 **Baldi S**, Menicatti M, Nannini G, Niccolai E, Russo E, Ricci F, Pallecchi M, Romano F, Pedone M, Poli G, Renzi D, Taddei A, Calabrò AS, Stingo FC, Bartolucci G, Amedei A. Free Fatty Acids Signature in Human Intestinal Disorders: Significant Association between Butyric Acid and Celiac Disease. *Nutrients* 2021; **13** [PMID: 33652681 DOI: 10.3390/nu13030742]
45 **McMurdie PJ**, Holmes S. phyloseq: an R package for reproducible interactive analysis and graphics of microbiome census data. *PLoS One* 2013; **8**: e61217 [PMID: 23630581 DOI: 10.1371/journal.pone.0061217]
46 **Love MI**, Huber W, Anders S. Moderated estimation of fold change and dispersion for RNA-seq data with DESeq2. *Genome Biol* 2014; **15**: 550 [PMID: 25516281 DOI: 10.1186/s13059-014-0550-8]
47 **Willis A**, Bunge J. Estimating diversity *via* frequency ratios. *Biometrics* 2015; **71**: 1042-1049 [PMID: 26038228 DOI: 10.1111/biom.12332]
48 **Russo E**, Giudici F, Ricci F, Scaringi S, Nannini G, Ficari F, Luceri C, Niccolai E, Baldi S, D'Ambrosio M, Ramazzotti M, Amedei A. Diving into Inflammation: A Pilot Study Exploring the Dynamics of the Immune-Microbiota Axis in Ileal Tissue Layers of Patients with Crohn's Disease. *J Crohns Colitis* 2021; **15**: 1500-1516 [PMID: 33611347 DOI: 10.1093/ecco-jcc/jjab034]
49 **Brenchley JM**, Douek DC. Microbial translocation across the GI tract. *Annu Rev Immunol* 2012; **30**: 149-173 [PMID: 22224779 DOI: 10.1146/annurev-immunol-020711-075001]
50 **Epple HJ**, Allers K, Tröger H, Kühl A, Erben U, Fromm M, Zeitz M, Loddenkemper C, Schulzke JD, Schneider T. Acute HIV infection induces mucosal infiltration with CD4+ and CD8+ T cells, epithelial apoptosis, and a mucosal barrier defect. *Gastroenterology* 2010; **139**: 1289-1300 [PMID: 20600014 DOI: 10.1053/j.gastro.2010.06.065]
51 **Raehtz KD**, Barrenäs F, Xu C, Busman-Sahay K, Valentine A, Law L, Ma D, Policicchio BB, Wijewardana V, Brocca-Cofano E, Trichel A, Gale M Jr, Keele BF, Estes JD, Apetrei C, Pandrea I. African green monkeys avoid SIV disease progression by preventing intestinal dysfunction and maintaining mucosal barrier integrity. *PLoS Pathog* 2020; **16**: e1008333 [PMID: 32119719 DOI: 10.1371/journal.ppat.1008333]
52 **Monaco CL**, Gootenberg DB, Zhao G, Handley SA, Ghebremichael MS, Lim ES, Lankowski A, Baldridge MT, Wilen CB, Flagg M, Norman JM, Keller BC, Luévano JM, Wang D, Boum Y, Martin JN, Hunt PW, Bangsberg DR, Siedner MJ, Kwon DS, Virgin HW. Altered Virome and Bacterial Microbiome in Human Immunodeficiency Virus-Associated Acquired Immunodeficiency Syndrome. *Cell Host Microbe* 2016; **19**: 311-322 [PMID: 26962942 DOI: 10.1016/j.chom.2016.02.011]
53 **Imahashi M**, Ode H, Kobayashi A, Nemoto M, Matsuda M, Hashiba C, Hamano A, Nakata Y, Mori M, Seko K, Nakahata M, Kogure A, Tanaka Y, Sugiura W, Yokomaku Y, Iwatani Y. Impact of long-term antiretroviral therapy on gut and oral microbiotas in HIV-1-infected patients. *Sci Rep* 2021; **11**: 960 [PMID: 33441754 DOI: 10.1038/s41598-020-80247-8]
54 **Noguera-Julian M**, Rocafort M, Guillén Y, Rivera J, Casadellà M, Nowak P, Hildebrand F, Zeller G, Parera M, Bellido R, Rodríguez C, Carrillo J, Mothe B, Coll J, Bravo I, Estany C, Herrero C, Saz J, Sirera G, Torrela A, Navarro J, Crespo M, Brander C, Negredo E, Blanco J, Guarner F, Calle ML, Bork P, Sönnerborg A, Clotet B, Paredes R. Gut Microbiota Linked to Sexual Preference and HIV Infection. *EBioMedicine* 2016; **5**: 135-146 [PMID: 27077120 DOI: 10.1016/j.ebiom.2016.01.032]
55 **Arpaia N**, Campbell C, Fan X, Dikiy S, van der Veeken J, deRoos P, Liu H, Cross JR, Pfeffer K, Coffer PJ, Rudensky AY. Metabolites produced by commensal bacteria promote peripheral regulatory T-cell generation. *Nature* 2013; **504**: 451-455 [PMID: 24226773 DOI: 10.1038/nature12726]
56 **Louis P**, Flint HJ. Diversity, metabolism and microbial ecology of butyrate-producing bacteria from the human large intestine. *FEMS Microbiol Lett* 2009; **294**: 1-8 [PMID: 19222573 DOI: 10.1111/j.1574-6968.2009.01514.x]
57 **Desai SN**, Landay AL. HIV and aging: role of the microbiome. *Curr Opin HIV AIDS* 2018; **13**: 22-27 [PMID: 29035948 DOI: 10.1097/COH.0000000000000433]
58 **Topping DL**, Clifton PM. Short-chain fatty acids and human colonic function: roles of resistant starch and nonstarch polysaccharides. *Physiol Rev* 2001; **81**: 1031-1064 [PMID: 11427691 DOI: 10.1152/physrev.2001.81.3.1031]
59 **Cummings JH**, Pomare EW, Branch WJ, Naylor CP, Macfarlane GT. Short chain fatty acids in human large intestine, portal, hepatic and venous blood. *Gut* 1987; **28**: 1221-1227 [PMID: 3678950 DOI: 10.1136/gut.28.10.1221]
60 **Bandera A**, De Benedetto I, Bozzi G, Gori A. Altered gut microbiome composition in HIV infection: causes, effects and potential intervention. *Curr Opin HIV AIDS* 2018; **13**: 73-80 [PMID: 29045252 DOI: 10.1097/COH.0000000000000429]
61 **Philips JA**. HIV-associated anaerobes ferment TB risk. *Sci Transl Med* 2017; **9** [PMID: 28490669 DOI: 10.1126/scitranslmed.aan3781]
62 **Villarroya F**, Domingo P, Giralt M. Drug-induced lipotoxicity: lipodystrophy associated with HIV-1 infection and antiretroviral treatment. *Biochim Biophys Acta* 2010; **1801**: 392-399 [PMID: 19800025 DOI: 10.1016/j.bbalip.2009.09.018]
63 **Hunt PW**. HIV and inflammation: mechanisms and consequences. *Curr HIV/AIDS Rep* 2012; **9**: 139-147 [PMID: 22528766 DOI: 10.1007/s11904-012-0118-8]
64 **Deeks SG**, Tracy R, Douek DC. Systemic effects of inflammation on health during chronic HIV infection. *Immunity* 2013; **39**: 633-645 [PMID: 24138880 DOI: 10.1016/j.immuni.2013.10.001]
65 **Yao Y**, Luo Y, He Y, Zheng Y, Zhang Q, Zhou H, Zeng S, Chen Z, He B, He M. The effect of a year of highly active antiretroviral therapy on immune reconstruction and cytokines in HIV/AIDS patients.

AIDS Res Hum Retroviruses 2013; **29**: 691-697 [PMID: 23151174 DOI: 10.1089/AID.2012.0275]

66 **Ramirez LA**, Arango TA, Thompson E, Naji M, Tebas P, Boyer JD. High IP-10 levels decrease T cell function in HIV-1-infected individuals on ART. *J Leukoc Biol* 2014; **96**: 1055-1063 [PMID: 25157027 DOI: 10.1189/jlb.3A0414-232RR]

67 **Cinque P**, Bestetti A, Marenzi R, Sala S, Gisslen M, Hagberg L, Price RW. Cerebrospinal fluid interferon-gamma-inducible protein 10 (IP-10, CXCL10) in HIV-1 infection. *J Neuroimmunol* 2005; **168**: 154-163 [PMID: 16091292 DOI: 10.1016/j.jneuroim.2005.07.002]

68 **Hattab S**, Guihot A, Guiguet M, Fourati S, Carcelain G, Caby F, Marcelin AG, Autran B, Costagliola D, Katlama C. Comparative impact of antiretroviral drugs on markers of inflammation and immune activation during the first two years of effective therapy for HIV-1 infection: an observational study. *BMC Infect Dis* 2014; **14**: 122 [PMID: 24589015 DOI: 10.1186/1471-2334-14-122]

69 **Relucio KI**, Beernink HT, Chen D, Israelski DM, Kim R, Holodniy M. Proteomic analysis of serum cytokine levels in response to highly active antiretroviral therapy (HAART). *J Proteome Res* 2005; **4**: 227-231 [PMID: 15822897 DOI: 10.1021/pr049930y]

70 **Jiao Y**, Zhang T, Wang R, Zhang H, Huang X, Yin J, Zhang L, Xu X, Wu H. Plasma IP-10 is associated with rapid disease progression in early HIV-1 infection. *Viral Immunol* 2012; **25**: 333-337 [PMID: 22788418 DOI: 10.1089/vim.2012.0011]

71 **Stylianou E**, Aukrust P, Bendtzen K, Müller F, Frøland SS. Interferons and interferon (IFN)-inducible protein 10 during highly active anti-retroviral therapy (HAART)-possible immunosuppressive role of IFN-alpha in HIV infection. *Clin Exp Immunol* 2000; **119**: 479-485 [PMID: 10691920 DOI: 10.1046/j.1365-2249.2000.01144.x]

72 **Ellwanger JH**, Valverde-Villegas JM, Kaminski VL, de Medeiros RM, Almeida SEM, Santos BR, de Melo MG, Hackenhaar FS, Chies JAB. Increased IL-8 levels in HIV-infected individuals who initiated ART with $CD4^+$ T cell counts <350 cells/mm^3 - A potential hallmark of chronic inflammation. *Microbes Infect* 2020; **22**: 474-480 [PMID: 32534178 DOI: 10.1016/j.micinf.2020.05.019]

73 **Nixon DE**, Landay AL. Biomarkers of immune dysfunction in HIV. *Curr Opin HIV AIDS* 2010; **5**: 498-503 [PMID: 20978393 DOI: 10.1097/COH.0b013e32833ed6f4]

74 **Klatt NR**, Chomont N, Douek DC, Deeks SG. Immune activation and HIV persistence: implications for curative approaches to HIV infection. *Immunol Rev* 2013; **254**: 326-342 [PMID: 23772629 DOI: 10.1111/imr.12065]

75 **Lederman MM**, Funderburg NT, Sekaly RP, Klatt NR, Hunt PW. Residual immune dysregulation syndrome in treated HIV infection. *Adv Immunol* 2013; **119**: 51-83 [PMID: 23886064 DOI: 10.1016/B978-0-12-407707-2.00002-3]

76 **Lu W**, Feng Y, Jing F, Han Y, Lyu N, Liu F, Li J, Song X, Xie J, Qiu Z, Zhu T, Routy B, Routy JP, Li T, Zhu B. Association Between Gut Microbiota and CD4 Recovery in HIV-1 Infected Patients. *Front Microbiol* 2018; **9**: 1451 [PMID: 30034377 DOI: 10.3389/fmicb.2018.01451]

77 **Ji Y**, Zhang F, Zhang R, Shen Y, Liu L, Wang J, Yang J, Tang Q, Xun J, Qi T, Wang Z, Song W, Tang Y, Chen J, Lu H. Changes in intestinal microbiota in HIV-1-infected subjects following cART initiation: influence of CD4+ T cell count. *Emerg Microbes Infect* 2018; **7**: 113 [PMID: 29934497 DOI: 10.1038/s41426-018-0117-y]

78 **Lee SC**, Chua LL, Yap SH, Khang TF, Leng CY, Raja Azwa RI, Lewin SR, Kamarulzaman A, Woo YL, Lim YAL, Loke P, Rajasuriar R. Enrichment of gut-derived Fusobacterium is associated with suboptimal immune recovery in HIV-infected individuals. *Sci Rep* 2018; **8**: 14277 [PMID: 30250162 DOI: 10.1038/s41598-018-32585-x]

79 **Siedner MJ**. START or SMART? *Open Forum Infect Dis* 2016; **3**: ofw032 [PMID: 26989755 DOI: 10.1093/ofid/ofw032]

80 **Havlir DV**, Currier JS. CROI 2015: Complications of HIV Infection and Antiretroviral Therapy. *Top Antivir Med* 2015; **23**: 56-65 [PMID: 25965312]

81 **Shaw KA**, Bertha M, Hofmekler T, Chopra P, Vatanen T, Srivatsa A, Prince J, Kumar A, Sauer C, Zwick ME, Satten GA, Kostic AD, Mulle JG, Xavier RJ, Kugathasan S. Dysbiosis, inflammation, and response to treatment: a longitudinal study of pediatric subjects with newly diagnosed inflammatory bowel disease. *Genome Med* 2016; **8**: 75 [PMID: 27412252 DOI: 10.1186/s13073-016-0331-y]

82 **Xie Y**, Sun J, Wei L, Jiang H, Hu C, Yang J, Huang Y, Ruan B, Zhu B. Altered gut microbiota correlate with different immune responses to HAART in HIV-infected individuals. *BMC Microbiol* 2021; **21**: 11 [PMID: 33407128 DOI: 10.1186/s12866-020-02074-1]

World Journal of Gastroenterology

Submit a Manuscript: https://www.f6publishing.com

World J Gastroenterol 2022 February 14; 28(6): 653-664

DOI: 10.3748/wjg.v28.i6.653

ISSN 1007-9327 (print) ISSN 2219-2840 (online)

ORIGINAL ARTICLE

Case Control Study

Atrophic gastritis and gastric cancer tissue miRNome analysis reveals hsa-miR-129-1 and hsa-miR-196a as potential early diagnostic biomarkers

Greta Varkalaite, Evelina Vaitkeviciute, Ruta Inciuraite, Violeta Salteniene, Simonas Juzenas, Vytenis Petkevicius, Rita Gudaityte, Antanas Mickevicius, Alexander Link, Limas Kupcinskas, Marcis Leja, Juozas Kupcinskas, Jurgita Skieceviciene

ORCID number: Greta Varkalaite 0000-0003-3488-2171; Evelina Vaitkeviciute 0000-0003-2525-1597; Ruta Inciuraite 0000-0002-5806-6155; Violeta Salteniene 0000-0002-7881-945X; Simonas Juzenas 0000-0001-9293-0691; Vytenis Petkevicius 0000-0002-1964-5226; Rita Gudaityte 0000-0001-7489-8069; Antanas Mickevicius 0000-0002-6208-7039; Alexander Link 0000-0002-9514-4562; Limas Kupčinskas 0000-0002-8689-9023; Marcis Leja 0000-0002-0319-8855; Juozas Kupcinskas 0000-0002-8760-7416; Jurgita Skieceviciene 0000-0002-4893-6612.

Author contributions: Varkalaite G, Leja M, Kupcinskas L, Kupcinskas J and Skieceviciene J contributed to study conception and designed the research; Gudaityte R, Petkevicius V and Mickevicius A collected material and clinical data from the participants; Varkalaite G and Vaitkeviciute E performed all the investigations, analysis of data and drafted the manuscript; Juzenas S and Inciuraite R reviewed and edited the manuscript; Salteniene V revised the article for important intellectual content; Link A, Kupcinskas J and Skieceviciene J approved the final version of the manuscript.

Greta Varkalaite, Evelina Vaitkeviciute, Ruta Inciuraite, Violeta Salteniene, Simonas Juzenas, Limas Kupcinskas, Jurgita Skieceviciene, Institute for Digestive Research, Lithuanian University of Health Sciences, Kaunas 44307, Lithuania

Vytenis Petkevicius, Juozas Kupcinskas, Department of Gastroenterology, Lithuanian University of Health Sciences, Kaunas 44307, Lithuania

Rita Gudaityte, Antanas Mickevicius, Department of Surgery, Lithuanian University of Health Sciences, Kaunas 44307, Lithuania

Alexander Link, Department of Gastroenterology, Hepatology and Infectious Diseases, Otto-von-Guericke University Hospital, Magdeburg 39120, Germany

Marcis Leja, Institute of Clinical and Preventive Medicine & Faculty of Medicine, University of Latvia, Riga 1586, Latvia

Corresponding author: Jurgita Skieceviciene, PhD, Senior Researcher, Institute for Digestive Research, Lithuanian University of Health Sciences, A. Mickeviciaus street 9, Kaunas 44307, Lithuania. jurgita.skieceviciene@lsmuni.lt

Abstract

BACKGROUND

Gastric cancer (GC) is one of the most frequently diagnosed tumor globally. In most cases, GC develops in a stepwise manner from chronic gastritis or atrophic gastritis (AG) to cancer. One of the major issues in clinical settings of GC is diagnosis at advanced disease stages resulting in poor prognosis. MicroRNAs (miRNAs) are small noncoding molecules that play an essential role in a variety of fundamental biological processes. However, clinical potential of miRNA profiling in the gastric cancerogenesis, especially in premalignant GC cases, remains unclear.

AIM

To evaluate the AG and GC tissue miRNomes and identify specific miRNAs' potential for clinical applications (*e.g.*, non-invasive diagnostics).

Institutional review board statement: The study was approved by the Kaunas Regional Biomedical Research Ethics Committee.

Informed consent statement: All study participants provided informed consent prior to study enrollment.

Conflict-of-interest statement: The authors have declared no conflicts of interest.

Data sharing statement: Technical appendix, statistical code, and dataset available from the corresponding author at jurgita.skieceviciene@lsmuni.lt.

STROBE statement: The authors have read the STROBE Statement-checklist of items, and the manuscript was prepared and revised according to the STROBE Statement-checklist of items.

Supported by the MULTIOMICS project that has received funding from European Social Fund (No. 09.3.3-LMT-K-712-01-0130) under grant agreement with the Research Council of Lithuania (LMTLT).

Country/Territory of origin: Lithuania

Specialty type: Gastroenterology and hepatology

Provenance and peer review: Unsolicited article; Externally peer reviewed.

Peer-review model: Single blind

Peer-review report's scientific quality classification

Grade A (Excellent): 0
Grade B (Very good): B, B
Grade C (Good): 0
Grade D (Fair): D
Grade E (Poor): 0

METHODS

Study included a total of 125 subjects: Controls (CON), AG, and GC patients. All study subjects were recruited at the Departments of Surgery or Gastroenterology, Hospital of Lithuanian University of Health Sciences and divided into the profiling (n = 60) and validation (n = 65) cohorts. Total RNA isolated from tissue samples was used for preparation of small RNA sequencing libraries and profiled using next-generation sequencing (NGS). Based on NGS data, deregulated miRNAs hsa-miR-129-1-3p and hsa-miR-196a-5p were analyzed in plasma samples of independent cohort consisting of CON, AG, and GC patients. Expression level of hsa-miR-129-1-3p and hsa-miR-196a-5p was determined using the quantitative real-time polymerase chain reaction and $2^{-\Delta\Delta Ct}$ method.

RESULTS

Results of tissue analysis revealed 20 differentially expressed miRNAs in AG group compared to CON group, 129 deregulated miRNAs in GC compared to CON, and 99 altered miRNAs comparing GC and AG groups. Only 2 miRNAs (hsa-miR-129-1-3p and hsa-miR-196a-5p) were identified to be step-wise deregulated in healthy-premalignant-malignant sequence. Area under the curve (AUC)-receiver operating characteristic analysis revealed that expression level of hsa-miR-196a-5p is significant for discrimination of CON *vs* AG, CON *vs* GC and AG *vs* GC and resulted in AUCs: 88.0%, 93.1% and 66.3%, respectively. Comparing results in tissue and plasma samples, hsa-miR-129-1-3p was significantly down-regulated in GC compared to AG (P = 0.0021 and P = 0.024, tissue and plasma, respectively). Moreover, analysis revealed that hsa-miR-215-3p/5p and hsa-miR-934 were significantly deregulated in GC based on *Helicobacter pylori* (*H. pylori*) infection status [log2 fold change (FC) = -4.52, P-adjusted = 0.02; log2FC = -4.00, P-adjusted = 0.02; log2FC = 6.09, P-adjusted = 0.02, respectively].

CONCLUSION

Comprehensive miRNome study provides evidence for gradual deregulation of hsa-miR-196a-5p and hsa-miR-129-1-3p in gastric carcinogenesis and found hsa-miR-215-3p/5p and hsa-miR-934 to be significantly deregulated in *H. pylori* carrying GC patients.

Key Words: Gastric cancer; Atrophic gastritis; Tumorigenesis; *Helicobacter pylori*; MicroRNAs; Biomarkers

Core Tip: In this research we aimed to evaluate microRNAs profiles of premalignant and malignant stages of gastric cancer (GC). To date this is the first study analyzing atrophic gastritis (AG) and GC tissue miRNomes in the subjects of European origin using next-generation sequencing approach. We showed that hsa-miR-196a-5p expression in tissue is significant for discrimination between controls and AG or GC, while hsa-miR-129-1-3p is potential candidate for non-invasive GC diagnostic. This study provides novel insights into complex GC pathogenesis cascade and might be highly significant for future studies of new AG or GC associated epigenetic markers or even diagnostic targets.

Citation: Varkalaite G, Vaitkeviciute E, Inciuraite R, Salteniene V, Juzenas S, Petkevicius V, Gudaityte R, Mickevicius A, Link A, Kupcinskas L, Leja M, Kupcinskas J, Skieceviciene J. Atrophic gastritis and gastric cancer tissue miRNome analysis reveals hsa-miR-129-1 and hsa-miR-196a as potential early diagnostic biomarkers. *World J Gastroenterol* 2022; 28(6): 653-664
URL: https://www.wjgnet.com/1007-9327/full/v28/i6/653.htm
DOI: https://dx.doi.org/10.3748/wjg.v28.i6.653

Received: September 13, 2021
Peer-review started: September 13, 2021
First decision: November 16, 2021
Revised: November 19, 2021
Accepted: January 19, 2022
Article in press: January 19, 2022
Published online: February 14, 2022

P-Reviewer: Gao W, Kotelevets SM
S-Editor: Wang JJ
L-Editor: A
P-Editor: Wang JJ

INTRODUCTION

Gastric cancer (GC) is the one of the most common malignancy and the fourth leading cause of cancer-related death worldwide[1]. Studies show, that in most cases GC development is a stepwise process: Chronic gastric mucosa inflammation progresses to atrophic gastritis (AG) or intestinal metaplasia (IM), which eventually may become predisposition to GC. This complex cascade involves many factors: *Helicobacter pylori* (*H. pylori*) infection, lifestyle, dietary habits, and genetic or epigenetic alterations, including miRNA expression changes[2,3]. One of the major concerns in diagnostics of GC is poor survival rate and prognosis, while this tumor is usually diagnosed at late stages. Therefore, investigation of the molecular mechanisms that are critical in the complex GC pathological cascade may help to identify novel therapeutic targets and consequently improve the disease prognosis. MicroRNAs (miRNAs) are small (approx 22 nt) non-coding RNA molecules that regulate gene expression by binding to the specific sites within 3′ untranslated regions of target mRNAs[4,5]. MiRNAs play very important role in many physiological and pathological processes as well as tumorigenesis and may function as either tumor-suppressors or as oncogenic miRNAs[6-8]. Studies have reported numerous differentially expressed miRNAs in malignant gastric tissues including members of miR-20, miR-451, miR-148, miR-223 families[9-11]. Despite the previous efforts and conducted miRNA studies in GC, the miRNome characterization of premalignant gastric condition - AG - remains largely unknown.

In this study, we aimed to investigate miRNome profile through GC tumorigenesis cascade including precancerous lesions, such as AG. Also, expression of two miRNAs (hsa-miR-129-1 and hsa-miR-196a) was analyzed in plasma samples of the independent cohort of AG and GC patients. Tissue miRNome analysis results revealed distinct miRNA profiles comparing controls (CON), AG, and GC groups. Also, our study findings show that two miRNAs: Hsa-miR-129-1 and hsa-miR-196a may be a relevant biomarker for GC diagnostics.

MATERIALS AND METHODS

Study population

The study included a total of 125 CON and patients diagnosed with AG and GC, who were divided into the profiling cohort of 60 subjects and validation cohort of 65 subjects. Tissue samples of profiling cohort were collected during the years 2007-2015, while plasma of participants in validation cohort was collected from years 2011-2019 at the Departments of Surgery and Gastroenterology, Hospital of Lithuanian University of Health Sciences (Kaunas, Lithuania). Clinical and phenotypic characteristics of subjects investigated in profiling and validation cohorts are presented in Table 1. *H. pylori* status was assessed using indirect ELISA to detect serum-specific IgG antigen (Virion/Serion GmbH, Germany). Control group consisted of subjects, who had no signs of atrophy or IM according to Operative Link on Gastritis Assessment (OLGA) staging system (stage 0)[12]. AG group consisted of individuals that had stage I-IV atrophy score in gastric mucosa by OLGA classification. Gastric adenocarcinoma in GC patients was verified by histology and classified according to the American Joint Committee on Cancer TNM Staging Classification and Lauren Classification[13,14]. Adjacent GC (GCaj) samples were biopsy samples obtained from endoscopically healthy appearing gastric mucosa at least 2 cm away from the primary tumor.

The study was approved by the Kaunas Regional Biomedical Research Ethics Committee (approval No BE-2-10 and BE-2-31) and performed in accordance with the Declaration of Helsinki. All study participants provided written informed consent before enrollment.

Total RNA extraction

Total RNA, including small RNA fraction, was isolated from CON, AG and GC tissues using miRNeasy Mini Kit (Qiagen, Germany) according to the manufacturer's instructions. Quantification of RNA was performed using Nanodrop2000 spectrophotometer (Thermo Fisher Scientific, United States) and quality of RNA samples was evaluated by Agilent 2100 Bioanalyzer (Agilent Technologies, United States). Circulating nucleic acids, including circulating miRNA fraction, was isolated using QIAamp Circulating Nucleic Acid Kit (Qiagen, Germany) according to manufacturer's instructions. All isolated samples were stored at -80 °C prior to further analysis.

Table 1 Demographic characteristics of profiling and validation cohorts

		Profiling cohort (*n* = 60)			Validation cohort (*n* = 65)		
		CON (*n* = 21)	AG (*n* = 19)	GC (*n* = 20)	CON (*n* = 11)	AG (*n* = 30)	GC (*n* = 24)
Age	Mean ± SD	58.29 ± 15.52	69.21 ± 8.78	64.95 ± 10.89	42.27 ± 12.89	68.01 ± 11.81	68.33 ± 11.27
Gender (*n*)	Male	5	3	15	5	9	18
	Female	16	16	5	6	21	6
***Helicobacter pylori* infection (*n*)**	Negative	12	10	8	-	17	9
	Positive	9	9	9	-	10	4
	Unknown	-	-	3	11	3	11
Differentiation grade (*n*)	G1	-	-	4	-	-	-
	G2	-	-	4	-	-	12
	G3	-	-	12	-	-	12
Lauren classification (*n*)	Diffuse	-	-	10	-	-	8
	Intestinal	-	-	10	-	-	13
	Mixed	-	-	-	-	-	2
	Unknown	-	-	-	-	-	1
T (*n*)	T1	-	-	6	-	-	3
	T2	-	-	2	-	-	5
	T3	-	-	8	-	-	9
	T4	-	-	4	-	-	6
	Unknown	-	-	-	-	-	1
N (*n*)	N0	-	-	10	-	-	6
	N1	-	-	2	-	-	5
	N2	-	-	3	-	-	4
	N3	-	-	5	-	-	8
	Unknown	-	-	-	-	-	1
M (*n*)	M0	-	-	7	-	-	14
	M1	-	-	2	-	-	9
	Unknown	-	-	11	-	-	1

SD: Standard deviation; CON: Control; AG: Atrophic gastritis; GC: Gastric cancer.

Small RNA-seq library preparation and next-generation sequencing

Small RNA libraries were prepared using Illumina TruSeq Small RNA Sample Preparation Kit (Illumina, United States) according to the manufacturer's protocol with 1 μg RNA input per sample followed by RNA 3′ adapter ligation, RNA 5′ adapter ligation, cDNA synthesis, polymerase chain reaction (PCR) amplification using unique barcode sequences for each sample and gel size-selection of small RNA library. The yield and quality of sequencing libraries were assessed using the Agilent 2100 Bioanalyzer (Agilent Technologies, United States). The small RNA libraries were randomized, pooled 24 samples per lane and sequenced using Illumina HiSeq 2500 (1 × 50 bp single-end reads).

Bioinformatics analysis of small RNA-seq data

Analysis of raw small RNA-seq data was performed by nf-core/smrnaseq pipeline v.1.0.0 including Nextflow v.20.07.1[15], Java v.11.0.7, and Docker v.19.03.12. In brief, all steps consisted of read quality control using FastQC v.0.11.9, removing 3′ adapter sequences with TrimGalore! v.0.6.5, mapping to mature and hairpin miRNAs (miRBase v.22.1[16]), and GRCh37 human reference genome with Bowtie v.1.3.0[17].

After alignment and trimming sorted BAM files were used for further analysis with edgeR v.3.32.1[18] and mirtop v.0.4.23. MiRNA quality was assessed and summarized using MultiQC v.1.9[19]. Normalized counts were generated using isomiRs package and differential expression analysis was carried out using the DESeq2 Bioconductor package v.1.26.0[20]. The threshold for significant differential expression was Bonferroni[21] adjusted P-value < 0.05 and absolute value of log2 fold change (FC) |log2FC| > 1.

Validation of miRNA expression in plasma by reverse transcription quantitative real-time PCR

To validate differentially expressed miRNAs in plasma samples, isolated plasma circulating microRNA was reverse transcribed to cDNA using the TaqMan™ MicroRNA Reverse Transcription Kit (Thermo Fisher Scientific, United States). The material was preamplified using the TaqMan PreAmp Master Mix (Applied Biosystems, United States) according to the manufacturer's protocol. Quantitative real-time PCR (RT-PCR) was performed using the TaqMan MicroRNA Assays: Hsa-miR-129* (Assay ID: 002298), hsa-miR-196a (Assay ID: 241070_mat) on 7500 Fast Real-Time PCR System (Applied Biosystems, United States). All RT-qPCR reactions were run in duplicate in a 20 μL reaction and the relative fold change in miRNA expression was estimated using the $2^{-\Delta\Delta Ct}$ method[22]. Ct values were normalized to the RNU6B (Assay ID: 001093, Thermo Fisher Scientific, United States) endogenous control.

Statistical analysis

Statistical analysis was performed using RStudio software (R v.3.6.3). Shapiro-Wilk normality test was used to test the normal distribution of data. For normally distributed data, statistical significance was assessed by Student's t-test. If the data did not pass normality tests was performed non-parametric Wilcoxon rank-sum test. A P < 0.05 was considered statistically significant. Area under the receiver operating characteristic curve (AUC-ROC) analysis was performed using pROC R package.

RESULTS

Small RNA sequencing reveals distinct miRNomes of healthy, premalignant, and malignant stages of GC

Small RNA sequencing of CON, AG, and paired GC (cancerous and adjacent) tissues in total identified 1037 miRNAs annotated in the miRBase v22.1. Sequencing yielded approx 250 M raw sequencing reads (from 359 K to 16 M reads per sample). After quality control steps 396 low-abundant and non-variable miRNAs and 5 outlying samples were removed resulting in 641 miRNAs and 75 samples which were used for further analysis (Supplementary Figures 1 and 2). The number of deregulated miRNAs corresponded to pathological cascade of GC development. The highest number of deregulated miRNAs were determined when comparing GC and CON groups (129 differentially expressed miRNAs, 82 up-regulated and 47 down-regulated; Supplementary Table 1). Next, 99 differentially expressed miRNAs were identified analyzing GC compared to AG (67 up-regulated and 32 down-regulated; Supplementary Table 2). The lowest number, 20 miRNAs, were found to be deregulated comparing AG and CON (6 up-regulated and 14 down-regulated; Supplementary Table 3). Differential expression results comparing GC *vs* GCaj, AG *vs* GCaj, and CON *vs* GCaj are presented in Supplementary Tables 4, 5 and 6 respectively.

Differential expression results and top five deregulated miRNAs in each case are represented in Figure 1A. Multidimensional scaling analysis of normalized expression values, assessing the similarity structure of miRNomes (Spearman's correlation distance), revealed 4 clusters, corresponding to the CON, AG, GC cancerous and adjacent tissues (Figure 1B). The AG cluster was intermediate between GC and CON, whereas GCaj was overlapping with AG and CON groups.

Hsa-miR-129-1-3p and hsa-miR-196a-5p may be employed for discrimination of healthy, premalignant, and malignant GC cases

To further study miRNome profiles, altered expression of miRNAs was analyzed in three main comparison groups: AG *vs* CON, GC *vs* CON and AG *vs* GC according to clinical significance. Analyzing uniquely deregulated miRNAs, 40 differentially expressed miRNAs were found when compared GC to CON (25.8% of all deregulated

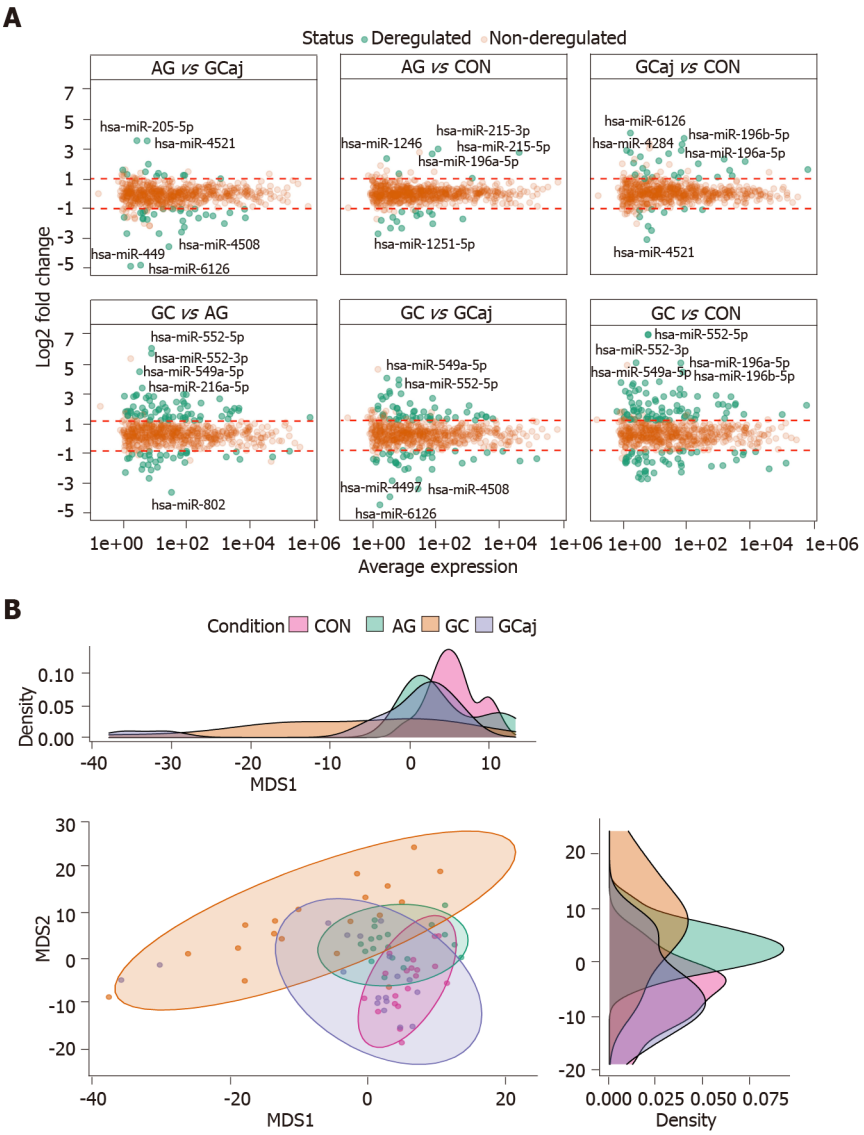

Figure 1 Results of microRNA differential expression analysis. A: Differentially expressed gastric tissue microRNAs among different conditions. *P*-adjusted < 0.05 and |log2 fold change| > 1; B: Multidimensional scaling plot based on normalized data showing a clustering corresponding to control, atrophic gastritis, gastric cancerous and adjacent tissues. The density plots show distributions of the first and second dimensions. CON: Control; AG: Atrophic gastritis; GC: Gastric cancerous; GCaj: Gastric adjacent tissue; MDS: Multidimensional scaling.

miRNAs), 18 (11.6%) - AG compared to GC, and 6 (3.9%) - AG compared to CON (Figure 2). Most of the deregulated miRNAs (n = 79, 68.7%) were similar between GC *vs* CON and GC *vs* AG comparison groups. 12 miRNAs (7.7%) were deregulated in both AG and GC groups when compared to CON. Four miRNAs (2.6%) were similarly deregulated between AG *vs* CON and AG *vs* GC groups. Finally, only 2 miRNAs (hsa-miR-129-1-3p and hsa-miR-196a-5p) (1.29%) were identified as deregulated between all comparison groups. AUC-ROC analysis revealed that expression level of hsa-miR-129-1-3p in tissues resulted in AUCs: 68.1%; 86.3%, and 78.1%, CON *vs* AG, CON *vs* GC, and AG *vs* GC, respectively (Figures 3A, 3B and 3C). In addition to this, expression level of hsa-miR-196a-5p could be significant for discrimination of CON *vs* AG, CON *vs* GC and AG *vs* GC and resulted in AUCs: 88.0%, 93.1% and 66.3% (Figures 3D, 3E and 3F).

Hsa-miR-129-1-3p and hsa-miR-196a-5p expression in the plasma follows the expression pattern of CON, AG, and GC tissues

Differential expression analysis of NGS data in tissue samples revealed that hsa-miR-129-1-3p was significantly down-regulated and hsa-miR-196a-5p was up-regulated in AG and GC tissues compared to CON (P = 0.002 and P = 0.00018; $P = 1.2 \times 10^{-5}$ and $P = 3.1 \times 10^{-5}$, respectively). Moreover, hsa-miR-129-1-3p was significantly down-regulated in the case of AG compared to GC (P = 0.0021) and reflected a stepwise process of a

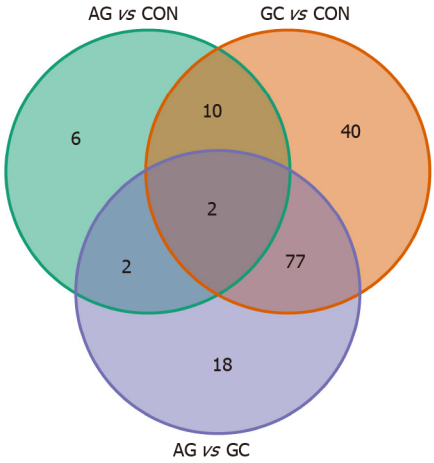

Figure 2 Venn diagram representing the number of commonly and uniquely differentially expressed microRNAs in three different comparison groups. *P*-adjusted < 0.05 and |log2 fold change| > 1. CON: Control; AG: Atrophic gastritis; GC: Gastric cancer.

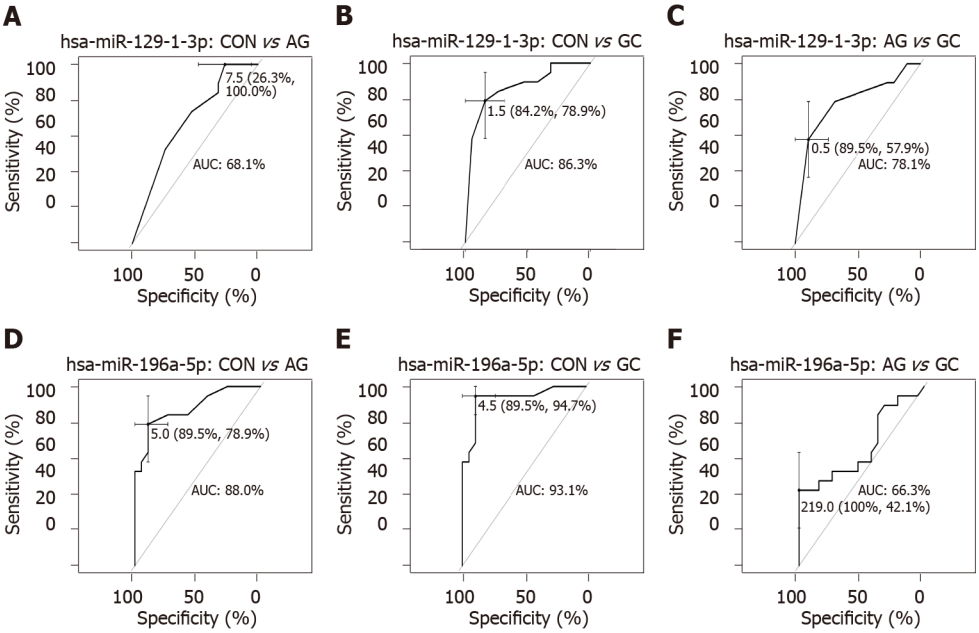

Figure 3 Receiver operating characteristic curves showing prediction performances of expression levels. A-C: Hsa-miR-129-1-3p; D-F: Hsa-miR-196a-5p in tissue samples between different comparison groups: Control *vs* atrophic gastritis; control *vs* gastric cancer; and atrophic gastritis *vs* gastric cancer. AUC: Area under the curve; CON: Control; AG: Atrophic gastritis; GC: Gastric cancer.

pathology (Figure 4A). Therefore, to identify whether the expression changes of these two miRNAs can be detected noninvasively in the body fluids of the patients, hsa-miR-129-1-3p and hsa-miR-196a-5p were selected for RT-qPCR analysis in plasma samples of independent cohort. The analysis showed similar expression patterns in the case of hsa-miR-129-1-3p, which was significantly down-regulated when comparing AG and GC groups (P = 0.024). There were no other significant findings between the groups (Figure 4B).

Hsa-miR-215-3p/5p and hsa-miR-934 may be associated with H. pylori-induced GC

To investigate role of miRNAs in AG atrophy progression (OLGA classification) and *H. pylori*-induced GC, differential miRNAs profile analysis in the subgroups of the study was performed. The analysis revealed a minor clustering in AG tissues corresponding to OLGA stages (Supplementary Figures 3A and 3H). *H. pylori* status in GC tissues (Supplementary Figure 3B). However, no significantly deregulated miRNAs were determined comparing I-II OLGA stages *vs* III-IV OLGA stages (AG tissue samples). On the other hand, analyzing GC group based on *H. pylori* infection status [*H. pylori* (neg.) *vs H. pylori* (pos.)], three miRNAs were shown to be significantly

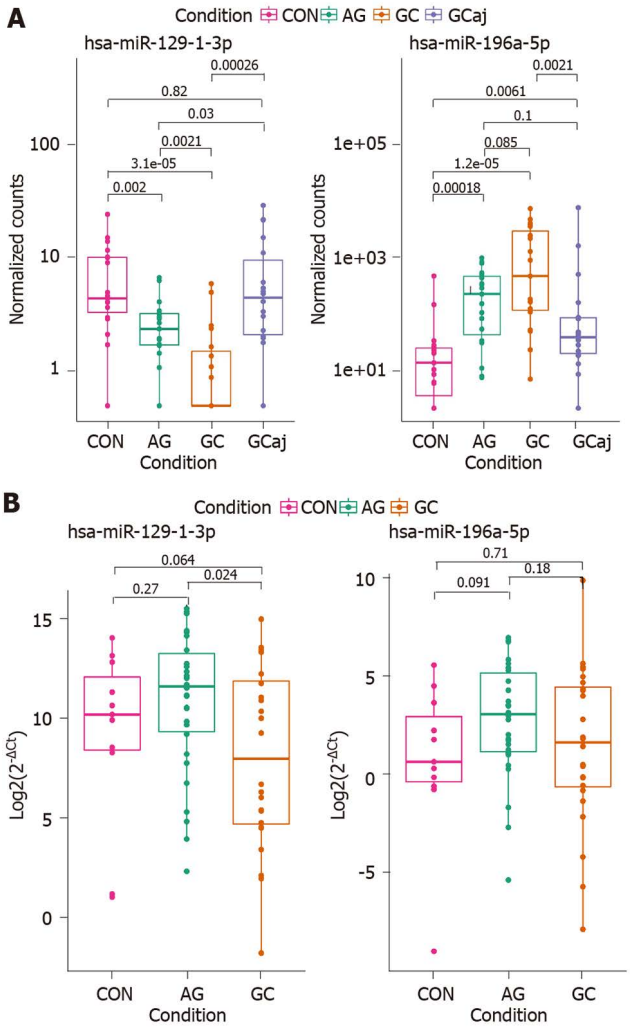

Figure 4 Hsa-miR-129-1-3p and hsa-miR-196a-5p expression levels in study comparison groups. A: Atrophic gastritis and gastric cancer tissue samples compared to controls; B: Atrophic gastritis and gastric cancer plasma samples compared to controls. Box plot graphs; boxes correspond to the median value and interquartile range. CON: Control; AG: Atrophic gastritis; GC: Gastric cancerous; GCaj: Gastric adjacent tissue.

deregulated: Hsa-miR-215-3p (log2FC = -4.52, *P*-adjusted = 0.02), hsa-miR-215-5p (log2FC = -4.00, *P*-adjusted = 0.02), and hsa-miR-934 (log2FC = 6.09, *P*-adjusted = 0.02).

DISCUSSION

This study represents comprehensive miRNome profiling of premalignant and malignant GC cases by implementing high throughput technologies such as NGS. Although there are several studies reporting profiles of GC tissue miRNAs[23,24], analysis of the association between miRNA expression and AG is very scarce reporting only individual miRNAs[25]. Moreover, based on small RNA-seq findings, two miRNAs were analyzed in subjects' plasma samples to investigate potential non-invasive markers. To our best knowledge this is the first study analyzing AG and GC tissue miRNomes in the subjects of European origin.

First, our study showed different profiles of deregulated miRNAs between tissue samples of studied groups. In total, 20 differentially expressed miRNAs were identified in AG and 129 - in GC comparing to CON; also 99 deregulated miRNAs - comparing GC and AG groups. MiRNAs such as hsa-miR-3131, hsa-miR-483, hsa-miR-150, hsa-miR-200a-3p, hsa-miR-873-5p were previously reported by the GC profiling studies of Pereira *et al*[23] and Assumpção *et al*[24]. Yet, we were able to identify number of novel miRNAs (of which hsa-miR-548ba, hsa-miR-4521, hsa-miR-549a were the most deregulated). There are no data showing the role of these novel miRNAs in inflammatory or tumorous processes of gastric tissue. However, recent studies have shown that hsa-miR-548ba was associated with bladder cancer, hsa-miR-549a with the

metastasis of renal cancer, and hsa-miR-4521 with *H. pylori* infection in esophageal epithelial cells[26-28]. Taking into consideration miRNome of AG, hsa-miR-3591-3p, hsa-miR-122-3p and hsa-miR-122-5p, hsa-miR-451a miRNAs were already reported by Liu *et al*[29], while the most deregulated miRNAs including hsa-miR-215, hsa-miR-4497, and hsa-miR-1251 were reported for the first time in our study. Previous research showed that hsa-miR-215-5p was deregulated in different lesions of the gastrointestinal tract (Barrett's esophagus, intraepithelial neoplastic lesions, ulcerative colitis)[30-32]. However, hsa-miR-4497 and hsa-miR-452 were not previously associated with AG but were reported to play an important role in GC development[33,34].

Next, we identified hsa-miR-215-3p and hsa-miR-215-5p to be down-regulated while hsa-miR-934 - up-regulated in GC group comparing negative and positive *H. pylori* infection status. Studies revealed the altered expression of various miRNAs in *H. pylori*-induced GC tissue samples, including miR-934, miR-146a, miR-375, miR-204[35-37]. Although, hsa-miR-215 deregulation was previously associated with GC[38-40], there is no data showing its link with *H. pylori* infection.

In addition to this, we showed that two miRNAs (hsa-miR-129-1-3p and hsa-miR-196a-5p) were gradually deregulated comparing all three study groups (CON, AG, and GC) which also corresponds to pathological cascade of GC. In concordance to our results, it has already been shown that hsa-miR-129-1-3p was down-regulated in GC tissues, function as a tumor suppressor in GC and even corresponds to the same expression pattern in gastric juice[41,42]. There is no data regarding the hsa-miR-196a expression in AG tissue, however, investigators have revealed that hsa-miR-196a is overexpressed in GC tissue, plasma, commercial cell lines and promotes cell proliferation[43,44]. ROC-AUC analysis suggests great potential of hsa-miR-196a-5p expression in tissue for discrimination of AG and GC in contrast to CON (AUC = 89.5% and AUC = 89.5%, respectively). Therefore, further studies are needed to confirm this finding.

Finally, selected miRNAs were analyzed in independent cohort of CON, AG, and GC plasma samples by using RT-qPCR. Results showed similar deregulation direction in plasma samples as in the tissue samples. However, significant differences were only determined comparing the expression of hsa-miR-129-1-3p between AG and GC suggesting its potential role in non-invasive diagnostics of malignant cases. No significant expression changes were observed between study groups and hsa-miR-196a-5p. Other studies have shown controversial results: Tsai *et al*[45] reported that miR-196a/b was up-regulated in both the plasma and tissue of metastatic GC patients, while miRNome profiling study revealed that miR-196a-5p was found to be down-regulated in plasma of patients with precursor lesions of GC compared to non-active gastritis[46].

In our study, using NGS and RT-qPCR techniques we have shown the distinct miRNome profiles of CON, AG, GC, GCaj tissues, and potential of specific miRNAs as non-invasive biomarkers. In addition to this, novel miRNAs not previously reported as AG or GC associated epigenetic markers were identified. We have shown that hsa-miR-196a-5p expression in tissue could be significant for discrimination between CON and AG or GC, confirmed hsa-miR-129-1-3p as non-invasive biomarker in disease progression monitoring, and showed that miRNAs could be a great candidate for future research of new diagnostic approaches.

CONCLUSION

In conclusion, we showed gradual deregulation of hsa-miR-196a-5p and hsa-miR-129-1-3p in the gastric carcinogenesis pathway and confirmed hsa-miR-129-1-3p as a possible non-invasive biomarker. We also found hsa-miR-215-3p/5p and hsa-miR-934 to be significantly deregulated in GC based on *H. pylori* infection status. These data provide novel insights into complex GC pathogenesis cascade which could be highly significant for future studies of new diagnostic GC targets.

ARTICLE HIGHLIGHTS

Research background

Gastric cancer (GC) is a complex disease arising from the interaction of environmental (*e.g.*, diet, smoking, *etc.*) and host-associated factors [*e.g.*, *Helicobacter pylori* (*H. pylori*) infection, genetics, *etc.*]. Due to its silent course, it is also one of the most lethal cancers

worldwide as it is usually diagnosed at the advanced stages.

Research motivation

Novel biomarkers that would help to improve GC patients' diagnosis and prognosis are highly needed. Studies show that microRNAs (miRNAs) play an important role in many cancers and could be a promising biomarker or even therapeutic target.

Research objectives

The objectives of the study were to analyze whole miRNome profiles of control, premalignant and malignant gastric tissues, and select the potential miRNA markers that could have a potential for minimally invasive GC diagnostics.

Research methods

Total RNA from gastric tissue samples was subjected for small RNA sequencing (smRNA-seq). Plasma total circulating nucleic acids were used for the expression analysis of the most tissue deregulated miRNAs by real-time quantitative polymerase chain reaction. Statistical analysis involved the differential expression and discrimination analyses.

Research results

The abundance of altered expression miRNAs corresponded to a pathological cascade of GC development. Hsa-miR-129-1-3p and has-miR-196a-5p were shown to be deregulated in healthy-premalignant-malignant sequence. In addition to this, we showed that down-regulation of hsa-miR-129-1-3p could also be detected non-invasively in GC patients' plasma samples. Finally, results indicated that hsa-miR-215-3p/5p and hsa-miR-934 were significantly deregulated based on *H. pylori* infection status for GC patients.

Research conclusions

Gastric tissue miRNome study provides extensive profiling of control, premalignant and malignant cases. Based on smRNA-seq results several miRNAs were shown as potential gastric carcinogenesis (hsa-miR-196a-5p and hsa-miR-129-1-3p); and *H. Pylori* -related (hsa-miR-215-3p/5p and hsa-miR-934) biomarkers.

Research perspectives

This study provides novel insights into complex GC pathogenesis cascade and could serve as a reference for future research to support our findings.

REFERENCES

1 **Sung H**, Ferlay J, Siegel RL, Laversanne M, Soerjomataram I, Jemal A, Bray F. Global Cancer Statistics 2020: GLOBOCAN Estimates of Incidence and Mortality Worldwide for 36 Cancers in 185 Countries. *CA Cancer J Clin* 2021; **71**: 209-249 [PMID: 33538338 DOI: 10.3322/caac.21660]

2 **McLean MH**, El-Omar EM. Genetics of gastric cancer. *Nat Rev Gastroenterol Hepatol* 2014; **11**: 664-674 [PMID: 25134511 DOI: 10.1038/nrgastro.2014.143]

3 **Tan P**, Yeoh KG. Genetics and Molecular Pathogenesis of Gastric Adenocarcinoma. *Gastroenterology* 2015; **149**: 1153-1162.e3 [PMID: 26073375 DOI: 10.1053/j.gastro.2015.05.059]

4 **Bartel DP**. Metazoan MicroRNAs. *Cell* 2018; **173**: 20-51 [PMID: 29570994 DOI: 10.1016/j.cell.2018.03.006]

5 **Bartel DP**. MicroRNAs: target recognition and regulatory functions. *Cell* 2009; **136**: 215-233 [PMID: 19167326 DOI: 10.1016/j.cell.2009.01.002]

6 **Bracken CP**, Scott HS, Goodall GJ. A network-biology perspective of microRNA function and dysfunction in cancer. *Nat Rev Genet* 2016; **17**: 719-732 [PMID: 27795564 DOI: 10.1038/nrg.2016.134]

7 **Farazi TA**, Hoell JI, Morozov P, Tuschl T. MicroRNAs in human cancer. *Adv Exp Med Biol* 2013; **774**: 1-20 [PMID: 23377965 DOI: 10.1007/978-94-007-5590-1_1]

8 **Gyvyte U**, Juzenas S, Salteniene V, Kupcinskas J, Poskiene L, Kucinskas L, Jarmalaite S, Stuopelyte K, Steponaitiene R, Hemmrich-Stanisak G, Hübenthal M, Link A, Franke S, Franke A, Pangonyte D, Lesauskaite V, Kupcinskas L, Skieceviciene J. MiRNA profiling of gastrointestinal stromal tumors by next-generation sequencing. *Oncotarget* 2017; **8**: 37225-37238 [PMID: 28402935 DOI: 10.18632/oncotarget.16664]

9 **Streleckiene G**, Inciuraite R, Juzenas S, Salteniene V, Steponaitiene R, Gyvyte U, Kiudelis G, Leja M, Ruzgys P, Satkauskas S, Kupcinskiene E, Franke S, Thon C, Link A, Kupcinskas J, Skieceviciene J. miR-20b and miR-451a Are Involved in Gastric Carcinogenesis through the PI3K/AKT/mTOR

Signaling Pathway: Data from Gastric Cancer Patients, Cell Lines and Ins-Gas Mouse Model. *Int J Mol Sci* 2020; **21** [PMID: 32013265 DOI: 10.3390/ijms21030877]

10 **Link A**, Kupcinskas J. MicroRNAs as non-invasive diagnostic biomarkers for gastric cancer: Current insights and future perspectives. *World J Gastroenterol* 2018; **24**: 3313-3329 [PMID: 30122873 DOI: 10.3748/wjg.v24.i30.3313]

11 **Juzėnas S**, Saltenienė V, Kupcinskas J, Link A, Kiudelis G, Jonaitis L, Jarmalaite S, Kupcinskas L, Malfertheiner P, Skieceviciene J. Analysis of Deregulated microRNAs and Their Target Genes in Gastric Cancer. *PLoS One* 2015; **10**: e0132327 [PMID: 26172537 DOI: 10.1371/journal.pone.0132327]

12 **Rugge M**, Correa P, Di Mario F, El-Omar E, Fiocca R, Geboes K, Genta RM, Graham DY, Hattori T, Malfertheiner P, Nakajima S, Sipponen P, Sung J, Weinstein W, Vieth M. OLGA staging for gastritis: a tutorial. *Dig Liver Dis* 2008; **40**: 650-658 [PMID: 18424244 DOI: 10.1016/j.dld.2008.02.030]

13 **Amin MB**, Greene FL, Edge SB, Compton CC, Gershenwald JE, Brookland RK, Meyer L, Gress DM, Byrd DR, Winchester DP. The Eighth Edition AJCC Cancer Staging Manual: Continuing to build a bridge from a population-based to a more "personalized" approach to cancer staging. *CA Cancer J Clin* 2017; **67**: 93-99 [PMID: 28094848 DOI: 10.3322/caac.21388]

14 **Lauren P**. The two histological main types of gastric carcinoma: diffuse and so-called intestinal-type carcinoma. An attempt at a histo-clinical classification. *Acta Pathol Microbiol Scand* 1965; **64**: 31-49 [PMID: 14320675 DOI: 10.1111/apm.1965.64.1.31]

15 **Kozomara A**, Birgaoanu M, Griffiths-Jones S. miRBase: from microRNA sequences to function. *Nucleic Acids Res* 2019; **47**: D155-D162 [PMID: 30423142 DOI: 10.1093/nar/gky1141]

16 **Di Tommaso P**, Chatzou M, Floden EW, Barja PP, Palumbo E, Notredame C. Nextflow enables reproducible computational workflows. *Nat Biotechnol* 2017; **35**: 316-319 [PMID: 28398311 DOI: 10.1038/nbt.3820]

17 **Langmead B**, Trapnell C, Pop M, Salzberg SL. Ultrafast and memory-efficient alignment of short DNA sequences to the human genome. *Genome Biol* 2009; **10**: R25 [PMID: 19261174 DOI: 10.1186/gb-2009-10-3-r25]

18 **Ewels P**, Magnusson M, Lundin S, Käller M. MultiQC: summarize analysis results for multiple tools and samples in a single report. *Bioinformatics* 2016; **32**: 3047-3048 [PMID: 27312411 DOI: 10.1093/bioinformatics/btw354]

19 **Robinson MD**, McCarthy DJ, Smyth GK. edgeR: a Bioconductor package for differential expression analysis of digital gene expression data. *Bioinformatics* 2010; **26**: 139-140 [PMID: 19910308 DOI: 10.1093/bioinformatics/btp616]

20 **Love MI**, Huber W, Anders S. Moderated estimation of fold change and dispersion for RNA-seq data with DESeq2. *Genome Biol* 2014; **15**: 550 [PMID: 25516281 DOI: 10.1186/s13059-014-0550-8]

21 **Ranstam J**. Multiple P-values and Bonferroni correction. *Osteoarthritis Cartilage* 2016; **24**: 763-764 [PMID: 26802548 DOI: 10.1016/j.joca.2016.01.008]

22 **Livak KJ**, Schmittgen TD. Analysis of relative gene expression data using real-time quantitative PCR and the 2(-Delta Delta C(T)) Method. *Methods* 2001; **25**: 402-408 [PMID: 11846609 DOI: 10.1006/meth.2001.1262]

23 **Pereira A**, Moreira F, Vinasco-Sandoval T, Cunha A, Vidal A, Ribeiro-Dos-Santos AM, Pinto P, Magalhães L, Assumpção M, Demachki S, Santos S, Assumpção P, Ribeiro-Dos-Santos Â. miRNome Reveals New Insights Into the Molecular Biology of Field Cancerization in Gastric Cancer. *Front Genet* 2019; **10**: 592 [PMID: 31275362 DOI: 10.3389/fgene.2019.00592]

24 **Assumpção MB**, Moreira FC, Hamoy IG, Magalhães L, Vidal A, Pereira A, Burbano R, Khayat A, Silva A, Santos S, Demachki S, Ribeiro-Dos-Santos Â, Assumpção P. High-Throughput miRNA Sequencing Reveals a Field Effect in Gastric Cancer and Suggests an Epigenetic Network Mechanism. *Bioinform Biol Insights* 2015; **9**: 111-117 [PMID: 26244015 DOI: 10.4137/BBI.S24066]

25 **Link A**, Schirrmeister W, Langner C, Varbanova M, Bornschein J, Wex T, Malfertheiner P. Differential expression of microRNAs in preneoplastic gastric mucosa. *Sci Rep* 2015; **5**: 8270 [PMID: 25652892 DOI: 10.1038/srep08270]

26 **Zhao F**, Ge YZ, Zhou LH, Xu LW, Xu Z, Ping WW, Wang M, Zhou CC, Wu R, Jia RP. Identification of hub miRNA biomarkers for bladder cancer by weighted gene coexpression network analysis. *Onco Targets Ther* 2017; **10**: 5551-5559 [PMID: 29200870 DOI: 10.2147/OTT.S146479]

27 **Xuan Z**, Chen C, Tang W, Ye S, Zheng J, Zhao Y, Shi Z, Zhang L, Sun H, Shao C. TKI-Resistant Renal Cancer Secretes Low-Level Exosomal miR-549a to Induce Vascular Permeability and Angiogenesis to Promote Tumor Metastasis. *Front Cell Dev Biol* 2021; **9**: 689947 [PMID: 34179017 DOI: 10.3389/fcell.2021.689947]

28 **Teng G**, Dai Y, Chu Y, Li J, Zhang H, Wu T, Shuai X, Wang W. Helicobacter pylori induces caudal-type homeobox protein 2 and cyclooxygenase 2 expression by modulating microRNAs in esophageal epithelial cells. *Cancer Sci* 2018; **109**: 297-307 [PMID: 29215765 DOI: 10.1111/cas.13462]

29 **Liu H**, Li PW, Yang WQ, Mi H, Pan JL, Huang YC, Hou ZK, Hou QK, Luo Q, Liu FB. Identification of non-invasive biomarkers for chronic atrophic gastritis from serum exosomal microRNAs. *BMC Cancer* 2019; **19**: 129 [PMID: 30736753 DOI: 10.1186/s12885-019-5328-7]

30 **Fassan M**, Croce CM, Rugge M. miRNAs in precancerous lesions of the gastrointestinal tract. *World J Gastroenterol* 2011; **17**: 5231-5239 [PMID: 22219591 DOI: 10.3748/wjg.v17.i48.5231]

31 **Fassan M**, Volinia S, Palatini J, Pizzi M, Baffa R, De Bernard M, Battaglia G, Parente P, Croce CM, Zaninotto G, Ancona E, Rugge M. MicroRNA expression profiling in human Barrett's carcinogenesis. *Int J Cancer* 2011; **129**: 1661-1670 [PMID: 21128279 DOI: 10.1002/ijc.25823]

32 **Wijnhoven BP**, Hussey DJ, Watson DI, Tsykin A, Smith CM, Michael MZ; South Australian Oesophageal Research Group. MicroRNA profiling of Barrett's oesophagus and oesophageal adenocarcinoma. *Br J Surg* 2010; **97**: 853-861 [PMID: 20301167 DOI: 10.1002/bjs.7000]

33 **Bibi F**, Naseer MI, Alvi SA, Yasir M, Jiman-Fatani AA, Sawan A, Abuzenadah AM, Al-Qahtani MH, Azhar EI. microRNA analysis of gastric cancer patients from Saudi Arabian population. *BMC Genomics* 2016; **17**: 751 [PMID: 27766962 DOI: 10.1186/s12864-016-3090-7]

34 **Yin C**, Zheng X, Xiang H, Li H, Gao M, Meng X, Yang K. Differential expression profile analysis of cisplatinregulated miRNAs in a human gastric cancer cell line. *Mol Med Rep* 2019; **20**: 1966-1976 [PMID: 31257509 DOI: 10.3892/mmr.2019.10430]

35 **Chang H**, Kim N, Park JH, Nam RH, Choi YJ, Lee HS, Yoon H, Shin CM, Park YS, Kim JM, Lee DH. Different microRNA expression levels in gastric cancer depending on Helicobacter pylori infection. *Gut Liver* 2015; **9**: 188-196 [PMID: 25167801 DOI: 10.5009/gnl13371]

36 **Prinz C**, Mese K, Weber D. MicroRNA Changes in Gastric Carcinogenesis: Differential Dysregulation during *Helicobacter pylori* and EBV Infection. *Genes (Basel)* 2021; **12** [PMID: 33921696 DOI: 10.3390/genes12040597]

37 **Wang F**, Sun G, Zou Y, Zhong F, Ma T, Li X. Protective role of Helicobacter pylori infection in prognosis of gastric cancer: evidence from 2,454 patients with gastric cancer. *PLoS One* 2013; **8**: e62440 [PMID: 23667477 DOI: 10.1371/journal.pone.0062440]

38 **Jin Z**, Selaru FM, Cheng Y, Kan T, Agarwal R, Mori Y, Olaru AV, Yang J, David S, Hamilton JP, Abraham JM, Harmon J, Duncan M, Montgomery EA, Meltzer SJ. MicroRNA-192 and -215 are upregulated in human gastric cancer *in vivo* and suppress ALCAM expression in vitro. *Oncogene* 2011; **30**: 1577-1585 [PMID: 21119604 DOI: 10.1038/onc.2010.534]

39 **Deng Y**, Huang Z, Xu Y, Jin J, Zhuo W, Zhang C, Zhang X, Shen M, Yan X, Wang L, Wang X, Kang Y, Si J, Zhou T. MiR-215 modulates gastric cancer cell proliferation by targeting RB1. *Cancer Lett* 2014; **342**: 27-35 [PMID: 23981575 DOI: 10.1016/j.canlet.2013.08.033]

40 **Li N**, Zhang QY, Zou JL, Li ZW, Tian TT, Dong B, Liu XJ, Ge S, Zhu Y, Gao J, Shen L. miR-215 promotes malignant progression of gastric cancer by targeting RUNX1. *Oncotarget* 2016; **7**: 4817-4828 [PMID: 26716895 DOI: 10.18632/oncotarget.6736]

41 **Wang D**, Luo L, Guo J. miR-129-1-3p inhibits cell migration by targeting BDKRB2 in gastric cancer. *Med Oncol* 2014; **31**: 98 [PMID: 25008064 DOI: 10.1007/s12032-014-0098-1]

42 **Yu X**, Luo L, Wu Y, Yu X, Liu Y, Zhao X, Zhang X, Cui L, Ye G, Le Y, Guo J. Gastric juice miR-129 as a potential biomarker for screening gastric cancer. *Med Oncol* 2013; **30**: 365 [PMID: 23307240 DOI: 10.1007/s12032-012-0365-y]

43 **Treece AL**, Duncan DL, Tang W, Elmore S, Morgan DR, Dominguez RL, Speck O, Meyers MO, Gulley ML. Gastric adenocarcinoma microRNA profiles in fixed tissue and in plasma reveal cancer-associated and Epstein-Barr virus-related expression patterns. *Lab Invest* 2016; **96**: 661-671 [PMID: 26950485 DOI: 10.1038/labinvest.2016.33]

44 **Sun M**, Liu XH, Li JH, Yang JS, Zhang EB, Yin DD, Liu ZL, Zhou J, Ding Y, Li SQ, Wang ZX, Cao XF, De W. MiR-196a is upregulated in gastric cancer and promotes cell proliferation by downregulating p27(kip1). *Mol Cancer Ther* 2012; **11**: 842-852 [PMID: 22343731 DOI: 10.1158/1535-7163.MCT-11-1015]

45 **Tsai MM**, Wang CS, Tsai CY, Huang CG, Lee KF, Huang HW, Lin YH, Chi HC, Kuo LM, Lu PH, Lin KH. Circulating microRNA-196a/b are novel biomarkers associated with metastatic gastric cancer. *Eur J Cancer* 2016; **64**: 137-148 [PMID: 27420607 DOI: 10.1016/j.ejca.2016.05.007]

46 **Lario S**, Brunet-Vega A, Quílez ME, Ramírez-Lázaro MJ, Lozano JJ, García-Martínez L, Pericay C, Miquel M, Junquera F, Campo R, Calvet X. Expression profile of circulating microRNAs in the Correa pathway of progression to gastric cancer. *United European Gastroenterol J* 2018; **6**: 691-701 [PMID: 30083331 DOI: 10.1177/2050640618759433]

World Journal of Gastroenterology

Submit a Manuscript: https://www.f6publishing.com

World J Gastroenterol 2022 February 14; 28(6): 665-674

DOI: 10.3748/wjg.v28.i6.665

ISSN 1007-9327 (print) ISSN 2219-2840 (online)

ORIGINAL ARTICLE

Retrospective Study

Validation of the PAGE-B score to predict hepatocellular carcinoma risk in caucasian chronic hepatitis B patients on treatment

Pinar Gokcen, Fatih Guzelbulut, Gupse Adali, Ayca Gokce Degirmenci Salturk, Oguzhan Ozturk, Ozgur Bahadir, Emine Kanatsiz, Mevlut Kiyak, Kamil Ozdil, Hamdi Levent Doganay

ORCID number: Pinar Gokcen 0000-0002-6742-6976; Fatih Guzelbulut 0000-0003-4889-208X; Gupse Adali 0000-0003-2157-0304; Ayca Gokce Degirmenci Salturk 0000-0002-1979-9145; Oguzhan Ozturk 0000-0002-7718-8684; Ozgur Bahadir 0000-0002-9472-5170; Emine Kanatsiz 0000-0003-2971-6443; Mevlut Kiyak 0000-0003-1672-5914; Kamil Ozdil 0000-0003-2556-3064; Hamdi Levent Doganay 0000-0002-2263-6689.

Author contributions: Doganay HL and Guzelbulut F equally contributed to this work. Doganay HL, Gokcen P, and Guzelbulut F contributed to the concept; Doganay HL, Gokcen P, Adali G, and Guzelbulut F designed this study; Doganay HL and Guzelbulut F supervised this study; Gokcen P, Kiyak M, Kanatsiz E, Bahadir O, Ozturk O and Ozdil K prepare the materials; Gokcen P, Guzelbulut F, Degirmenci Salturk AG, Kanatsiz E, Kiyak M, Ozturk O and Ozdil K collected and/or processed the data; Gokcen P, Doganay HL, Guzelbulut F and Adali G analyzed and/or interpreted the data; Gokcen P, Guzelbulut F., Kanatsiz E, Kiyak M, Degirmenci Salturk AG and Bahadir O searched the literature; Gokcen P, Doganay HL, Adali G and

Pinar Gokcen, Gupse Adali, Oguzhan Ozturk, Kamil Ozdil, Hamdi Levent Doganay, Department of Gastroenterology, Health Sciences University, Umraniye Teaching and Research Hospital, Istanbul 34764, Turkey

Fatih Guzelbulut, Ayca Gokce Degirmenci Salturk, Ozgur Bahadir, Emine Kanatsiz, Mevlut Kiyak, Department of Gastroenterology, Health Sciences University, Haydarpasa Numune Teaching and Research Hospital, Istanbul 34668, Turkey

Corresponding author: Hamdi Levent Doganay, MD, Professor, Department of Gastroenterology, Health Sciences University, Umraniye Teaching and Research Hospital, No. 1 Adem Yavuz Street, Elmalikent, Umraniye, Istanbul 34764, Turkey.
ldoganay@hotmail.com

Abstract

BACKGROUND

Several risk scores have been developed to predict hepatocellular carcinoma (HCC) risk in chronic hepatitis B (CHB) patients. The majority of risk scores are based on pretreatment variables that are no longer considered risk factors for HCC development due to the suppression of hepatitis B virus replication early in the course of potent antiviral treatment in most patients. The PAGE-B score, which is based on platelet levels, age and sex, has been shown to accurately predict HCC risk in CHB patients on antiviral treatment in various populations.

AIM

We aimed to evaluate the PAGE-B score in predicting HCC risk in Turkish CHB patients on antiviral treatment.

METHODS

In this study, we recruited 742 CHB patients who had been treated with tenofovir disoproxil fumarate or entecavir for ≥ 1 year. Risk groups were determined according to the PAGE-B scores as follows: ≤ 9, low; 10-17, moderate and ≥ 18, high. The cumulative HCC incidences in each risk group were computed using Kaplan-Meier analysis and were compared using the log-rank test. The accuracy of the PAGE-B score in predicting HCC risk was evaluated using a time-dependent area under the receiver operating characteristic (AUROC) curve at all study time points. Univariate and multivariate logistic regression analyses were

Guzelbulut F wrote the Manuscript; Doganay HL, Guzelbulut F and Adali G contributed to review critical.

Institutional review board statement: The study was approved by the local ethics committees of Umraniye Training and Research Hospital and Haydarpasa Numune Training and Research Hospital.

Conflict-of-interest statement: The authors report no conflicts of interest.

Data sharing statement: No additional data are available.

STROBE statement: The authors have read the STROBE guidelines, and the manuscript was prepared and revised according to the STROBE guidelines.

Country/Territory of origin: Turkey

Specialty type: Gastroenterology and Hepatology

Provenance and peer review: Unsolicited article; Externally peer reviewed.

Peer-review model: Single blind

Peer-review report's scientific quality classification

Grade A (Excellent): 0
Grade B (Very good): B
Grade C (Good): C
Grade D (Fair): 0
Grade E (Poor): 0

used to assess the risk factors for HCC development.

RESULTS

The mean follow-up time was 54.7 ± 1.2 mo. HCC was diagnosed in 26 patients (3.5%). The cumulative HCC incidences at 1, 3, 5 and 10 years were 0%, 0%, 0% and 0.4% in the PAGE-B low-risk group; 0%, 1.2%, 1.5% and 2.1% in the PAGE-B moderate-risk group; and 5%, 11.7%, 12.5%, and 15% in the PAGE-B high-risk group, respectively (log-rank $P < 0.001$). The AUROCs of the PAGE-B score in the prediction of HCC development at 1, 3, 5 and 10 years were 0.977, 0.903, 0.903 and 0.865, respectively. In the multivariable analysis, older age, male sex, lower platelet levels, presence of cirrhosis, and absence of alanine aminotransferase normalization at month 6 were associated with HCC development (all $P < 0.05$).

CONCLUSION

The PAGE-B score is a practical tool to predict HCC risk in Turkish patients with CHB and may be helpful to improve surveillance strategies.

Key Words: Chronic hepatitis B; Hepatocellular carcinoma; PAGE-B score; Surveillance

Core Tip: We evaluated the accuracy of the PAGE-B score in predicting hepatocellular carcinoma (HCC) risk in Turkish patients with chronic hepatitis B on antiviral treatment. The cumulative HCC incidences at 5 and 10 years were 0% and 0.4%, 1.5% and 2.1%, and 12.5% and 15.0% in the low-, moderate- and high-risk groups based on the PAGE-B score, respectively. The area under the receiver operating characteristics of the PAGE-B score in the prediction of HCC risk at 5 and 10 years were 0.903 and 0.865, respectively. The PAGE-B score was found to be highly negative predictive and reliable for a cutoff value of ≤ 9 in predicting HCC development.

Citation: Gokcen P, Guzelbulut F, Adali G, Degirmenci Salturk AG, Ozturk O, Bahadir O, Kanatsiz E, Kiyak M, Ozdil K, Doganay HL. Validation of the PAGE-B score to predict hepatocellular carcinoma risk in caucasian chronic hepatitis B patients on treatment. *World J Gastroenterol* 2022; 28(6): 665-674
URL: https://www.wjgnet.com/1007-9327/full/v28/i6/665.htm
DOI: https://dx.doi.org/10.3748/wjg.v28.i6.665

INTRODUCTION

Hepatocellular carcinoma (HCC) is the 7th most prevalent among all cancers and ranks 4th in cancer-related mortality[1]. Chronic hepatitis B (CHB) virus infection affects 257 million people worldwide and is one of the most common etiologies of HCC, accounting for 33% of HCC-related mortality[2]. Nucleos(t)ide analogs suppress hepatitis B virus (HBV) replication in most patients; however, the risk of HCC persists even in patients with suppressed viral replication. Treatment options for advanced-stage HCC are quite limited, and the 5-year survival rate is 18.1%[3]. Therefore, identifying patients who are at high risk for HCC development and detecting tumors at early stages are crucial. Recent guidelines recommend HCC surveillance with ultrasound (USG) twice a year in patients who are at high risk for HCC development [4]. However, not all patients with CHB have the same risk for HCC. There is an ongoing need for a scoring system to predict HCC risk that offers an easy application in clinical practice and a high predictive value to perform effective surveillance in high-risk patients and eliminate unnecessary surveillance in low-risk patients.

Various risk scores have been developed to identify CHB patients at high risk for HCC development. However, many of the risk scores for HCC have focused on untreated patients, and they are mostly based on pretreatment risk factors for HCC, such as hepatitis B e antigen (HBeAg) status, serum HBV DNA, alanine aminotransferase (ALT), albumin and bilirubin levels[5,6]. Most of the baseline virological factors are no longer considered risk factors for HCC, as HBV replication is suppressed early

Received: June 20, 2021
Peer-review started: June 20, 2021
First decision: July 14, 2021
Revised: July 27, 2021
Accepted: January 19, 2021
Article in press: January 19, 2022
Published online: February 14, 2022

P-Reviewer: Huang CF, Xu J
S-Editor: Chang KL
L-Editor: A
P-Editor: Chang KL

in the majority of patients receiving potent antiviral treatment. Therefore, risk scores that include parameters not easily modified by treatment are needed. Among these, the PAGE-B is a practical risk score that includes platelet count, age and sex and has been validated in various patient populations[7-9]. In this study, we aimed to evaluate the accuracy of the PAGE-B score in predicting HCC risk in Turkish CHB patients on tenofovir disoproxil fumarate (TDF) or entecavir (ETV) therapy.

MATERIALS AND METHODS

Patient population and Follow-up Definitions

Medical records of CHB patients who were on follow-up in hepatology outpatient clinics at Umraniye Training and Research Hospital (Istanbul, Turkey) and Haydarpaşa Numune Training and Research Hospital (Istanbul, Turkey) between January 2007 to December 2018 were retrospectively evaluated. The inclusion criteria were as follows: Age ≥ 16 years, HBsAg positivity for ≥ 6 mo, and treatment with TDF or ETV for at least 12 mo. The exclusion criteria were as follows: Age < 16 years, decompensated cirrhosis, having HCC diagnosis before or during the first 6 mo of therapy, history of liver transplantation, and coinfection with hepatitis C virus, hepatitis D virus or human immunodeficiency virus.

Laboratory tests, including HBeAg, anti-HBe, HBV DNA, aspartate aminotransferase, ALT, albumin, bilirubin and alpha-fetoprotein (AFP) levels, international normalized ratio, and complete blood count at the start of therapy and during follow-up at 3-6 mo intervals, were recorded. The results of imaging studies, *e.g.*, USG, triphasic computed tomography (CT) and dynamic contrast-enhanced magnetic resonance imaging (MRI), at the start of therapy and during follow-up were recorded. The presence of comorbidities and liver biopsy results, if available, were also recorded. Virological response was defined as a serum HBV DNA level < 80 IU/mL. Maintained virological response was defined as serum HBV DNA negativity without subsequent positivity. A biochemical response was achieved when the serum ALT level dropped below 42 U/L. Hepatic flare was defined as an elevation of ALT ≥ 2 × upper limit of normal with subsequent HBV DNA positivity in patients with virological response. Liver biopsies were evaluated according to the ISHAK staging system[10]. Patients with pretreatment fibrosis scores between 0 and 4 (F0-4) were considered noncirrhotic. Patients with fibrosis scores 5 and 6 (F5-6) or those with radiological (nodular appearance of liver surface, parenchymal thickening, caudate lobe enlargement, portal vein diameter > 13 mm) or endoscopic (varices, portal gastropathy) findings of cirrhosis were considered compensated cirrhotic. Decompensated cirrhosis was defined as the presence of ascites, variceal bleeding or hepatic encephalopathy. Patients underwent HCC surveillance with abdominal USG at 6-12 mo intervals. In the presence of suspicious lesions on USG, cross-sectional imaging with triphasic CT and/or dynamic contrast-enhanced MRI were performed. A diagnosis of HCC was made following the current guidelines[5]. The PAGE-B score included the parameters of platelet count, age, and sex. Scoring was performed as follows: (1) For age 16-29 years, 0 points; 30-39 years, 2 points; 40-49 years, 4 points; 50-59 years, 6 points; 60-69 years, 8 points; ≥ 70 years, 10 points; (2) For female gender, 0 points and for male gender, 6 points; and (3) For platelet count (/mm^3) ≥ 200000, 0 points; 100000-199999, 6 points; < 100000, 9 points. The score ranged from 0-25 points. Based on their PAGE-B scores, patients were classified as ≤ 9, low risk; 10-17, moderate risk; and ≥ 18, high risk [7].

Statistical analysis

Statistical data were analyzed using SPSS v.23.0 (SPSS Inc., Chicago, IL, USA). Descriptive statistics are presented as the mean ± standard error of the mean for continuous variables. Variables were tested for normality using the Kolmogorov-Smirnov test. Independent *t*-tests were used to compare parametric variables, and chi-squared tests, continuity correction, or Fisher's exact tests were used to compare categorical variables. The cumulative effect of PAGE-B risk groups on survival was assessed using the log-rank test. Survival rates were computed by Kaplan-Meier survival analysis. Accuracy in predicting HCC occurrence was evaluated using a time-dependent area under the receiver operating characteristic (AUROC) curve at all study time points. Univariate and multivariate logistic regression analysis models were used to determine the effects of the variables on the risk of developing HCC. Cirrhosis and platelet count were analyzed separately in logistic regression model as they showed collinearity. Tests were interpreted at a 95% confidence interval. A *P* value ≤ 0.05 was

Table 1 Demographic and follow-up characteristics of study population

	***n* = 742**
Age, yr ± SE	45.0 ± 0.5
Gender, male *n* (%)	472 (63.6)
Follow-up, mo ± SE	54.7 ± 1.2
Diabetes mellitus, *n* (%)	116 (15.7)
HBeAg positivity, *n* (%)	171 (23.0)
Cirrhosis, *n* (%)	161 (21.7)
NA(s) before ETV/TDF, *n* (%)	162 (21.8)
Antiviral treatment (ETV/TDF), *n* (%)	240 (32.3)/502(67.7)
MVR, *n* (%)	633 (85.3)
Hepatic flare, *n* (%)	25 (3.4)
ALT normalization at 6 mo, *n* (%)	620 (85.9)
Virological response at 6 mo, *n* (%)	597 (85.4)
PAGE-B score ± SE	11.1 ± 0.2
PAGE-B score-risk groups, *n* (%)	
Low	281 (37.9)
Moderate	341 (46)
High	120 (16.2)
HCC cases during follow up, *n* (%)	26 (3.5)

HBeAg: Hepatitis B e antigen; ALT: Alanine transaminase; ETV: Entecavir; HCC: Hepatocellular carcinoma; MVR: Maintained virological response; NA(s): Nucleos(t)ide analogue(s); TDF: Tenofovir disoproxil fumarate; SE: Standard error of mean.

considered statistically significant.

The study was approved by the local ethics committees of Umraniye Training and Research Hospital and Haydarpasa Numune Training and Research Hospital.

RESULTS

A total of 742 patients were enrolled in the study. The mean age was 45.0 ± 0.5 (17-93) years, and 472 (63.6%) patients were male. One hundred and sixty-one patients (21.7%) had cirrhosis. Of the total patients, 502 (67.7%) received TDF, and 240 (32.3%) received ETV. One hundred and sixty-two (21.8%) of patients were lamivudine-experienced. At month 12, 597 patients (85.4%) achieved virological response, and 620 patients (85.9%) achieved ALT normalization. Twenty-five (3.4%) patients had hepatic flare. The mean follow-up time was 54.7 ± 1.2 (5-145) mo. The demographic and clinical characteristics and follow-up data of the patients are presented in Table 1.

During the follow-up period, 26 patients (3.5%) developed HCC. Patients who developed HCC were older, male predominant, had lower albumin and platelet levels, and had higher AFP levels than those who did not develop HCC (all $P < 0.05$). Cirrhosis and diabetes mellitus were more common in patients who developed HCC than in those who did not develop HCC (both $P < 0.05$) (Table 2).

In the univariable analysis, older age, male sex, lower platelet levels, presence of diabetes mellitus, presence of cirrhosis, absence of ALT normalization at month 6, and pretreatment AFP levels were associated with HCC development (all $P < 0.05$). HCC was not detected in any patients with hepatic flare. In the multivariable analysis, older age [odd ratio (OR) = 1.1; 95% confidence interval (CI): 1.0-1.1], male sex (OR = 8.9; 95%CI: 1.1-70.7), lower platelet levels (OR = 1.0; 95%CI: 1.0-1.0), presence of cirrhosis (OR = 3.1; 95%CI: 1.1-8.2), and absence of ALT normalization at month 6 (OR = 0.2; 95%CI: 0.1-0.7) were associated with HCC occurrence (all $P < 0.05$) (Table 3).

Table 2 Comparison of baseline characteristics of patients with and without hepatocellular carcinoma

	Patients with HCC	Patients without HCC	*P* value
Age (yr) mean ± SE	57.8 ± 2.3	44.5 ± 0.5	< 0.001
Male gender, *n* (%)	24 (92.3)	448 (62.6)	0.004
Cirrhosis, *n* (%)	16 (61.5)	145 (20.3)	< 0.001
Diabetes mellitus, *n* (%)	8 (32)	108(15.1)	0.043
Antiviral treatment (ETV/TDF), *n* (%)	10 (38.5)/16 (61.5)	230 (32.1)/486 (67.9)	0.642
Laboratory (mean ± SE)			
HBeAg positivity, *n* (%)	6 (23.1)	165 (23.0)	1.000
ALT (IU/L)	92.9 ± 25.7	98.3 ± 5.7	0.856
Albumin (g/dL)	3.9 ± 0.1	4.1 ± 0.0	0.014
Total bilirubin (mg/dL)	0.9 ± 0.1	1.0 ± 0.1	0.709
AFP (ng/mL)	23.3 ± 9.6	5.2 ± 0.4	< 0.001
INR	1.1 ± 0.0	1.1 ± 0.0	0.143
Platelet (10^3/mL)	128.8 ± 8.6	203.5 ± 2.5	< 0.001
HBV-DNA (log IU/mL)	5.4 ± 0.3	5.5 ± 0.1	0.859

ALT: Alanine transaminase; AFP: Alpha-fetoprotein; ETV: Entecavir; HCC: Hepatocellular carcinoma; SE: Standard error of mean; TDF: Tenofovir disoproxil fumarate; HBeAg: Hepatitis B e antigen; INR: International normalized ratio; HBV: Hepatitis B virus.

Validation of PAGE-B risk score

The mean PAGE-B score was 11.1 ± 0.2. According to the PAGE-B score, 281 (37.9%), 341 (46%) and 120 (16.2%) patients had low-risk, moderate-risk and high-risk of HCC development, respectively. Nineteen (6.8%), 78 (22.9%) and 64 (53.3%) patients had cirrhosis in the low-, moderate- and high-risk groups, respectively ($P < 0.001$). One (0.4%), 7 (2.1%) and 18 (15%) patients developed HCC in the low-, moderate- and high-risk groups, respectively ($P < 0.001$). For a PAGE-B score cutoff value ≤ 9, the sensitivity, specificity, positive and negative predictive values for the prediction of HCC were 96.2%, 39.1%, 5.4% and 99.6%, respectively. The AUROCs of the PAGE-B score in the prediction of HCC risk at 1, 3, 5 and 10 years were 0.977, 0.903, 0.903 and 0.865, respectively (Figure 1). The cumulative HCC incidences at 1, 3, 5 and 10 years were 0%, 0%, 0% and 0.4%, respectively, in the PAGE-B low-risk group; 0%, 1.2%, 1.5% and 2.1%, respectively, in the PAGE-B moderate-risk group; and 5.0%, 11.7%, 12.5%, and 15.0%, respectively, in the PAGE-B high-risk group (log-rank $P < 0.001$) (Figure 2).

DISCUSSION

The ultimate goal of CHB therapy is to extend the survival of patients by preventing progression to cirrhosis, HCC development and the need for transplantation. This objective has been achieved substantially with the widespread use of TDF and ETV, which have a high genetic barrier to resistance. However, the risk of HCC is not eliminated despite effective antiviral drugs. Various studies have aimed to evaluate the risk of HCC development in various populations using risk scores that include clinical or laboratory parameters. The REACH-B (age, sex, HBsAg status, and HBV DNA concentration) score was the first scoring system that did not include cirrhosis as a parameter, and it was associated with a 5-year HCC incidence of 2.6% in the low-risk group[11]. The GAG-HCC (age, sex, HBV DNA, core promoter mutations and cirrhosis) and CU-HCC (age, viral load, bilirubin, albumin, cirrhosis) scores have a negative predictive value of 98.3% for 5-year HCC incidence in treatment-naive Asian patients[12]. These scoring systems, which were validated in untreated patients, were less predictive when applied to patients on antiviral treatment[13]. For example, a high serum HBV DNA level, which is included in REACH-B, is no longer regarded as a risk factor for HCC with the use of potent antivirals[8]. Moreover, detection of core promoter mutations that are included in the GAG-HCC scoring system is not always

Table 3 Risk factors associated with the risk of hepatocellular carcinoma development

	Univariate analysis, OR (95% CI)	*P* value	Multivariate analysis, OR (95% CI)	*P* value
Age (per yr increase)	1.1 (1.0-1.1)	< 0.001	1.1 (1.0-1.1)	< 0.001
Gender (male *vs* female)	7.2 (1.7-30.6)	0.004	8.9 (1.1-70.7)	0.038
Platelet[1] (10^3/mL)	1.0 (1.0-1.0)	< 0.001	1.0 (1.0-1.0)	< 0.001
AFP (ng/mL)	1.0 (1.0-1.0)	< 0.001	1.0 (1.0-1.0)	0.141
HBeAg status (positive *vs* negative)	1.0 (0.4-2.5)	1.000		
Diabetes mellitus (yes *vs* no)	2.7 (1.1-6.3)	0.043	0.6 (0.2-1.7)	0.308
NA(s) before ETV/TDF (yes *vs* no)	2.0 (0.9-4.5)	0.143		
Cirrhosis[1] (yes *vs* no)	6.3 (2.8-14.2)	< 0.001	3.1 (1.1-8.2)	0.026
Antiviral treatment (ETV *vs* TDF)	0.8 (0.3-1.7)	0.642		
MVR (no *vs* yes)	0.6 (0.2-1.4)	0.253		
ALT normalization at month 6 (no *vs* yes)	0.4 (0.2-0.9)	0.043	0.2 (0.1-0.7)	0.009
ALT normalization at month 12 (no *vs* yes)	0.4 (0.2-1.0)	0.101		
Virological response at month 6 (no *vs* yes)	0.8 (0.3-1.9)	0.622		
Virological response at month 6 (no *vs* yes)	0.7 (0.2-2.2)	0.530		

[1]Cirrhosis and platelet count were analyzed separately among with other independent variables in logistic regression model as they showed collinearity. AFP: Alpha-fetoprotein; HBeAg: Hepatitis B e antigen; CI: Confidence interval; ETV: Entecavir; MVR: Maintained virological response; NA(s): Nucleos(t)ide analogue(s); TDF: Tenofovir disoproxil fumarate.

possible. To solve these problems, novel scoring systems were developed in patients on treatment. The PAGE-B (age, sex and platelet count), CAGE-B (age, presence of baseline cirrhosis), SAGE-B (age, liver stiffness measurements), CAMD (cirrhosis, age, male sex, diabetes mellitus) and HCC-RESCUE (age, sex, cirrhosis) scoring systems all have high negative predictive values for HCC development in their low-risk groups[7,14-16]. Among current scoring systems, the PAGE-B is the only one that does not include cirrhosis as a parameter. The presence of cirrhosis is the most important risk factor for HCC development, and the annual risk of HCC in patients with cirrhosis is 2.5%-4%[17]. Liver biopsy is the gold standard method for the diagnosis of cirrhosis. However, biopsy is associated with certain disadvantages, such as being an invasive method that can lead to potential complications, requiring tissue samples of an appropriate amount and from an appropriate localization, and producing false-negative results in the early period. Meanwhile, noninvasive methods that assess fibrosis, such as transient elastography, can produce operator-dependent false-positive results. It should also be emphasized that liver biopsy is not performed in patients with lamivudine, adefovir or telbivudine resistance prior to the start of new antiviral agents with a high genetic barrier to resistance. Therefore, these nucleos(t)ide analog-experienced patients may not have cirrhosis at the start of rescue therapy due to the resolution of cirrhosis after years of therapy. Our cohort also included 162 patients (21.8%) who had received lamivudine and developed resistance prior to the start of TDF/ETV treatment. Therefore, definitive confirmation of cirrhosis for all patients is impractical. To that point, the PAGE-B score has an advantage compared to the other scoring systems that include cirrhosis as a parameter. Supporting this, implementing ISHAK stage in the PAGE-B score did not improve the prediction of HCC risk[18].

In the present study, the incidence of HCC was determined to be 3.5%, and the cumulative HCC incidences at 5 years in the low-, moderate-, and high-risk groups were 0%, 1.5% and 12.5%, respectively. These rates were lower than those in the PAGE-B database (0%, 3%, 17%) but higher than those in Spain's CIBERHEP database (0%, 2.8%, 5%), which was used for the validation of the PAGE-B score. All three databases (ours, PAGE-B, CIBERHEP) had similar reliability of the PAGE-B score in the prediction of overall HCC development for a cutoff value ≥ 10[7,9]. It was thought

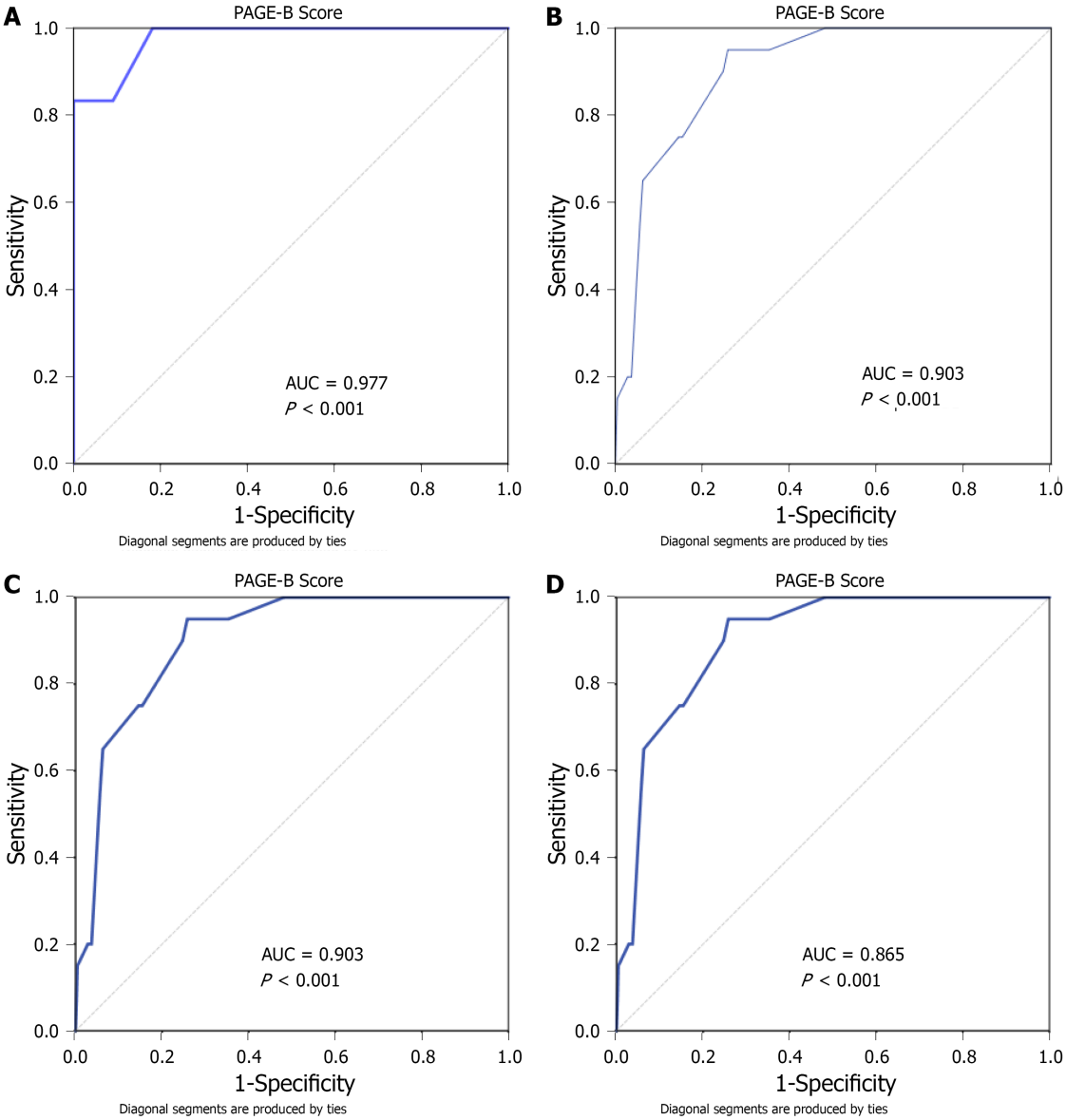

Figure 1 Receiver operating characteristic curves of the PAGE-B score for hepatocellular carcinoma development according to years. A: 1st year; B: 3rd year; C: 5th year; D: 10th year.

that the lower HCC rates in CIBERHEP may be related to the relatively low total number of patients and the number of patients who completed the 5-year follow-up [9]. The present study included 267 (36%) patients who had completed the 5-year follow-up, which was similar to the PAGE-B database; however, patients were younger on average than the PAGE-B database (45 *vs* 52). This might be a reason for the lower HCC incidence seen in this study. Additionally, the present study included mainly genotype D patients who are known to have less risk for HCC development, while genotypes A, B, D predominated in the PAGE-B database and genotype B and D in the CIBERHEP database.

In this study, we also evaluated 10-year HCC incidence. Although we did not find any cases of HCC in the low-risk group during the first 5 years of follow-up, one patient developed HCC at month 80. This 37-year-old noncirrhotic male patient was treated with ETV, did not have comorbidities, and had a PAGE-B score of 8. The study by Brouwer *et al*[18] showed that the estimated HCC incidences at 10 years in PAGE-B low-, moderate-, and high-risk groups were < 1.5%, 1.5%-17.5% and ≥ 17.5%, respectively, supporting our results (0.4%, 2.1%, 15%).

Current international guidelines recommend that patients with cirrhosis should undergo HCC surveillance systematically. However, there is no consensus about noncirrhotic CHB patients[19-22]. Diverging from other guidelines, the European Association for the Study of the Liver suggests that only patients with a PAGE-B score ≥ 10 in the noncirrhotic group should be included in screening[19]. In the present

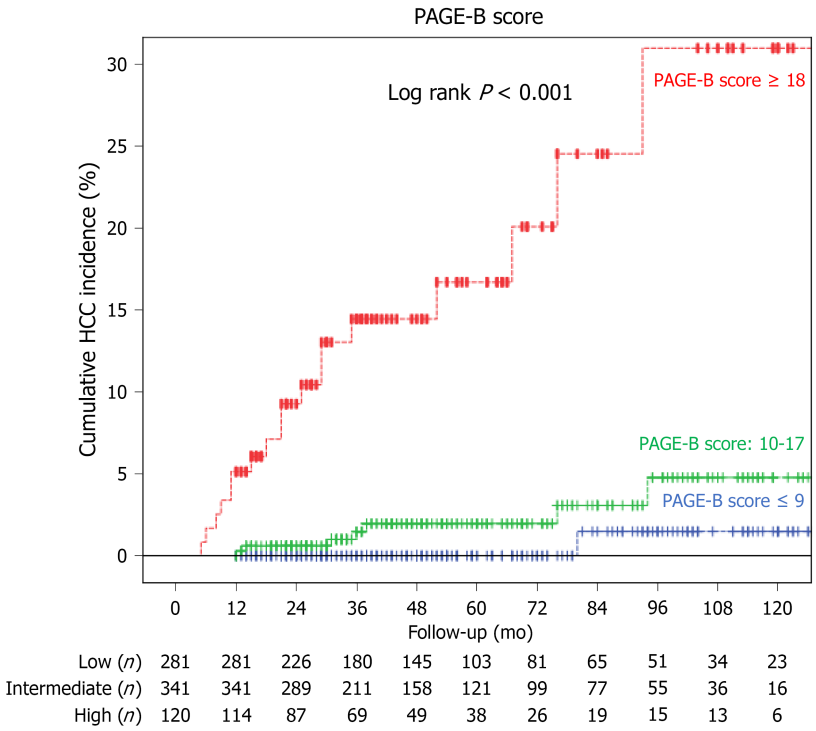

Figure 2 Cumulative hepatocellular carcinoma incidences according to PAGE-B risk scores. Low risk *vs* intermediate risk, log rank $P = 0.06$; low risk *vs* high risk, log rank $P < 0.001$; intermediate risk *vs* high risk, log rank $P < 0.001$.

study, unnecessary tests would be prevented in 281 (37.9%) patients with low-risk HCC by following this cost-effective approach.

The present study has some limitations. First, it is a retrospective study, so the effect of treatment non-compliance could not be determined precisely. Second, the patient number was relatively low. Third, only one-third of the patients completed the 5-year follow-up. Fourth, in Turkey, almost all patients are infected with genotype D virus (32), so no interpretation could be made for other genotypes.

CONCLUSION

PAGE–B successfully predicted patients who had a low risk for HCC during treatment with genetically high barrier antivirals. Ease of use without the need for biopsy or an impractical molecular test justifies implementing this score in clinical practice.

ARTICLE HIGHLIGHTS

Research background

Chronic hepatitis B (CHB) infection is an important health issue worldwide. Novel antiviral treatments lead to complete suppression of the virus and maintained suppression of viral replication prevents cirrhosis, decompensation in already cirrhotic patients and hepatocellular carcinoma (HCC). However, HCC risk is not totally eliminated and in pursuance of detecting cancer in early stages comprehensive follow up is needed. It is critical to stratify patients for risk predictions, especially to prevent unnecessary tests in low-risk patients.

Research motivation

Various risk scores have been developed to predict the development of HCC in CHB patients. The majority of studies on the risk scores had focused on untreated patients. Currently, almost all patients with CHB are treated with antiviral agents and better risk scores for patients under treatment is needed. The PAGE-B is a risk scoring system that includes platelet count, age and sex and has been validated in patients treated with antivirals.

Research objectives

We aimed to evaluate the accuracy of the PAGE-B scoring system in the prediction of HCC risk in CHB patients receiving entecavir (ETV) or tenofovir disoproxil fumarat therapy.

Research methods

We recruited 742 CHB patients who had been treated with tenofovir disoproxil fumarate or ETV for more than 1 year. Risk groups were determined according to the PAGE-B scores. We evaluated the accuracy of the PAGE-B score in predicting HCC.

Research results

HCC was diagnosed in 26 patients (3.5%) during 54.7 ± 1.2 mo mean follow up. The cumulative HCC incidences at 5 years were 0% in the PAGE-B low-risk group; 1.5% moderate-risk group; and 12.5%, in the high-risk group (log-rank $p < 0.001$). The AUROCs of the PAGE-B score in the prediction of HCC development at 5 years follow up was 0.903.

Research conclusions

PAGE–B had successfully predicted the patients who had a low risk of HCC during treatment with genetically high barrier antivirals.

Research perspectives

PAGE-B is a simple score that does not require biopsy or any impractical molecular test. The efficiency of PAGE-B justifies implementing this score in daily clinical practice.

REFERENCES

1 **Global Burden of Disease Cancer Collaboration**. Global, Regional, and National Cancer Incidence, Mortality, Years of Life Lost, Years Lived With Disability, and Disability-Adjusted Life-Years for 29 Cancer Groups, 1990 to 2016: A Systematic Analysis for the Global Burden of Disease Study. *JAMA Oncol* 2018; **4**: 1553-1568 [PMID: 29860482 DOI: 10.1001/jamaoncol.2018.2706]

2 **Global Burden of Disease Liver Cancer Collaboration**. The Burden of Primary Liver Cancer and Underlying Etiologies From 1990 to 2015 at the Global, Regional, and National Level: Results From the Global Burden of Disease Study 2015. *JAMA Oncol* 2017; **3**: 1683-1691 [PMID: 28983565 DOI: 10.1001/jamaoncol.2017.3055]

3 **Jemal A**, Ward EM, Johnson CJ, Cronin KA, Ma J, Ryerson B, Mariotto A, Lake AJ, Wilson R, Sherman RL, Anderson RN, Henley SJ, Kohler BA, Penberthy L, Feuer EJ, Weir HK. Annual Report to the Nation on the Status of Cancer, 1975-2014, Featuring Survival. *J Natl Cancer Inst* 2017; **109** [PMID: 28376154 DOI: 10.1093/jnci/djx030]

4 **Marrero JA**, Kulik LM, Sirlin CB, Zhu AX, Finn RS, Abecassis MM, Roberts LR, Heimbach JK. Diagnosis, Staging, and Management of Hepatocellular Carcinoma: 2018 Practice Guidance by the American Association for the Study of Liver Diseases. *Hepatology* 2018; **68**: 723-750 [PMID: 29624699 DOI: 10.1002/hep.29913]

5 **Yang HI**, Yuen MF, Chan HL, Han KH, Chen PJ, Kim DY, Ahn SH, Chen CJ, Wong VW, Seto WK; REACH-B Working Group. Risk estimation for hepatocellular carcinoma in chronic hepatitis B (REACH-B): development and validation of a predictive score. *Lancet Oncol* 2011; **12**: 568-574 [PMID: 21497551 DOI: 10.1016/S1470-2045(11)70077-8]

6 **Wong VW**, Chan SL, Mo F, Chan TC, Loong HH, Wong GL, Lui YY, Chan AT, Sung JJ, Yeo W, Chan HL, Mok TS. Clinical scoring system to predict hepatocellular carcinoma in chronic hepatitis B carriers. *J Clin Oncol* 2010; **28**: 1660-1665 [PMID: 20194845 DOI: 10.1200/JCO.2009.26.2675]

7 **Papatheodoridis G**, Dalekos G, Sypsa V, Yurdaydin C, Buti M, Goulis J, Calleja JL, Chi H, Manolakopoulos S, Mangia G, Gatselis N, Keskin O, Savvidou S, de la Revilla J, Hansen BE, Vlachogiannakos I, Galanis K, Idilman R, Colombo M, Esteban R, Janssen HL, Lampertico P. PAGE-B predicts the risk of developing hepatocellular carcinoma in Caucasians with chronic hepatitis B on 5-year antiviral therapy. *J Hepatol* 2016; **64**: 800-806 [PMID: 26678008 DOI: 10.1016/j.jhep.2015.11.035]

8 **Kim MN**, Hwang SG, Rim KS, Kim BK, Park JY, Kim DY, Ahn SH, Han KH, Kim SU. Validation of PAGE-B model in Asian chronic hepatitis B patients receiving entecavir or tenofovir. *Liver Int* 2017; **37**: 1788-1795 [PMID: 28418595 DOI: 10.1111/Liv.13450]

9 **Riveiro-Barciela M**, Tabernero D, Calleja JL, Lens S, Manzano ML, Rodríguez FG, Crespo J, Piqueras B, Pascasio JM, Comas C, Gutierrez ML, Aguirre A, Suárez E, García-Samaniego J, Rivero M, Acero D, Fernandez-Bermejo M, Moreno D, Sánchez-Pobre P, de Cuenca B, Moreno-Palomares JJ, Esteban R, Buti M. Effectiveness and Safety of Entecavir or Tenofovir in a Spanish Cohort of Chronic Hepatitis B Patients: Validation of the Page-B Score to Predict Hepatocellular Carcinoma.

Dig Dis Sci 2017; **62**: 784-793 [PMID: 28078526 DOI: 10.1007/s10620-017-4448-7]

10 **Ishak K**, Baptista A, Bianchi L, Callea F, De Groote J, Gudat F, Denk H, Desmet V, Korb G, MacSween RN. Histological grading and staging of chronic hepatitis. *J Hepatol* 1995; **22**: 696-699 [PMID: 7560864 DOI: 10.1016/0168-8278(95)80226-6]

11 **Yang HI**, Sherman M, Su J, Chen PJ, Liaw YF, Iloeje UH, Chen CJ. Nomograms for risk of hepatocellular carcinoma in patients with chronic hepatitis B virus infection. *J Clin Oncol* 2010; **28**: 2437-2444 [PMID: 20368541 DOI: 10.1200/JCO.2009.27.4456]

12 **Wong GL**, Chan HL, Chan HY, Tse PC, Tse YK, Mak CW, Lee SK, Ip ZM, Lam AT, Iu HW, Leung JM, Wong VW. Accuracy of risk scores for patients with chronic hepatitis B receiving entecavir treatment. *Gastroenterology* 2013; **144**: 933-944 [PMID: 23415803 DOI: 10.1053/j.gastro.2013.02.002]

13 **Arends P**, Sonneveld MJ, Zoutendijk R, Carey I, Brown A, Fasano M, Mutimer D, Deterding K, Reijnders JG, Oo Y, Petersen J, van Bömmel F, de Knegt RJ, Santantonio T, Berg T, Welzel TM, Wedemeyer H, Buti M, Pradat P, Zoulim F, Hansen B, Janssen HL; VIRGIL Surveillance Study Group. Entecavir treatment does not eliminate the risk of hepatocellular carcinoma in chronic hepatitis B: limited role for risk scores in Caucasians. *Gut* 2015; **64**: 1289-1295 [PMID: 25011935 DOI: 10.1136/gutjnl-2014-307023]

14 **Ji JH**, Park SY, Son WJ, Shin HJ, Lee H, Lee HW, Lee JS, Kim SU, Park JY, Kim DY, Ahn SH, Kim BK. External validation of CAGE-B and SAGE-B scores for Asian chronic hepatitis B patients with well-controlled viremia by antivirals. *J Viral Hepat* 2021; **28**: 951-958 [PMID: 33763928 DOI: 10.1111/jvh.13506]

15 **Kim SU**, Seo YS, Lee HA, Kim MN, Kim EH, Kim HY, Lee YR, Lee HW, Park JY, Kim DY, Ahn SH, Han KH, Hwang SG, Rim KS, Um SH, Tak WY, Kweon YO, Kim BK, Park SY. Validation of the CAMD Score in Patients With Chronic Hepatitis B Virus Infection Receiving Antiviral Therapy. *Clin Gastroenterol Hepatol* 2020; **18**: 693-699.e1 [PMID: 31252188 DOI: 10.1016/j.cgh.2019.06.028]

16 **Güzelbulut F**, Gökçen P, Can G, Adalı G, Değirmenci Saltürk AG, Bahadır Ö, Özdil K, Doğanay HL. Validation of the HCC-RESCUE score to predict hepatocellular carcinoma risk in Caucasian chronic hepatitis B patients under entecavir or tenofovir therapy. *J Viral Hepat* 2021; **28**: 826-836 [PMID: 33586270 DOI: 10.1111/jvh.13485]

17 **Mair RD**, Valenzuela A, Ha NB, Ayoub WS, Daugherty T, Lutchman GA, Garcia G, Ahmed A, Nguyen MH. Incidence of hepatocellular carcinoma among US patients with cirrhosis of viral or nonviral etiologies. *Clin Gastroenterol Hepatol* 2012; **10**: 1412-1417 [PMID: 22902757 DOI: 10.1016/j.cgh.2012.08.011]

18 **Brouwer WP**, van der Meer AJP, Boonstra A, Plompen EPC, Pas SD, de Knegt RJ, de Man RA, Ten Kate FJW, Janssen HLA, Hansen BE. Prediction of long-term clinical outcome in a diverse chronic hepatitis B population: Role of the PAGE-B score. *J Viral Hepat* 2017; **24**: 1023-1031 [PMID: 28544398 DOI: 10.1111/jvh.12727]

19 **European Association for the Study of the Liver**. EASL Clinical Practice Guidelines: Management of hepatocellular carcinoma. *J Hepatol* 2018; **69**: 182-236 [PMID: 29628281 DOI: 10.1016/j.jhep.2018.03.019]

20 **Heimbach JK**, Kulik LM, Finn RS, Sirlin CB, Abecassis MM, Roberts LR, Zhu AX, Murad MH, Marrero JA. AASLD guidelines for the treatment of hepatocellular carcinoma. *Hepatology* 2018; **67**: 358-380 [PMID: 28130846 DOI: 10.1002/hep.29086]

21 **Omata M**, Cheng AL, Kokudo N, Kudo M, Lee JM, Jia J, Tateishi R, Han KH, Chawla YK, Shiina S, Jafri W, Payawal DA, Ohki T, Ogasawara S, Chen PJ, Lesmana CRA, Lesmana LA, Gani RA, Obi S, Dokmeci AK, Sarin SK. Asia-Pacific clinical practice guidelines on the management of hepatocellular carcinoma: a 2017 update. *Hepatol Int* 2017; **11**: 317-370 [PMID: 28620797 DOI: 10.1007/s12072-017-9799-9]

22 **Kokudo N**, Hasegawa K, Akahane M, Igaki H, Izumi N, Ichida T, Uemoto S, Kaneko S, Kawasaki S, Ku Y, Kudo M, Kubo S, Takayama T, Tateishi R, Fukuda T, Matsui O, Matsuyama Y, Murakami T, Arii S, Okazaki M, Makuuchi M. Evidence-based Clinical Practice Guidelines for Hepatocellular Carcinoma: The Japan Society of Hepatology 2013 update (3rd JSH-HCC Guidelines). *Hepatol Res* 2015; **45** [PMID: 25625806 DOI: 10.1111/hepr.12464]

World Journal of Gastroenterology

Submit a Manuscript: https://www.f6publishing.com

World J Gastroenterol 2022 February 14; 28(6): 675-682

DOI: 10.3748/wjg.v28.i6.675

ISSN 1007-9327 (print) ISSN 2219-2840 (online)

CASE REPORT

Gallbladder Burkitt's lymphoma mimicking gallbladder cancer: A case report

Kiyotaka Hosoda, Akira Shimizu, Koji Kubota, Tsuyoshi Notake, Hikaru Hayashi, Koya Yasukawa, Kentaro Umemura, Atsushi Kamachi, Takamune Goto, Hidenori Tomida, Shiori Yamazaki, Yuri Narusawa, Naoko Asano, Takeshi Uehara, Yuji Soejima

ORCID number: Kiyotaka Hosoda 0000-0001-6928-3676; Akira Shimizu 0000-0002-5015-1697; Koji Kubota 0000-0003-0164-7685; Tsuyoshi Notake 0000-0002-2277-5347; Hikaru Hayashi 0000-0002-3724-1751; Koya Yasukawa 0000-0002-3643-0921; Kentaro Umemura 0000-0003-1259-5438; Atsushi Kamachi 0000-0002-4012-0459; Takamune Goto 0000-0003-2410-0770; Hidenori Tomida 0000-0001-9278-7418; Shiori Yamazaki 0000-0001-8162-0620; Yuri Narusawa 0000-0003-0346-6220; Naoko Asano 0000-0001-7536-6179; Takeshi Uehara 0000-0002-7694-9015; Yuji Soejima 0000-0001-5539-9280.

Author contributions: Hosoda K, Kubota K, Notake T, Hayashi H, Umemura K, Kamachi A, Goto T, Tomida H, and Yamazaki S were the patient's hepato-biliary-pancreatic surgeons, they reviewed the literature and contributed to manuscript drafting; Narusawa Y, Asano N, and Uehara T were involved in pathology evaluation; Shimizu A and Soejima Y were responsible for revising the manuscript for important intellectual content; all the authors provided final approval for the version of the manuscript to be submitted.

Informed consent statement:

Kiyotaka Hosoda, Akira Shimizu, Koji Kubota, Tsuyoshi Notake, Hikaru Hayashi, Koya Yasukawa, Kentaro Umemura, Atsushi Kamachi, Takamune Goto, Hidenori Tomida, Shiori Yamazaki, Yuji Soejima, Division of Gastroenterological, Hepato-Biliary-Pancreatic, Transplantation and Pediatric Surgery, Department of Surgery, Shinshu University School of Medicine, Matsumoto 390-8621, Japan

Yuri Narusawa, Naoko Asano, Takeshi Uehara, Department of Laboratory Medicine, Shinshu University School of Medicine, Matsumoto 390-8621, Japan

Corresponding author: Akira Shimizu, MD, PhD, Associate Professor, Division of Gastroenterological, Hepato-Biliary-Pancreatic, Transplantation and Pediatric Surgery, Department of Surgery, Shinshu University School of Medicine, 3-1-1 Asahi, Matsumoto 390-8621, Japan. ashimizu@shinshu-u.ac.jp

Abstract

BACKGROUND

Malignant lymphoma is a rare form of gallbladder malignancy. Most of these malignancies are diffuse large B-cell lymphomas or mucosa-associated lymphoid tissue-type lymphomas; however, Burkitt's lymphoma of the gallbladder is extremely rare, and only two previous reports are available in the literature. Herein, we report a rare case of Burkitt's lymphoma of the gallbladder mimicking gallbladder adenocarcinoma.

CASE SUMMARY

An 83-year-old man with no abdominal complaints was found to have a gallbladder tumor and periportal lymph node enlargement on computed tomography (CT) performed for hypertension screening. His laboratory data revealed slightly elevated serum levels of carcinoembryonic antigen and soluble interleukin 2 receptor. Imaging examinations revealed two irregular and contrast-enhanced masses extending into the gallbladder lumen, but these did not infiltrate the serosa. Moreover, a periportal lymph node had enlarged to 30 mm. Based on these findings, we diagnosed the patient as having gallbladder adenocarcinoma with lymph node metastasis, which was treated using bile duct resection with gallbladder bed resection and periportal lymph node dissection. However, the patient was finally diagnosed as having Burkitt's lymphoma. Although the surgical margin was pathologically negative, recurrence was noted at the hepatic

Written informed consent was obtained from the patient for the publication of this report and any accompanying images.

Conflict-of-interest statement: The authors declare that they have no conflicts of interest.

CARE Checklist (2016) statement: The authors have read the CARE Checklist (2016), and the manuscript was prepared and revised according to the CARE Checklist (2016).

Country/Territory of origin: Japan

Specialty type: Gastroenterology and hepatology

Provenance and peer review: Unsolicited article; Externally peer reviewed.

Peer-review model: Single blind

Peer-review report's scientific quality classification
Grade A (Excellent): A
Grade B (Very good): B
Grade C (Good): 0
Grade D (Fair): 0
Grade E (Poor): 0

Received: October 1, 2021
Peer-review started: October 1, 2021
First decision: November 7, 2021
Revised: November 23, 2021
Accepted: January 19, 2022
Article in press: January 19, 2022
Published online: February 14, 2022

P-Reviewer: Gupta P, Zhu CF

radical margin and superior pancreaticoduodenal lymph nodes on positron emission tomography/CT soon after discharge. Thus, he was referred to a hematologist and started receiving treatment with reduced-dose cyclophosphamide, doxorubicin, vincristine, and prednisone.

CONCLUSION
Burkitt's lymphoma can occur in the gallbladder. Biopsy can be useful in cases with findings suggestive of gallbladder malignant lymphoma.

Key Words: Gallbladder; Malignant lymphoma; Burkitt's lymphoma; Gallbladder cancer; Lymphadenopathy; Case report

Core Tip: Malignant lymphoma is a rare form of gallbladder malignancy, and Burkitt's lymphoma of the gallbladder is especially rare, with only two previous reports available in the literature. We report a case of gallbladder Burkitt's lymphoma that was preoperatively indistinguishable from gallbladder carcinoma. Unfortunately, the patient had lymphoma recurrence immediately after the surgery because of delayed chemotherapy initiation owing to postoperative complications due to an extended surgery. Although accurate preoperative diagnosis of gallbladder malignant lymphoma is quite difficult, some findings are suggestive of gallbladder malignant lymphoma, and hence, biopsy is recommended in these cases.

Citation: Hosoda K, Shimizu A, Kubota K, Notake T, Hayashi H, Yasukawa K, Umemura K, Kamachi A, Goto T, Tomida H, Yamazaki S, Narusawa Y, Asano N, Uehara T, Soejima Y. Gallbladder Burkitt's lymphoma mimicking gallbladder cancer: A case report. *World J Gastroenterol* 2022; 28(6): 675-682
URL: https://www.wjgnet.com/1007-9327/full/v28/i6/675.htm
DOI: https://dx.doi.org/10.3748/wjg.v28.i6.675

INTRODUCTION

Malignant lymphoma of the gallbladder is extremely rare[1-4]. In almost all cases of this malignancy, patients are diagnosed as having gallbladder adenocarcinoma or cholecystitis at the time of surgery, and preoperative diagnosis is extremely difficult. Although several reports have documented malignant lymphomas of the gallbladder, most of these malignancies are diffuse large B-cell lymphomas and mucosa-associated lymphoid tissue-type lymphomas (MALTomas)[2,4,5], and only two reports have previously documented Burkitt's lymphoma of the gallbladder[6,7]. Herein, we report the case of a patient with Burkitt's lymphoma of the gallbladder mimicking gallbladder adenocarcinoma.

CASE PRESENTATION

Chief complaints

An 83-year-old man with no abdominal complaints was found to have a gallbladder tumor along with periportal lymph node enlargement and was admitted to our institution for further investigation.

History of present illness

The tumor was detected during contrast-enhanced computed tomography (CT) performed for a detailed examination of hypertension.

History of past illness

The patient had a history of cerebral artery stenosis and paroxysmal atrial fibrillation.

S-Editor: Fan JR
L-Editor: A
P-Editor: Fan JR

Personal and family history

No personal and family history.

Physical examination

Abdominal examination revealed no palpable mass or tenderness.

Laboratory examinations

Laboratory examinations performed upon admission revealed mild to moderate renal dysfunction (creatinine: 1.21 mg/dL) and slightly elevated levels of serum carcinoembryonic antigen and serum soluble interleukin 2 receptor (6.1 ng/mL and 635 IU/mL, respectively). Other laboratory data were within normal limits.

Imaging examinations

A contrast-enhanced abdominal CT scan revealed two irregular and highly contrast-enhanced masses at the neck and body of the gallbladder as well as periportal lymph node enlargement, measuring 30 mm × 20 mm in diameter and consistent with gallbladder cancer lymph node metastasis (Figure 1). Magnetic resonance imaging revealed that the tumor signal was hypointense on T1-weighted imaging and hyperintense on T2-weighted and diffusion-weighted imaging (Figure 2). Positron emission tomography (PET) revealed increased ^{18}F-fluorodeoxyglucose uptake in the tumor (Figure 3). Endoscopic ultrasonography (EUS) showed a heterogeneous echoic mass extending into the lumen, but it did not infiltrate the serosa (Figure 4).

FINAL DIAGNOSIS

The final diagnosis was gallbladder adenocarcinoma with lymph node metastasis.

TREATMENT

On the basis of these findings, the patient underwent bile duct resection with gallbladder bed resection and periportal lymph node dissection. The surgical findings revealed the gallbladder tumor was relatively softer than ordinary gallbladder cancers. The swollen lymph node was firm but did not invade the portal vein. However, the patient developed severe aspiration pneumonia and bile leakage after the surgery, which were treated conservatively. The patient was discharged 2 mo after the surgery.

OUTCOME AND FOLLOW-UP

Histologic examination revealed periportal lymphadenopathy and two tumors at the neck and body of the gallbladder, measuring 27 mm × 20 mm and 20 mm × 18 mm in diameter, respectively. Histological findings also showed monotonous lymphoid cells with hemophagocytosis by macrophages. Immunohistochemical staining for markers showed the presence of CD10, BCL6, and c-Myc and the absence of BCL2. The Ki-67 index was > 80% (Figure 5). Therefore, the patient was finally diagnosed as having Burkitt's lymphoma. Although the surgical margin was pathologically negative, recurrence was noted at the hepatic radical margin and superior pancreaticoduodenal lymph nodes on PET-CT immediately after discharge. Thus, he was referred to a hematologist and started receiving treatment with reduced-dose cyclophosphamide, doxorubicin, vincristine, and prednisone.

DISCUSSION

Malignant lymphoma of the gallbladder is a rare form of gallbladder malignancy, which accounts for 0.1%-0.2% of all gallbladder cancers[1-3]. In previous reports, most of these malignancies were documented to be diffuse large B-cell lymphomas and MALTomas[2,4], and only two reports had documented Burkitt's lymphoma of the gallbladder[6,7]. Compared to previous cases, the present case yielded some interesting clinical and imaging findings.

Table 1 Diagnostic criteria for gastrointestinal malignant lymphoma

Ref.	Diagnostic criteria
Dawson *et al*[8]	Absence of palpable superficial lymphadenopathy
	Absence of obvious enlargement of mediastinal lymph nodes
	Normal level of total and differential white blood cell counts
	The bowel lesion predominating and the only lymph node obviously affected being those in its immediate neighborhood
	Absence of tumor in the liver and spleen
Lewin *et al*[9]	Exhibiting gastroinetstinal symptoms or predominant lesions in the gastrointestinal tract

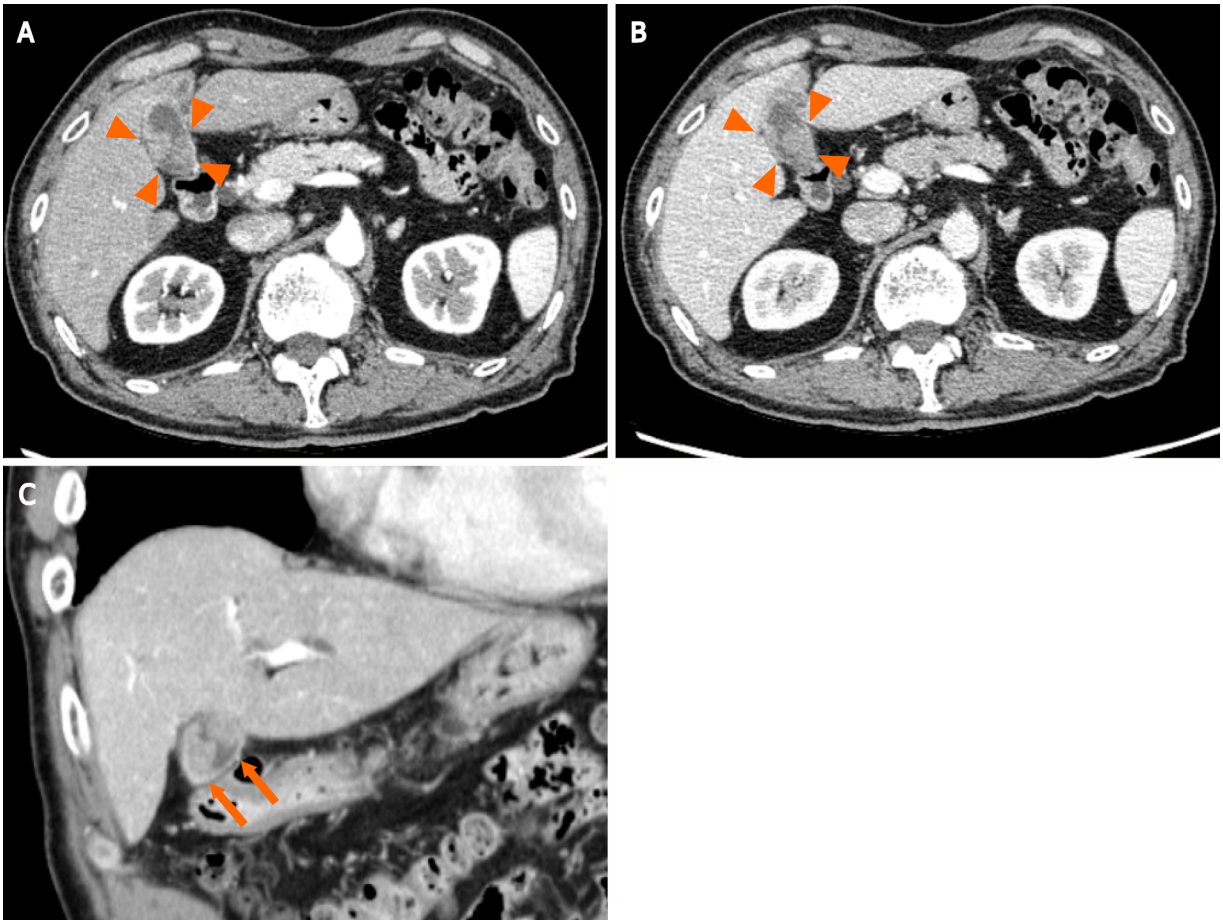

Figure 1 A contrast-enhanced abdominal computed tomography scan shows two irregular and highly contrast-enhanced masses (arrowheads and arrow) at the neck and body of the gallbladder as well as periportal lymph node enlargement, which is consistent with gallbladder cancer lymph node metastasis. A: Axial section image in the early phase showing neck of the gallbladder; B: Axial section image in the delayed phase showing neck of the gallbladder in the delayed phase; C: Coronal sectional image showing body of the gallbladder.

First, this is potentially the first reported case of "primary" gallbladder Burkitt's lymphoma. According to the diagnostic criteria of primary gastrointestinal lymphoma (Table 1) defined by Dawson *et al*[8] and Lewin *et al*[9], the previous two cases were diagnosed as "secondary" gallbladder Burkitt's lymphoma because they included extra-gallbladder lesions, such as duodenal, hepatic, or central nervous system lesions. In contrast, in the present case, the tumor was localized in the gallbladder and a periportal lymph node. Although no gastrointestinal symptoms were observed because the primary site was the gallbladder, other criteria were fulfilled. Therefore, the patient was diagnosed as having "primary" gallbladder Burkitt's lymphoma, and the case was considered novel.

Second, gallbladder Burkitt's lymphoma can present as a localized disease that mimics gallbladder cancer. The imaging features of malignant lymphoma were reported by Ono *et al*[3], who reported that high-grade malignant lymphomas showed

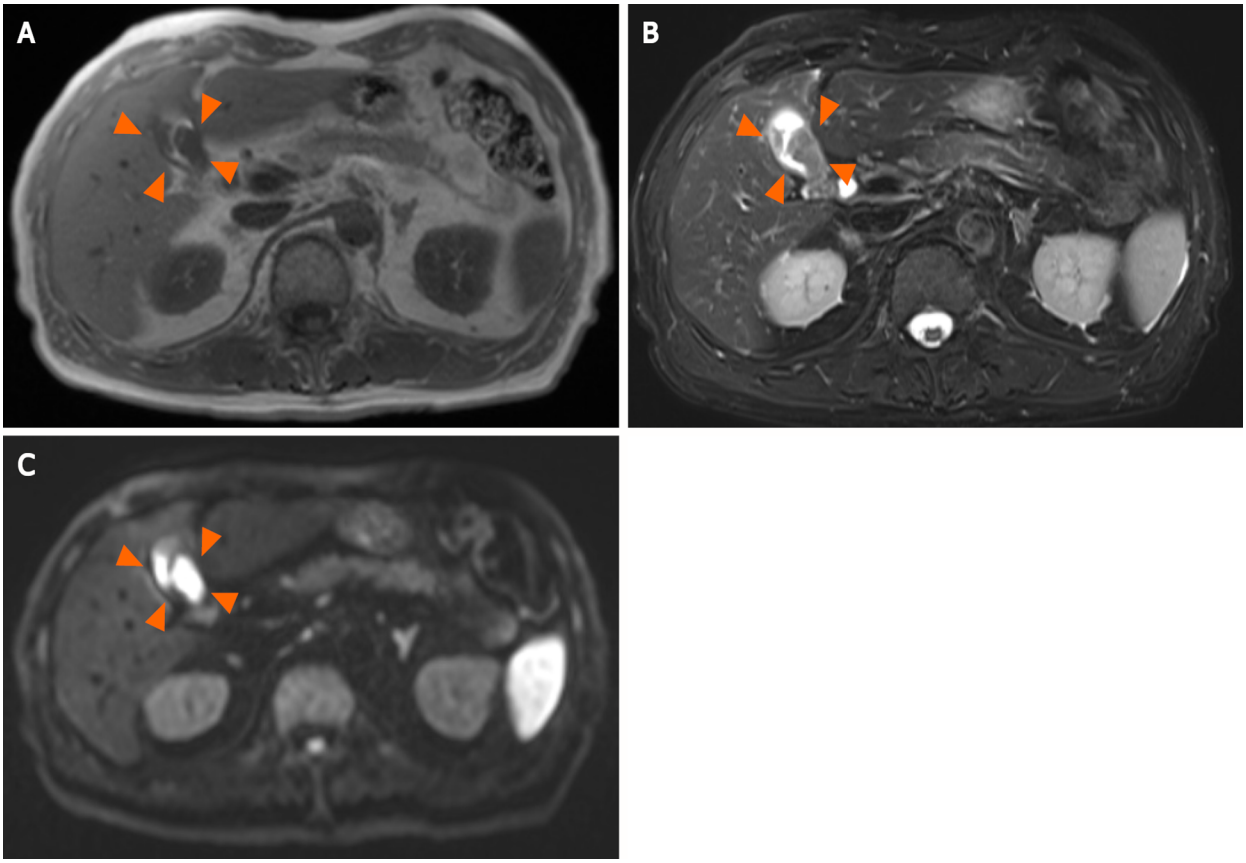

Figure 2 Magnetic resonance imaging reveals a hypointense tumor signal. A: T1-weighted imaging (arrowheads); B: A hyperintense signal on T2-weighted imaging (arrowheads); C: Diffusion-weighted imaging (arrowheads).

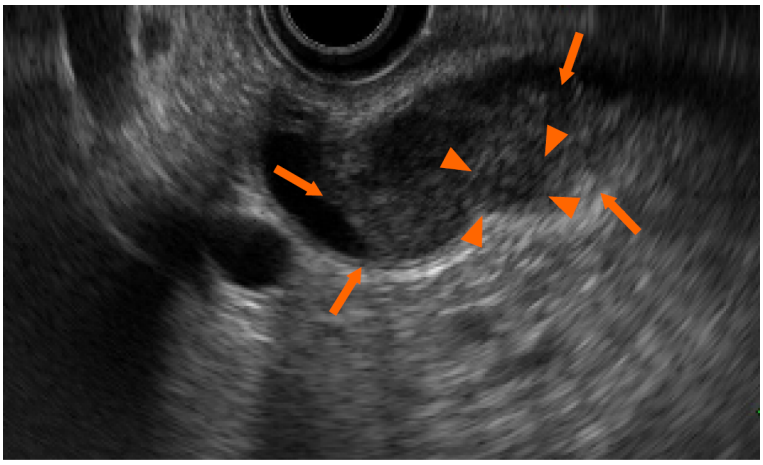

Figure 3 Endoscopic ultrasonography shows a heterogeneous echoic mass (arrows) with internal partially low echo (arrowheads). The mass extends into the lumen but does not infiltrate the serosa.

solid and bulky masses or irregular wall thickening. In addition, because Burkitt's lymphoma is a highly aggressive and rapidly progressive disease, some extranodal sites are generally involved at the time of diagnosis[10] and tumor localization around the primary lesion is rare[11]. In this case, the malignancy was localized in the body of the gallbladder and a periportal lymph node. Since these findings were consistent with the imaging findings of gallbladder adenocarcinoma, we could not confirm a preoperative diagnosis of malignant lymphoma.

Unfortunately, the patient had lymphoma recurrence 2 mo after the surgery because the introduction of chemotherapy had to be delayed owing to postoperative complications. Burkitt's lymphoma is a highly aggressive disease, but it is highly sensitive to chemotherapy. Therefore, chemotherapy has the highest priority in the treatment of

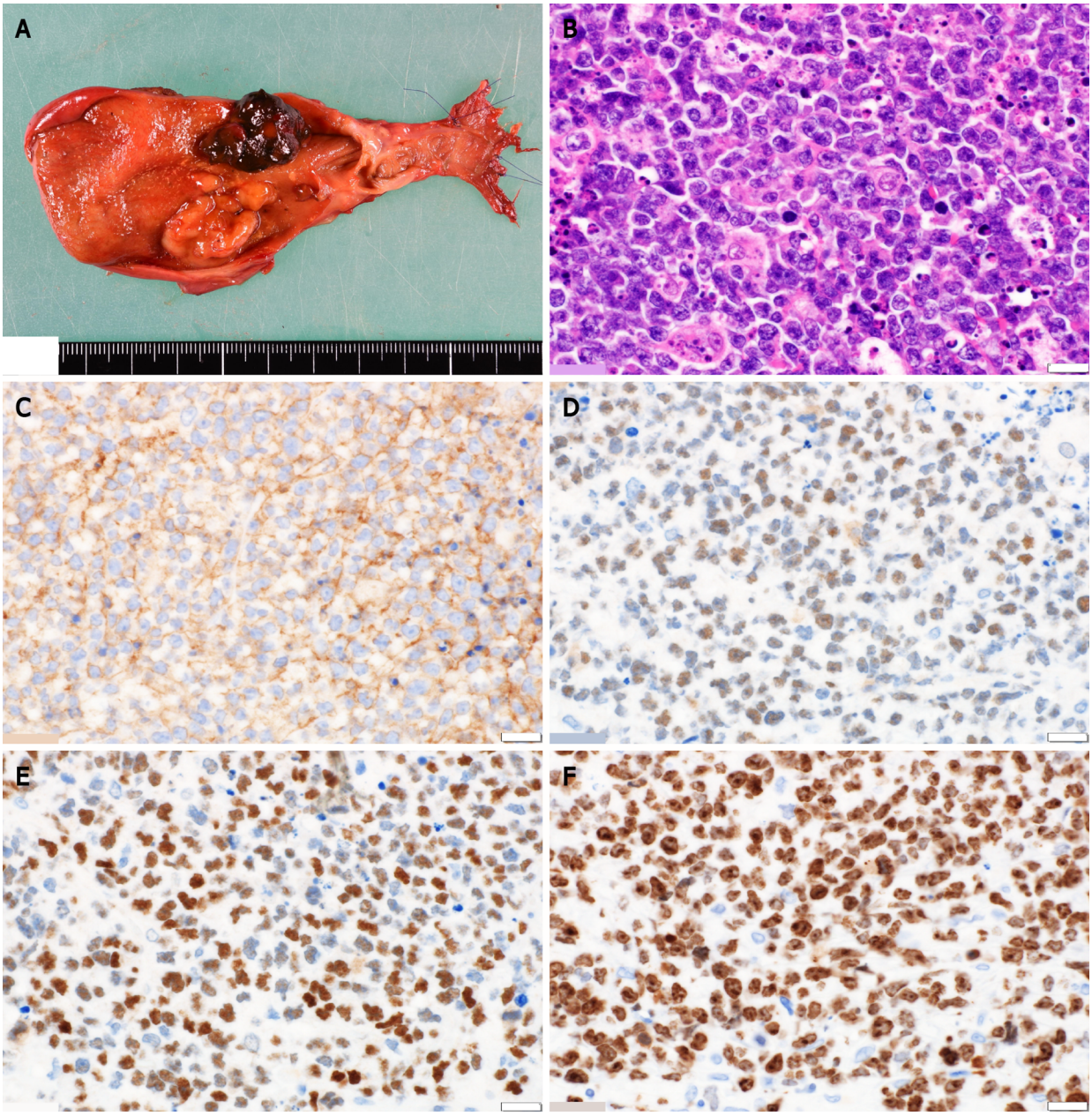

Figure 4 Histologic examination. A: Periportal lymphadenopathy and two tumors at the neck and body of the gallbladder, measuring 27 mm × 20 mm and 20 mm × 18 mm in diameter, respectively; B: Histological findings reveal monotonous lymphoid cells with hemophagocytosis by macrophages; C-E: Immunohistochemical staining for markers shows the presence of CD10 (C), BCL6 (D), and c-Myc (E) and the absence of BCL2; F: The Ki-67 index is > 80%. The white scale bars represent 1 mm.

Burkitt's lymphoma[10], and we should have introduced chemotherapy as soon as possible after the surgery. If we had been aware of the possibility of gallbladder malignant lymphoma, we could have avoided the extended procedure and could have initiated chemotherapy at the appropriate time.

Although the accurate preoperative diagnosis of gallbladder malignant lymphoma is quite difficult[2,12], some previous reports[3,12,13] have suggested the possibility of a precise preoperative diagnosis based on imaging findings. Specifically, Ono *et al*[3] showed that the signal intensity of the gallbladder wall on T2-weighted imaging is more hypointense in malignant lymphoma than in carcinoma. In addition, Kato *et al*[12] reported the usefulness of an internal partially low echo in distinguishing malignant lymphoma from carcinoma. On a retrospective review of the present case, although no obvious differences were observed in the intensity of T2-weighted imaging when compared to that of gallbladder cancers, EUS revealed an internal partially low echo of the tumor. Furthermore, in this case, a discrepancy existed in that no serosal invasion was observed despite the size of the tumor and presence of lymphadenopathy. We think this might be a characteristic finding that distinguishes

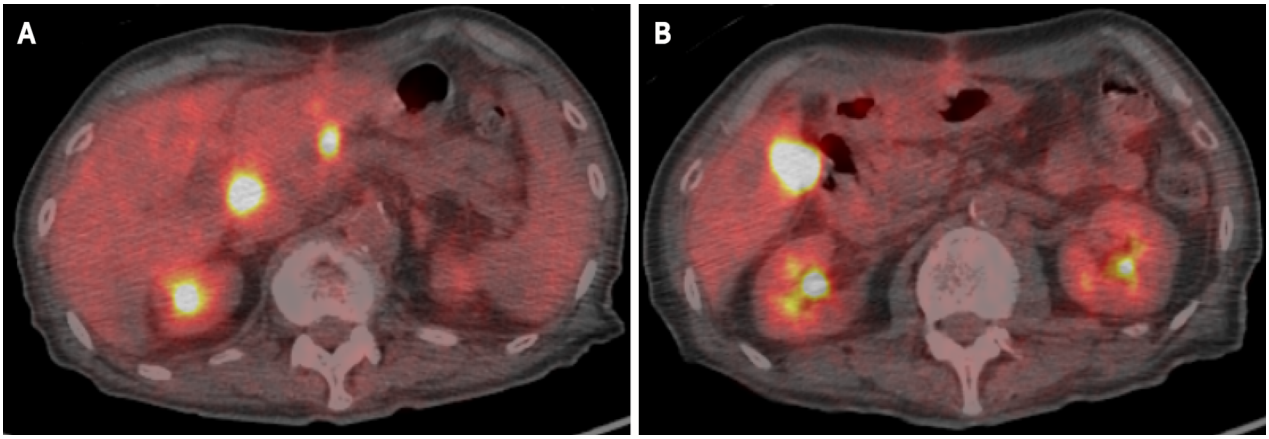

Figure 5 Positron emission tomography reveals increased ^{18}F-fluorodeoxyglucose uptake at the superior pancreaticoduodenal lymph nodes and hepatic radical margin. A: Superior pancreaticoduodenal lymph nodes; B: Hepatic radical margin.

gallbladder malignant lymphoma from carcinoma.

Nevertheless, a biopsy examination seems the best diagnostic technique in the present case, considering the possibility of malignant lymphoma, and hence, biopsy should be planned for patients with the above imaging findings.

CONCLUSION

Burkitt's lymphoma can occur in the gallbladder. Therefore, this disease should be considered in the differential diagnosis of a gallbladder tumor, and biopsy can be useful in facilitating the early introduction of chemotherapy in cases with suggestive imaging findings.

REFERENCES

1 **Yasuma T**, Yanaka M. Primary sarcoma of the gallbladder--report of three cases. *Acta Pathol Jpn* 1971; **21**: 285-304 [PMID: 4937525 DOI: 10.1111/j.1440-1827.1971.tb00125.x]
2 **Jelic TM**, Barreta TM, Yu M, Frame JN, Estallila OC, Mellen PF, Newman SS, Chang HH. Primary, extranodal, follicular non-Hodgkin lymphoma of the gallbladder: case report and a review of the literature. *Leuk Lymphoma* 2004; **45**: 381-387 [PMID: 15101728 DOI: 10.1080/10428190310001597919]
3 **Ono A**, Tanoue S, Yamada Y, Takaji Y, Okada F, Matsumoto S, Mori H. Primary malignant lymphoma of the gallbladder: a case report and literature review. *Br J Radiol* 2009; **82**: e15-e19 [PMID: 19095809 DOI: 10.1259/bjr/30768802]
4 **Ayub A**, Rehmani S, Al-Ayoubi AM, Lewis E, Santana-Rodríguez N, Raad W, Bhora F, Kim G. Primary Non-Hodgkin's Lymphoma of the Gallbladder: A Population-based Analysis. *Anticancer Res* 2017; **37**: 2581-2586 [PMID: 28476830 DOI: 10.21873/anticanres.11602]
5 **Mani H**, Climent F, Colomo L, Pittaluga S, Raffeld M, Jaffe ES. Gall bladder and extrahepatic bile duct lymphomas: clinicopathological observations and biological implications. *Am J Surg Pathol* 2010; **34**: 1277-1286 [PMID: 20679881 DOI: 10.1097/PAS.0b013e3181e9bb8b]
6 **Doherty B**, Palmer W, Cvinar J, Sadek N. A Rare Case of Systemic Adult Burkitt Lymphoma Presenting as Acute Acalculous Cholecystitis. *ACG Case Rep J* 2019; **6**: e00048 [PMID: 31616732 DOI: 10.14309/crj.0000000000000048]
7 **Repine TB**, DeArmond G, López JD. Unusual sites of metastatic malignancy: case 2. Burkitt's lymphoma involving the gallbladder. *J Clin Oncol* 2004; **22**: 5014-5015 [PMID: 15611517 DOI: 10.1200/jco.2004.11.026]
8 **Dawson IM**, Cornes JS, Morson BC. Primary malignant lymphoid tumours of the intestinal tract. Report of 37 cases with a study of factors influencing prognosis. *Br J Surg* 1961; **49**: 80-89 [PMID: 13884035 DOI: 10.1002/bjs.18004921319]
9 **Lewin KJ**, Ranchod M, Dorfman RF. Lymphomas of the gastrointestinal tract: a study of 117 cases presenting with gastrointestinal disease. *Cancer* 1978; **42**: 693-707 [PMID: 354774 DOI: 10.1002/1097-0142(197808)42:2<693::aid-cncr2820420241>3.0.co;2-j]
10 **Crombie J**, LaCasce A. The treatment of Burkitt lymphoma in adults. *Blood* 2021; **137**: 743-750 [PMID: 33171490 DOI: 10.1182/blood.2019004099]
11 **Čubranić A**, Golčić M, Fučkar-Čupić D, Brozović B, Gajski D, Brumini I. BURKITT LYMPHOMA

IN GASTROINTESTINAL TRACT: A REPORT OF TWO CASES. *Acta Clin Croat* 2019; **58**: 386-390 [PMID: 31819338 DOI: 10.20471/acc.2019.58.02.25]

12 **Kato H**, Naganuma T, Iizawa Y, Kitagawa M, Tanaka M, Isaji S. Primary non-Hodgkin's lymphoma of the gallbladder diagnosed by laparoscopic cholecystectomy. *J Hepatobiliary Pancreat Surg* 2008; **15**: 659-663 [PMID: 18987940 DOI: 10.1007/s00534-007-1283-9]

13 **Gupta P**, Marodia Y, Bansal A, Kalra N, Kumar-M P, Sharma V, Dutta U, Sandhu MS. Imaging-based algorithmic approach to gallbladder wall thickening. *World J Gastroenterol* 2020; **26**: 6163-6181 [PMID: 33177791 DOI: 10.3748/wjg.v26.i40.6163]

World Journal of Gastroenterology

Submit a Manuscript: https://www.f6publishing.com

World J Gastroenterol 2022 February 14; 28(6): 683-688

DOI: 10.3748/wjg.v28.i6.683

ISSN 1007-9327 (print) ISSN 2219-2840 (online)

LETTER TO THE EDITOR

COVID-19, liver dysfunction and pathophysiology: A conceptual discussion

Jucier Gonçalves Júnior

ORCID number: Jucier Gonçalves Júnior 0000-0001-5077-7959.

Author contributions: The author worked on all aspects of manuscript preparation and has read and approved the final manuscript; The author meets the criteria for authorship established by the International Committee of Medical Journal Editors.

Conflict-of-interest statement: The author declares no conflict of interest.

Country/Territory of origin: Brazil

Specialty type: Gastroenterology and hepatology

Provenance and peer review: Invited article; Externally peer reviewed.

Peer-review model: Single blind

Peer-review report's scientific quality classification

Grade A (Excellent): 0
Grade B (Very good): 0
Grade C (Good): 0
Grade D (Fair): D
Grade E (Poor): 0

Jucier Gonçalves Júnior, Department of Internal Medicine, Division of Rheumatology, São Paulo University, São Paulo 01246-903, State, Brazil

Corresponding author: Jucier Gonçalves Júnior, MD, PhD, Academic Research, Department of Internal Medicine, Division of Rheumatology, São Paulo University, Av. Dr. Arnaldo, 455, 3º Andar-Sala 3131 Cerqueira César, São Paulo 01246-903, State, Brazil.
juciergjunior@hotmail.com

Abstract

The intra and extracellular pathways of hepatic injury by coronavirus disease 2019 (COVID-19) are still being studied. Understanding them is important to treat this viral disease and other liver and biliary tract disorders. Thus, this paper aims to present three hypotheses about liver injury caused by COVID-19: (1) The interactions between severe acute respiratory syndrome coronavirus 2 spike protein and membrane receptors in the hepatocyte; (2) The dysbiosis and "gut-liver axis" disruption in patients with serious clinical presentations of COVID-19; and (3) The inflammatory response exacerbated through the production of interleukins such as interleukin-6. However, despite these new perspectives, the pathophysiological process of liver injury caused by COVID-19 is still complex and multifactorial. Thus, understanding all these variables is a challenge to science but also the key to propose individualized and effective patient therapies.

Key Words: COVID-19; Intracellular signaling peptides and proteins; Immunopathology; Liver diseases; Liver injury; SARS-CoV-2

Core Tip: This paper aimed to present new hypotheses on the pathophysiology of liver injury caused by severe acute respiratory syndrome coronavirus 2 (SARS-CoV-2) infection. Interactions between SARS-CoV-2 spike protein and other membrane receptors in the liver; "gut-liver axis" disruption and dysbiosis; and increased inflammatory process mediated by interleukin-6 and AT1R-metalloprotease 17 seem to be factors that contribute to such injury.

Citation: Gonçalves Júnior J. COVID-19, liver dysfunction and pathophysiology: A conceptual

Received: July 18, 2021
Peer-review started: July 18, 2021
First decision: August 15, 2021
Revised: August 21, 2021
Accepted: January 19, 2022
Article in press: January 19, 2022
Published online: February 14, 2022

P-Reviewer: Ssekandi AM
S-Editor: Fan JR
L-Editor: Filipodia
P-Editor: Fan JR

discussion. *World J Gastroenterol* 2022; 28(6): 683-688
URL: https://www.wjgnet.com/1007-9327/full/v28/i6/683.htm
DOI: https://dx.doi.org/10.3748/wjg.v28.i6.683

TO THE EDITOR

I have read the work of Prof. Gracia-Ramos *et al*[1] about the clinical aspects of the relationship between liver dysfunction and coronavirus disease 2019 (COVID-19). The author aimed to summarize the pathophysiology, clinical importance, and management of COVID-19 in patients with or without preexisting liver disease.

I would like to highlight some hypotheses for the pathophysiological impairment of the liver in COVID-19. To facilitate visualization, I have summarized the findings in Figure 1. I believe the information provided will enrich the current discussion and may enhance the results of the aforementioned paper[1].

The first theory states that liver cells have two receptors that have an affinity with severe acute respiratory syndrome coronavirus 2 (SARS-CoV-2) spike protein. The first receptor is the Cluster of Differentiation 147 (CD147) or basigin (BSG) or Extracellular Matrix Metalloproteinase Inducer (EMMPRIN)[2], and the second receptor is the Liver/Lymph node-specific intercellular adhesion molecule-3-grabbing non-integrin (L-SIGN)[3].

CD147 is a transmembrane glycoprotein of the immunoglobulin superfamily overexpressed in an inflammatory process triggered by viral infections (*e.g.*, Severe Acute Respiratory Syndrome in 2002), bacterial infections, and parasitic infections (*e.g.*, Plasmodium falciparum)[2] (Figure 1). Evidence of CD147 protein expression in the liver tissue was found in 1999[4]. Recently, a United States publication in Nature journal highlighted the possibility that a chimeric anti-CD147 receptor would be a possible treatment for hepatocellular carcinoma[5]. Experimental research has shown affinity between CD147 and SARS-CoV-2 spike protein. A Chinese study published in Nature journal evaluating the *in vitro* association between the CD147 receptor and the SARS-CoV-2 spike protein by enzyme-linked immunosorbent assay and plasmon resonance demonstrated an affinity of 1.85 × 10–7 Michaelis between them. In parallel, the authors demonstrated that in cell cultures, when the CD147 protein is blocked by specific autoantibodies (*e.g.*, meplazumab), SARS-CoV-2 amplification is inhibited. Additionally, the virus was able to enter into naturally non-susceptible cells (*e.g.*, cells of baby hamster lineage) more easily when CD147 expression was induced in this population[6]. Moreover, increased expression of CD147 in tissues outside the lung has also been shown as an alternative pathway for SARS-CoV-2 infection in bioinformatics studies[7] and systematic reviews[8]. Therefore, an interesting hypothesis would be that the affinity between the CD147 receptor and the SARS-CoV-2 spike protein represents another way for the virus to infect liver cells.

L-SIGN is a liver-specific membrane receptor related to viral capture[3]. L-SIGN is already widely studied in diseases that affect the liver, such as diseases caused by the hepatitis C virus, the human immunodeficiency virus, the Rift Valley fever virus, the Uukuniemi virus, and the Toscana virus[9]. A recent study supports this hypothesis by suggesting that L-SIGN may provide a new way for SARS-CoV-2 to enter human cells [10]. In COVID-19, autopsy studies showed that SARS-CoV-2-infected hepatic sinusoid cells expressed more L-SIGN receptors compared to control groups[11]. Besides that, the literature has shown *in vitro* interactions between L-SIGN and the spike protein[12, 13], in which this receptor binds to angiotensin II (ACE2), increasing the capacity of SARS-CoV-2 to infect liver cells[8,14] (Figure 1).

The second hypothesis (Figure 1) highlights the apparent "gut–liver axis disruption"[15] caused by COVID-19. More than half (60%) of the patients infected with SARS-CoV-2 developed liver injury[16], and some studies have already shown that the hepatic clearance of toxins is negatively impacted by COVID-19[17]. This shows there are varying degrees of dysfunction. Past infections by H1N1[15] and SARS-like viruses[18] led to severe cytopathic alterations in the gastrointestinal tract within 48 h of the beginning of the infectious process[19]. Thus, the disruption of this cross-talk would lead to two consequences: (1) Bacterial translocation stimulating septic shock; and (2) Perpetuation of the septic shock that would lead to a worsened ischemic state[15,20].

The literature has shown a decrease in commensal bacteria and pathogenic microorganisms in patients with COVID-19. This situation persists even after the absence of symptoms and an undetectable viral load by reverse transcription-polymerase chain

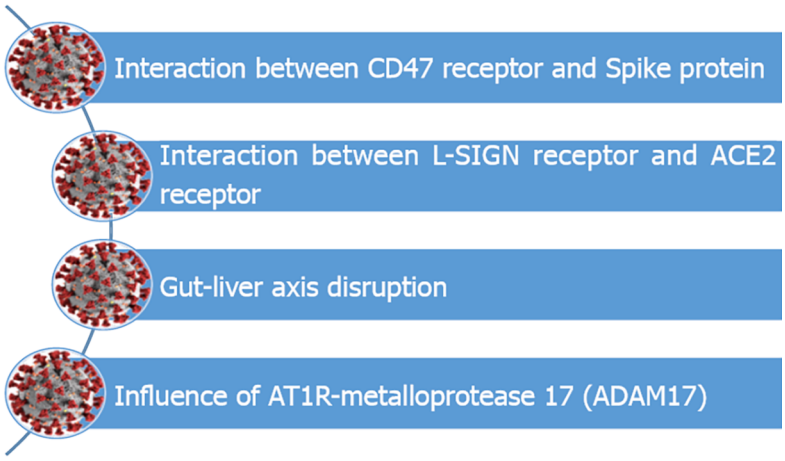

Figure 1 Pathophysiological hypotheses explaining liver injury by severe acute respiratory syndrome coronavirus-2. ACE2: Angiotensin II; ADAM17: AT1R-metalloprotease 17; CD147: Cluster of Differentiation 147; L-SIGN: Liver/Lymph node-specific intercellular adhesion molecule-3-grabbing non-integrin.

reaction. Increased colony-forming units of opportunistic bacteria, such as Veillonella spp., Rothia spp., Actinomyces spp.[20], Faecalibacterium prausnitzii, Clostridium ramosum, and Clostridium hathewayi, in the fecal sample of patients with COVID-19, have been associated with more severe illness by SARS-CoV-2[19]. Furthermore, subspecies of Bacteroides sp. (which decrease ACE2 expression in murine intestine models), when present in human fecal samples, have been correlated with a lower viral load of SARS-CoV-2[21,22]. Besides that, epidemiological studies[23] and meta-analyses[24] have shown that COVID-19 can cause cellular dysfunction in enterocytes. More than half (54%) of the patients infected with COVID-19 had SARS-CoV-2 RNA in their fecal samples in a Chinese study[25]. A paper published by Mazza *et al*[26] demonstrated the presence of fecal calprotectin in a patient infected with COVID-19 showing direct damage to the gastric mucosa. Thus, the disruption of the gastric mucosa feeds back the "cytokine storm" caused by COVID-19 and can lead to hepatic tissue injury[27].

Parohan *et al*[28], when analyzing 3428 patients with COVID-19, demonstrated a significant increase in serum aspartate aminotransferase, alanine aminotransferase, and total bilirubin levels with lower levels of albumin in critically ill patients. An epidemiological survey showed that 62% of the patients admitted to intensive care units (ICUs) had increased liver enzymes. Furthermore, in these ICUs, patients had higher values of pro-inflammatory cytokines such as interleukins (IL) 10, 7, 2; monocyte chemoattractant protein-1 (MCP1); gamma induced protein 10 (IP-10); granulocyte colony-stimulating factor (GCSF); and tumor necrosis factor α (TNF-α) when compared to their controls not admitted to ICUs[29]. Indeed, autopsy studies of patients with severe acute respiratory syndrome caused by COVID-19 showed centrilobular sinusoidal dilation and lobular infiltration by small lymphocytes[30]. Percutaneous liver biopsy of patients infected with coronavirus showed histopathological findings suggestive of liver injury, such as acidophilic bodies, hepatocyte ballooning, and lobular activity without fibrin deposition or fibrosis[16].

The third theory is that SARS-CoV-2 endocytosis by immune system cells is caused by AT1R-metalloprotease 17 (ADAM17), which is also involved in the genesis of liver injury (Figure 1). The mechanism by which ADAM17 facilitates viral entry is not yet known. However, it is known that the increase in its activity can lead to the cleavage of pro-inflammatory molecules (*e.g.*, IL-6; TNF-α), reinforcing the inflammatory process and injury to various organs, including the liver, during SARS-CoV-2 infection[31,32]. Additionally, ADAM17 breaks down several proteins that are responsible for liver regeneration/protection. Among ADAM17 substrates are the epidermal growth factor receptor (EGFR) ligand amphiregulin (AR), the heparin-binding-EGF-like growth factor (HB-EGF), and the hepatocyte growth factor (HGF). ADAM17 deletion in cell cultures of hepatocytes led to a decrease in EGFR and HB-EGF (responsible for preventing liver injury). These molecules increased the apoptosis of hepatocytes and decreased their proliferation[33].

Interestingly, studies have shown increased serum levels of ADAMS17 in comorbidities known to be risk factors for severe cases of COVID-19, such as heart failure[34], COPD[35], diabetes mellitus[36], kidney disease[37], and increasing age

[34]. On the other hand, decreased ADAM17 activity is correlated with decreased ACE2 receptors, thus having a protective effect against SARS-CoV-2 infections[38].

Therefore, the pathophysiological process of liver injury caused by COVID-19 is complex, multifactorial, and extensive. There are many (intra and extracellular) inflammatory pathways we are not yet aware of, in addition to local and systemic environmental factors that interfere. Understanding all these variables is a challenge to science. Additionally, only with this understanding, we will be able to propose individualized and effective therapies.

ACKNOWLEDGEMENTS

The author is grateful to Hospital das Clínicas, Faculdade de Medicina, Universidade de São Paulo, SP, Brazil.

REFERENCES

1 **Gracia-Ramos AE**, Jaquez-Quintana JO, Contreras-Omaña R, Auron M. Liver dysfunction and SARS-CoV-2 infection. *World J Gastroenterol* 2021; **27**: 3951-3970 [PMID: 34326607 DOI: 10.3748/wjg.v27.i26.3951]

2 **Xiong L**, Edwards CK 3rd, Zhou L. The biological function and clinical utilization of CD147 in human diseases: a review of the current scientific literature. *Int J Mol Sci* 2014; **15**: 17411-17441 [PMID: 25268615 DOI: 10.3390/ijms151017411]

3 **Jeffers SA**, Tusell SM, Gillim-Ross L, Hemmila EM, Achenbach JE, Babcock GJ, Thomas WD Jr, Thackray LB, Young MD, Mason RJ, Ambrosino DM, Wentworth DE, Demartini JC, Holmes KV. CD209L (L-SIGN) is a receptor for severe acute respiratory syndrome coronavirus. *Proc Natl Acad Sci U S A* 2004; **101**: 15748-15753 [PMID: 15496474 DOI: 10.1073/pnas.0403812101]

4 **Frayne J**, Ingram C, Love S, Hall L. Localisation of phosphatidylethanolamine-binding protein in the brain and other tissues of the rat. *Cell Tissue Res* 1999; **298**: 415-423 [PMID: 10639732 DOI: 10.1007/s004419900113]

5 **Prince KC**, Diviacco B. On "Coherent control in the extreme ultraviolet and attosecond regime by synchrotron radiation" by Hikosaka *et al*, Nat. Comm. 10, 4988 (2019). *Nat Commun* 2021; **12**: 3784 [PMID: 34145233 DOI: 10.1038/s41467-021-24024-9]

6 **Wang K**, Chen W, Zhang Z, Deng Y, Lian JQ, Du P, Wei D, Zhang Y, Sun XX, Gong L, Yang X, He L, Zhang L, Yang Z, Geng JJ, Chen R, Zhang H, Wang B, Zhu YM, Nan G, Jiang JL, Li L, Wu J, Lin P, Huang W, Xie L, Zheng ZH, Zhang K, Miao JL, Cui HY, Huang M, Zhang J, Fu L, Yang XM, Zhao Z, Sun S, Gu H, Wang Z, Wang CF, Lu Y, Liu YY, Wang QY, Bian H, Zhu P, Chen ZN. CD147-spike protein is a novel route for SARS-CoV-2 infection to host cells. *Signal Transduct Target Ther* 2020; **5**: 283 [PMID: 33277466 DOI: 10.1038/s41392-020-00426-x]

7 **He C**, Hua X, Sun S, Li S, Wang J, Huang X. Integrated Bioinformatic Analysis of SARS-CoV-2 Infection Related Genes ACE2, BSG and TMPRSS2 in Aerodigestive Cancers. *J Inflamm Res* 2021; **14**: 791-802 [PMID: 33732005 DOI: 10.2147/JIR.S300127]

8 **Qiao J**, Li W, Bao J, Peng Q, Wen D, Wang J, Sun B. The expression of SARS-CoV-2 receptor ACE2 and CD147, and protease TMPRSS2 in human and mouse brain cells and mouse brain tissues. *Biochem Biophys Res Commun* 2020; **533**: 867-871 [PMID: 33008593 DOI: 10.1016/j.bbrc.2020.09.042]

9 **Léger P**, Tetard M, Youness B, Cordes N, Rouxel RN, Flamand M, Lozach PY. Differential Use of the C-Type Lectins L-SIGN and DC-SIGN for Phlebovirus Endocytosis. *Traffic* 2016; **17**: 639-656 [PMID: 26990254 DOI: 10.1111/tra.12393]

10 **Raghav PK**, Kalyanaraman K, Kumar D. Human cell receptors: potential drug targets to combat COVID-19. *Amino Acids* 2021; **53**: 813-842 [PMID: 33950300 DOI: 10.1007/s00726-021-02991-z]

11 **Kondo Y**, Larabee JL, Gao L, Shi H, Shao B, Hoover CM, McDaniel JM, Ho YC, Silasi-Mansat R, Archer-Hartmann SA, Azadi P, Srinivasan RS, Rezaie AR, Borczuk A, Laurence JC, Lupu F, Ahamed J, McEver RP, Papin JF, Yu Z, Xia L. L-SIGN is a receptor on liver sinusoidal endothelial cells for SARS-CoV-2 virus. *JCI Insight* 2021; **6** [PMID: 34291736 DOI: 10.1172/jci.insight.148999]

12 **Gao C**, Zeng J, Jia N, Stavenhagen K, Matsumoto Y, Zhang H, Li J, Hume AJ, Mühlberger E, van Die I, Kwan J, Tantisira K, Emili A, Cummings RD. SARS-CoV-2 Spike protein interacts with multiple innate immune receptors. 2020 Preprint. Available from: bioRxiv:2020.07.29.227462 [PMID: 32766577 DOI: 10.1101/2020.07.29.227462]

13 **Zhang Q**, Xiang R, Huo S, Zhou Y, Jiang S, Wang Q, Yu F. Molecular mechanism of interaction between SARS-CoV-2 and host cells and interventional therapy. *Signal Transduct Target Ther* 2021; **6**: 233 [PMID: 34117216 DOI: 10.1038/s41392-021-00653-w]

14 **Gadanec LK**, McSweeney KR, Qaradakhi T, Ali B, Zulli A, Apostolopoulos V. Can SARS-CoV-2 Virus Use Multiple Receptors to Enter Host Cells? *Int J Mol Sci* 2021; **22** [PMID: 33498183 DOI: 10.3390/ijms22030992]

15 **Gu S**, Chen Y, Wu Z, Gao H, Lv L, Guo F, Zhang X, Luo R, Huang C, Lu H, Zheng B, Zhang J, Yan

R, Zhang H, Jiang H, Xu Q, Guo J, Gong Y, Tang L, Li L. Alterations of the Gut Microbiota in Patients With Coronavirus Disease 2019 or H1N1 Influenza. *Clin Infect Dis* 2020; **71**: 2669-2678 [PMID: 32497191 DOI: 10.1093/cid/ciaa709]

16 **Chau TN**, Lee KC, Yao H, Tsang TY, Chow TC, Yeung YC, Choi KW, Tso YK, Lau T, Lai ST, Lai CL. SARS-associated viral hepatitis caused by a novel coronavirus: report of three cases. *Hepatology* 2004; **39**: 302-310 [PMID: 14767982 DOI: 10.1002/hep.20111]

17 **Rodriguez-Morales AJ**, Cardona-Ospina JA, Gutiérrez-Ocampo E, Villamizar-Peña R, Holguin-Rivera Y, Escalera-Antezana JP, Alvarado-Arnez LE, Bonilla-Aldana DK, Franco-Paredes C, Henao-Martinez AF, Paniz-Mondolfi A, Lagos-Grisales GJ, Ramírez-Vallejo E, Suárez JA, Zambrano LI, Villamil-Gómez WE, Balbin-Ramon GJ, Rabaan AA, Harapan H, Dhama K, Nishiura H, Kataoka H, Ahmad T, Sah R. Clinical, laboratory and imaging features of COVID-19: A systematic review and meta-analysis. *Travel Med Infect Dis* 2020; **34**: 101623 [PMID: 32179124 DOI: 10.1016/j.tmaid.2020.101623]

18 **Cheng VC**, Lau SK, Woo PC, Yuen KY. Severe acute respiratory syndrome coronavirus as an agent of emerging and reemerging infection. *Clin Microbiol Rev* 2007; **20**: 660-694 [PMID: 17934078 DOI: 10.1128/CMR.00023-07]

19 **Vodnar DC**, Mitrea L, Teleky BE, Szabo K, Călinoiu LF, Nemeş SA, Martău GA. Coronavirus Disease (COVID-19) Caused by (SARS-CoV-2) Infections: A Real Challenge for Human Gut Microbiota. *Front Cell Infect Microbiol* 2020; **10**: 575559 [PMID: 33363049 DOI: 10.3389/fcimb.2020.575559]

20 **Watson AJ**, Hughes KR. TNF-α-induced intestinal epithelial cell shedding: implications for intestinal barrier function. *Ann N Y Acad Sci* 2012; **1258**: 1-8 [PMID: 22731709 DOI: 10.1111/j.1749-6632.2012.06523.x]

21 **Amirian ES**. Potential fecal transmission of SARS-CoV-2: Current evidence and implications for public health. *Int J Infect Dis* 2020; **95**: 363-370 [PMID: 32335340 DOI: 10.1016/j.ijid.2020.04.057]

22 **Zuo T**, Zhang F, Lui GCY, Yeoh YK, Li AYL, Zhan H, Wan Y, Chung ACK, Cheung CP, Chen N, Lai CKC, Chen Z, Tso EYK, Fung KSC, Chan V, Ling L, Joynt G, Hui DSC, Chan FKL, Chan PKS, Ng SC. Alterations in Gut Microbiota of Patients With COVID-19 During Time of Hospitalization. *Gastroenterology* 2020; **159**: 944-955.e8 [PMID: 32442562 DOI: 10.1053/j.gastro.2020.05.048]

23 **Jin X**, Lian JS, Hu JH, Gao J, Zheng L, Zhang YM, Hao SR, Jia HY, Cai H, Zhang XL, Yu GD, Xu KJ, Wang XY, Gu JQ, Zhang SY, Ye CY, Jin CL, Lu YF, Yu X, Yu XP, Huang JR, Xu KL, Ni Q, Yu CB, Zhu B, Li YT, Liu J, Zhao H, Zhang X, Yu L, Guo YZ, Su JW, Tao JJ, Lang GJ, Wu XX, Wu WR, Qv TT, Xiang DR, Yi P, Shi D, Chen Y, Ren Y, Qiu YQ, Li LJ, Sheng J, Yang Y. Epidemiological, clinical and virological characteristics of 74 cases of coronavirus-infected disease 2019 (COVID-19) with gastrointestinal symptoms. *Gut* 2020; **69**: 1002-1009 [PMID: 32213556 DOI: 10.1136/gutjnl-2020-320926]

24 **Parasa S**, Desai M, Thoguluva Chandrasekar V, Patel HK, Kennedy KF, Roesch T, Spadaccini M, Colombo M, Gabbiadini R, Artifon ELA, Repici A, Sharma P. Prevalence of Gastrointestinal Symptoms and Fecal Viral Shedding in Patients With Coronavirus Disease 2019: A Systematic Review and Meta-analysis. *JAMA Netw Open* 2020; **3**: e2011335 [PMID: 32525549 DOI: 10.1001/jamanetworkopen.2020.11335]

25 **Xie C**, Jiang L, Huang G, Pu H, Gong B, Lin H, Ma S, Chen X, Long B, Si G, Yu H, Yang X, Shi Y, Yang Z. Comparison of different samples for 2019 novel coronavirus detection by nucleic acid amplification tests. *Int J Infect Dis* 2020; **93**: 264-267 [PMID: 32114193 DOI: 10.1016/j.ijid.2020.02.050]

26 **Mazza S**, Sorce A, Peyvandi F, Vecchi M, Caprioli F. A fatal case of COVID-19 pneumonia occurring in a patient with severe acute ulcerative colitis. *Gut* 2020; **69**: 1148-1149 [PMID: 32245909 DOI: 10.1136/gutjnl-2020-321183]

27 **Cardinale V**, Capurso G, Ianiro G, Gasbarrini A, Arcidiacono PG, Alvaro D. Intestinal permeability changes with bacterial translocation as key events modulating systemic host immune response to SARS-CoV-2: A working hypothesis. *Dig Liver Dis* 2020; **52**: 1383-1389 [PMID: 33023827 DOI: 10.1016/j.dld.2020.09.009]

28 **Parohan M**, Yaghoubi S, Seraji A. Liver injury is associated with severe coronavirus disease 2019 (COVID-19) infection: A systematic review and meta-analysis of retrospective studies. *Hepatol Res* 2020; **50**: 924-935 [PMID: 32386449 DOI: 10.1111/hepr.13510]

29 **Huang C**, Wang Y, Li X, Ren L, Zhao J, Hu Y, Zhang L, Fan G, Xu J, Gu X, Cheng Z, Yu T, Xia J, Wei Y, Wu W, Xie X, Yin W, Li H, Liu M, Xiao Y, Gao H, Guo L, Xie J, Wang G, Jiang R, Gao Z, Jin Q, Wang J, Cao B. Clinical features of patients infected with 2019 novel coronavirus in Wuhan, China. *Lancet* 2020; **395**: 497-506 [PMID: 31986264 DOI: 10.1016/S0140-6736(20)30183-5]

30 **Tian S**, Xiong Y, Liu H, Niu L, Guo J, Liao M, Xiao SY. Pathological study of the 2019 novel coronavirus disease (COVID-19) through postmortem core biopsies. *Mod Pathol* 2020; **33**: 1007-1014 [PMID: 32291399 DOI: 10.1038/s41379-020-0536-x]

31 **Zipeto D**, Palmeira JDF, Argañaraz GA, Argañaraz ER. ACE2/ADAM17/TMPRSS2 Interplay May Be the Main Risk Factor for COVID-19. *Front Immunol* 2020; **11**: 576745 [PMID: 33117379 DOI: 10.3389/fimmu.2020.576745]

32 **Li D**, Ding X, Xie M, Tian D, Xia L. COVID-19-associated liver injury: from bedside to bench. *J Gastroenterol* 2021; **56**: 218-230 [PMID: 33527211 DOI: 10.1007/s00535-021-01760-9]

33 **Al-Salihi M**, Bornikoel A, Zhuang Y, Stachura P, Scheller J, Lang KS, Lang PA. The role of ADAM17 during liver damage. *Biol Chem* 2021; **402**: 1115-1128 [PMID: 34192832 DOI: 10.1515/hsz-2021-0149]

34 **Sama IE**, Ravera A, Santema BT, van Goor H, Ter Maaten JM, Cleland JGF, Rienstra M, Friedrich AW, Samani NJ, Ng LL, Dickstein K, Lang CC, Filippatos G, Anker SD, Ponikowski P, Metra M, van Veldhuisen DJ, Voors AA. Circulating plasma concentrations of angiotensin-converting enzyme 2 in men and women with heart failure and effects of renin-angiotensin-aldosterone inhibitors. *Eur Heart J* 2020; **41**: 1810-1817 [PMID: 32388565 DOI: 10.1093/eurheartj/ehaa373]

35 **Saheb Sharif-Askari N**, Saheb Sharif-Askari F, Alabed M, Temsah MH, Al Heialy S, Hamid Q, Halwani R. Airways Expression of SARS-CoV-2 Receptor, ACE2, and TMPRSS2 Is Lower in Children Than Adults and Increases with Smoking and COPD. *Mol Ther Methods Clin Dev* 2020; **18**: 1-6 [PMID: 32537478 DOI: 10.1016/j.omtm.2020.05.013]

36 **Fiorentino L**, Vivanti A, Cavalera M, Marzano V, Ronci M, Fabrizi M, Menini S, Pugliese G, Menghini R, Khokha R, Lauro R, Urbani A, Federici M. Increased tumor necrosis factor alpha-converting enzyme activity induces insulin resistance and hepatosteatosis in mice. *Hepatology* 2010; **51**: 103-110 [PMID: 19877183 DOI: 10.1002/hep.23250]

37 **Salem ES**, Grobe N, Elased KM. Insulin treatment attenuates renal ADAM17 and ACE2 shedding in diabetic Akita mice. *Am J Physiol Renal Physiol* 2014; **306**: F629-F639 [PMID: 24452639 DOI: 10.1152/ajprenal.00516.2013]

38 **Riera M**, Anguiano L, Clotet S, Roca-Ho H, Rebull M, Pascual J, Soler MJ. Paricalcitol modulates ACE2 shedding and renal ADAM17 in NOD mice beyond proteinuria. *Am J Physiol Renal Physiol* 2016; **310**: F534-F546 [PMID: 26697977 DOI: 10.1152/ajprenal.00082.2015]

World Journal of Gastroenterology

Submit a Manuscript: https://www.f6publishing.com

World J Gastroenterol 2022 February 14; 28(6): 689-692

DOI: 10.3748/wjg.v28.i6.689

ISSN 1007-9327 (print) ISSN 2219-2840 (online)

LETTER TO THE EDITOR

Comments on validation of conventional non-invasive fibrosis scoring systems in patients with metabolic associated fatty liver disease

Jian-Guo Hong, Lun-Jie Yan, Xian Li, Sheng-Yu Yao, Peng Su, Hai-Chao Li, Zi-Niu Ding, Dong-Xu Wang, Zhao-Ru Dong, Tao Li

ORCID number: Jian-Guo Hong 0000-0003-1529-1106; Lun-Jie Yan 0000-0002-1102-1144; Xian Li 0000-0001-7347-8628; Sheng-Yu Yao 0000-0002-6911-0465; Peng Su 0000-0003-1495-2689; Hai-Chao Li 0000-0002-4220-1295; Zi-Niu Ding 0000-0002-2308-8629; Dong-Xu Wang 0000-0002-4550-4611; Zhao-Ru Dong 0000-0003-2906-0210; Tao Li 0000-0002-5378-3059.

Author contributions: Li X and Yao SY designed and performed the research; Yan LJ, Li HC and Ding ZN analyzed the data; Li T and Hong JG wrote the letter; Yan LJ, Su P, Wang DX and Dong ZR revised the letter; Hong JG, Yan LJ, Li X, Yao SY, and Su P contributed equally to this article.

Conflict-of-interest statement: The authors have no conflicts of interest to disclose.

Country/Territory of origin: China

Specialty type: Gastroenterology and hepatology

Provenance and peer review: Invited article; Externally peer reviewed.

Peer-review model: Single blind

Peer-review report's scientific

Jian-Guo Hong, Lun-Jie Yan, Xian Li, Sheng-Yu Yao, Hai-Chao Li, Zi-Niu Ding, Dong-Xu Wang, Zhao-Ru Dong, Tao Li, Department of General Surgery, Qilu Hospital of Shandong University, Jinan 250012, Shandong Province, China

Peng Su, Department of Pathology, Qilu Hospital of Shandong University, Jinan 250012, Shandong Province, China

Corresponding author: Tao Li, MD, Chief Doctor, Department of General Surgery, Qilu Hospital of Shandong University, No. 107 West Wenhua Road, Jinan 250012, Shandong Province, China. litao7709@126.com

Abstract

To evaluate and predict liver fibrosis in patients with nonalcoholic fatty liver disease (NAFLD), several non-invasive scoring systems were built and widely used in the progress of diagnosis and treatment, which showed great diagnostic efficiency, such as aspartate aminotransferase to platelet ratio index, fibrosis-4 index, body mass index, aspartate aminotransferase to alanine aminotransferase ratio, diabetes score and NAFLD fibrosis score. Since the new concept of metabolic associated fatty liver disease (MAFLD) was proposed, the clinical application value of the non-invasive scoring systems mentioned above has not been assessed in MAFLD. The evaluation of the diagnostic performance of these non-invasive scoring systems will provide references for clinicians in the diagnosis of MAFLD.

Key Words: Metabolic associated fatty liver disease; Prediction model; Calibration; Normal distribution; Nonalcoholic fatty liver disease

Core Tip: The concept of metabolic associated fatty liver disease (MAFLD) was proposed in 2020. Unlike the concept of nonalcoholic fatty liver disease, the exclusion of chronic liver disease was not required in the establishment of diagnosis of MAFLD,

quality classification
Grade A (Excellent): A
Grade B (Very good): B
Grade C (Good): 0
Grade D (Fair): 0
Grade E (Poor): 0

Received: October 5, 2021
Peer-review started: October 5, 2021
First decision: November 15, 2021
Revised: December 5, 2021
Accepted: January 17, 2022
Article in press: January 17, 2022
Published online: February 14, 2022

P-Reviewer: Par G, Zaiou M
S-Editor: Fan JR
L-Editor: A
P-Editor: Fan JR

but the presence of metabolic associated disease or dysfunction is required. The clinical prediction values and the optimal cutoff values of non-invasive fibrosis scores remain unknown. We read the recent article entitled "Validation of Conventional Non-invasive Fibrosis Scoring Systems in Patients with Metabolic Associated Fatty Liver Disease" with great interest. We would like to share our opinions and criticisms about this valuable work.

Citation: Hong JG, Yan LJ, Li X, Yao SY, Su P, Li HC, Ding ZN, Wang DX, Dong ZR, Li T. Comments on validation of conventional non-invasive fibrosis scoring systems in patients with metabolic associated fatty liver disease. *World J Gastroenterol* 2022; 28(6): 689-692
URL: https://www.wjgnet.com/1007-9327/full/v28/i6/689.htm
DOI: https://dx.doi.org/10.3748/wjg.v28.i6.689

TO THE EDITOR

We read the recent article entitled "Validation of Conventional Non-invasive Fibrosis Scoring Systems in Patients with Metabolic Associated Fatty Liver Disease" published by Wu *et al*[1] with great interest. In the article, the authors designed and performed a retrospective study to evaluate the diagnostic performance of four non-invasive scoring systems, including aspartate aminotransferase to platelet ratio index (APRI), fibrosis-4 index (FIB-4), body mass index (BMI), aspartate aminotransferase to alanine aminotransferase (ALT) ratio, diabetes score (BARD score) and nonalcoholic fatty liver disease fibrosis score (NFS), in patients with metabolic associated fatty liver disease (MAFLD). We would like to share our opinions and criticisms about this valuable work.

The specificity, sensitivity, positive predictive value (PPV), negative predictive value (NPV) and discrimination of the scoring systems mentioned above were evaluated in the prediction of advanced fibrosis in patients with MAFLD in the study by Wu *et al*[1]. Clinical characteristics, laboratory variables and non-invasive scores were compared between patients with advanced fibrosis and those with mild fibrosis or without fibrosis. The results showed that the FIB-4 ($P < 0.001$), NFS ($P < 0.001$), APRI ($P = 0.003$) and BARD ($P < 0.001$) scores were all significantly higher in patients with advanced fibrosis. Unfortunately, only univariate analysis was performed in this study. In our opinion, multivariate analysis should be performed to recognize the independent variables in the prediction of advanced fibrosis, as in the study by Nielsen *et al*[2].

The authors evaluated the diagnostic efficiency of the prediction scores using the following statistical indices: Sensitivity, specificity, accuracy, PPV, NPV and the area under the receiver operating characteristic curve (AUROC). All the above indices are important statistical variables in the development and validation of prediction models. In our opinion, it would be better if the authors had evaluated the calibration of the prediction scores in the study. In fact, calibration of the prediction model is a critical statistical index in the evaluation of diagnostic efficiency[3]. Calibration of the prediction scores can be performed using the Hosmer–Lemeshow goodness-of-fit test and calibration curves, the latter of which can be easily plotted using R software. We advise the authors to evaluate the calibration of prediction models in future studies.

The calculations of PPV and NPV are very important in the development and validation of prediction models. Unlike sensitivity and specificity, PPV and NPV cannot be compared directly among different samples, except for samples with the same prevalence rate of the disease. This is because both PPV and NPV can be affected by the prevalence rate of disease[4,5]. The authors compared the PPV and NPV in table 4 and stated that "PPV and NPV was better in the HBV-MAFLD group" in the article. In our opinion, the comparisons of PPV and NPV between the HBV-MAFLD group and the pure MAFLD group will be valuable only when advanced fibrosis accounts for the same proportion of the two groups.

Although the authors stated that the continuous variables were expressed in the format of mean ± SD or median value with interquartile range (IQR) and the differences were calculated using Student's *t* test in the case of normally distributed data or the Mann–Whitney test in the remaining cases, there were no continuous variables expressed as the median (IQR) in the article. Normally, the distribution of

continuous variables should be tested; then, the continuous variables in normal distribution will be expressed as the mean ± SD, and the non-normally distributed continuous variables will be expressed as the median (IQR). If all the continuous variables are expressed as the mean ± SD but the authors do not indicate that all the continuous variables fit a normal distribution, the readers will doubt whether the normal distribution tests were performed in the study. After all, it rarely happens that all the laboratory variables fit a normal distribution in one study. In most studies, the laboratory variables and scores, including ALT, AST, APRI and other variables, do not fit a normal distribution and should be expressed as the median (interquartile range) [2,6-8]. For any parameter in biomedical research, a true normal distribution is rare. The European Medicines Agency has issued the general guidance that data should be checked for normality of distribution and should be analyzed and presented based on the results of normal distribution tests. It is also possible that some continuous variables did not fit a normal distribution, but these variables were accidentally expressed as the mean ± SD in the study conducted by Wu *et al*[1]. Of course, this situation indeed does not affect the accuracy of the study. We advise that the authors indicate whether the continuous variables fit a normal distribution and if the normal distribution tests have been performed in future studies.

The authors compared the diagnostic ability of the NFS, FIB-4, APRI and BARD score for a late stage of fibrosis in MAFLD. The results demonstrated that the APRI and BARD scores performed poorly, but the FIB-4 and NFS showed a promising prospect in clinical use. The new thresholds of the FIB-4 and NFS proposed in this study were 1.05 and -2.1, respectively. The two thresholds proposed by the authors were determined based on their specific study sample. The diagnostic efficiency of the thresholds in the prediction of advanced fibrosis should be further evaluated in an external validation cohort and/or in a prospective validation cohort. Additionally, if possible, the authors can try to develop models based on multiple variables, including the FIB-4 and/or NFS, to predict advanced fibrosis in patients with MAFLD. He *et al*[9] proposed that a diagnostic model containing valuable parameters extracted from more examination tools might provide more satisfactory results[9]. Compared to using a single variable, we believe that prediction models based on multiple variables, including clinical characteristics, radiology examinations and laboratory examinations, would exhibit higher sensitivity, higher specificity, higher accuracy, higher PPV, higher NPV, better discrimination and better calibration in the prediction of advanced fibrosis in patients with MAFLD. Because there is now evidence from a prospective cohort that common genetic variants can capture additional prognostic insights not conveyed by validated clinical/biochemical parameters[10], we encourage the integration of genetics (perhaps epigenetics) with clinical fibrosis scores, as it may refine individual risk and improve risk stratification and prediction of severe liver disease.

In general, we are very interested in the study by Wu *et al*[1]. The authors demonstrated the prediction values of APRI, FIB-4, NFS and BARD in a large sample of histology-proven MAFLD. As MAFLD is a new entity, this study will provide important references for clinicians in the prediction of advanced fibrosis in MAFLD patients. The study performed by Wu *et al*[1] could also provide important references for other studies of non-invasive scores and prediction models.

REFERENCES

1 **Wu YL**, Kumar R, Wang MF, Singh M, Huang JF, Zhu YY, Lin S. Validation of conventional non-invasive fibrosis scoring systems in patients with metabolic associated fatty liver disease. *World J Gastroenterol* 2021; **27**: 5753-5763 [PMID: 34629799 DOI: 10.3748/wjg.v27.i34.5753]

2 **Nielsen MJ**, Leeming DJ, Goodman Z, Friedman S, Frederiksen P, Rasmussen DGK, Vig P, Seyedkazemi S, Fischer L, Torstenson R, Karsdal MA, Lefebvre E, Sanyal AJ, Ratziu V. Comparison of ADAPT, FIB-4 and APRI as non-invasive predictors of liver fibrosis and NASH within the CENTAUR screening population. *J Hepatol* 2021; **75**: 1292-1300 [PMID: 34454994 DOI: 10.1016/j.jhep.2021.08.016]

3 **Assel M**, Sjoberg D, Elders A, Wang X, Huo D, Botchway A, Delfino K, Fan Y, Zhao Z, Koyama T, Hollenbeck B, Qin R, Zahnd W, Zabor EC, Kattan MW, Vickers AJ. Guidelines for Reporting of Statistics for Clinical Research in Urology. *Eur Urol* 2019; **75**: 358-367 [PMID: 30580902 DOI: 10.1016/j.eururo.2018.12.014]

4 **Monaghan TF**, Rahman SN, Agudelo CW, Wein AJ, Lazar JM, Everaert K, Dmochowski RR. Foundational Statistical Principles in Medical Research: Sensitivity, Specificity, Positive Predictive Value, and Negative Predictive Value. *Medicina (Kaunas)* 2021; **57** [PMID: 34065637 DOI: 10.3390/medicina57050503]

5 **Akobeng AK**. Understanding diagnostic tests 2: likelihood ratios, pre- and post-test probabilities and their use in clinical practice. *Acta Paediatr* 2007; **96**: 487-491 [PMID: 17306009 DOI: 10.1111/j.1651-2227.2006.00179.x]

6 **Abdel-Hameed EA**, Rouster SD, Kottilil S, Sherman KE. The Enhanced Liver Fibrosis Index Predicts Hepatic Fibrosis Superior to FIB4 and APRI in HIV/HCV Infected Patients. *Clin Infect Dis* 2021; **73**: 450-459 [PMID: 32459305 DOI: 10.1093/cid/ciaa646]

7 **Lee J**, Vali Y, Boursier J, Spijker R, Anstee QM, Bossuyt PM, Zafarmand MH. Prognostic accuracy of FIB-4, NAFLD fibrosis score and APRI for NAFLD-related events: A systematic review. *Liver Int* 2021; **41**: 261-270 [PMID: 32946642 DOI: 10.1111/liv.14669]

8 **Amiri M**, Murgas S, Stang A, Michel MC. Do overactive bladder symptoms and their treatment-associated changes exhibit a normal distribution? *Neurourol Urodyn* 2020; **39**: 754-761 [PMID: 31945207 DOI: 10.1002/nau.24275]

9 **He Y**, Zhu Z, Chen Y, Chen F, Wang Y, Ouyang C, Yang H, Huang M, Zhuang X, Mao R, Ben-Horin S, Wu X, Ouyang Q, Qian J, Lu N, Hu P, Chen M. Development and Validation of a Novel Diagnostic Nomogram to Differentiate Between Intestinal Tuberculosis and Crohn's Disease: A 6-year Prospective Multicenter Study. *Am J Gastroenterol* 2019; **114**: 490-499 [PMID: 30741735 DOI: 10.14309/ajg.0000000000000064]

10 **De Vincentis A**, Tavaglione F, Jamialahmadi O, Picardi A, Antonelli Incalzi R, Valenti L, Romeo S, Vespasiani-Gentilucci U. A Polygenic Risk Score to Refine Risk Stratification and Prediction for Severe Liver Disease by Clinical Fibrosis Scores. *Clin Gastroenterol Hepatol* 2021 [PMID: 34091049 DOI: 10.1016/j.cgh.2021.05.056]

Published by **Baishideng Publishing Group Inc**
7041 Koll Center Parkway, Suite 160, Pleasanton, CA 94566, USA
Telephone: +1-925-3991568
E-mail: bpgoffice@wjgnet.com
Help Desk: https://www.f6publishing.com/helpdesk
https://www.wjgnet.com